2001

Synthesis of Phosphonopeptides and Alpha, Alpha-Dialkylated Amino Acid-Rich Peptides.

Sheila Denise Rushing
Louisiana State University and Agricultural & Mechanical College

INFORMATION TO USERS

This manuscript has been reproduced from the microfilm master. UMI films the text directly from the original or copy submitted. Thus, some thesis and dissertation copies are in typewriter face, while others may be from any type of computer printer.

The quality of this reproduction is dependent upon the quality of the copy submitted. Broken or indistinct print, colored or poor quality illustrations and photographs, print bleedthrough, substandard margins, and improper alignment can adversely affect reproduction..

In the unlikely event that the author did not send UMI a complete manuscript and there are missing pages, these will be noted. Also, if unauthorized copyright material had to be removed, a note will indicate the deletion.

Oversize materials (e.g., maps, drawings, charts) are reproduced by sectioning the original, beginning at the upper left-hand corner and continuing from left to right in equal sections with small overlaps.

Photographs included in the original manuscript have been reproduced xerographically in this copy. Higher quality 6" x 9" black and white photographic prints are available for any photographs or illustrations appearing in this copy for an additional charge. Contact UMI directly to order.

ProQuest Information and Learning
300 North Zeeb Road, Ann Arbor, MI 48106-1346 USA
800-521-0600

SYNTHESIS OF PHOSPHONOPEPTIDES AND ALPHA, ALPHA-DIALKYLATED AMINO ACID-RICH PEPTIDES

A Dissertation

Submitted to the Graduate Faculty of the
Louisiana State University and
Agricultural and Mechanical College
in partial fulfillment of the
requirements for the degree of
Doctor of Philosophy

in

The Department of Chemistry

by
Sheila Denise Rushing
B.S., Tougaloo College, 1996
May, 2001

This dissertation is dedicated to:

my compassionate and supportive husband,

Judson

It's reaping time!!!

and to my parents (Mr. and Mrs. Rushing) and grandmother (Thelma Mobley)

for all of your love, encouragement, and support.

Acknowledgements

Hallelujah!!! I would first like to thank God for providing me with the strength, wisdom, and intense desire needed for successful completion of my formal educational training.

I give thanks and appreciation to my advisor, Dr. Robert P. Hammer, for his support, guidance, and expressive belief in my abilities as a scientist. Working in his bioorganic group was truly a rewarding experience-especially in terms of skills and knowledge gained and professional and personal growth.

An abundant of love and gratitude goes to my wonderful, supportive husband, Dr. Judson L. Haynes, III. Thanks for countless encouraging words and actions and for very insightful and beneficial information you provided about the graduate school process.

I give special thanks and honor to my parents, Johnnie Mae and Clifton Rushing, for their innumerable prayers for me as well as their inspiring words of encouragement and never-ending faith in me. I also acknowledge my siblings-Sandra, Curtis, Clifton, Diane, Steven, Jeffrey, Johnny, and Jennifer-for their emotional and spiritual support. In addition, I give special acknowledgements to the Haynes family, particularly, Ornita and Judson Haynes and Chiara Haynes, for their genuine concern and prayers for me during my tenure at LSU.

A significant amount of thanks is given to Martha Juban for help with peptide synthesis, Dr. Tracy McCarley for mass specs, Dr. Dale Treleavan and Dr. Frank Zhou for assistance with NMR techniques, Natha Booth for biological studies, Henry Hurtado and Luz Barona for assistance in drafting shop. I also greatly appreciate the contributions and support from members of Hammer's group: Dr. Maria Fernandez, Dr. Hong Fan, Yanwen Fu, Christopher Wysong, Dr. Kristofer Moffett, Dr. Tod Miller, Hannah

Farquar, Dr. Andrea Saurage, and Courtney Brown. In addition, I give thanks and appreciation to the faculty and staff of LSU.

Finally, I would like to thank all of my committee members, Dr. Robert P. Hammer, Dr. Mark McLaughlin, Dr. Robert Strongin, Dr. Isiah M. Warner, and Dr. Frederick Enright.

Table of Contents

List of Tables

List of Figures

List of Schemes

List of Abbreviations

ααAA	α,α-disubstituted amino acid
Aib	α-aminoisobutyric acid
Ac	acetyl
Api	4-aminopiperidine-4-carboxylic acid
ATCC	American Type Culture Collection
Boc	tert-butyloxycarbonyl
BOP	benzotriazolyloxy-tris(dimethylamino)phosphonium hexafluorophosphate
bs	broad singlet
CCA	α-cyano-4-hydroxycinnamic acid
CH_3CN	acetonitrile
Cbz	benzyloxycarbonyl
d	doublet
dab	2,4 diaminobutanoic acid
dap	2,3 diaminopropanoic acid
DBU	1,8-diazobicyclo[4.5.0]undec-7-ene
DCC	dicyclohexyl carbodiimide
dd	double of doublets
Dde	5,5-dimethyl-2-acetyl-1,3-cyclohexandione
Deg	degree
DIC	1,3-diisopropylcarbodiimide
DIEA	diisopropylethylamine

dmol	decimole
DMF	*N,N*-dimethylformamide
DMSO	dimethylsulfoxide
EDC	1-[3-(dimethylamino)propyl]-3-ethylcarbodiimide hydrochloride
Et_3N	triethylamine
Et_2O	diethyl ether
EtOAc	ethyl acetate
EtOH	ethanol
FABMS	fast atom bombardment mass spectrometry
FCS	fetal calf serum
Fmoc	9-fluorenylmethyloxycarbonyl
Fmoc-Cl	9-fluorenylmethyl chloroformate
GC-MS	gas chromatography-mass spectrometry
HATU	*N*-[(dimethylamino)-1H-1,2,3-triazolo[4,5-b]pyridin-1-ylmethylene]-*N*-methyl-methanaminium hexafluorophosphate *N*-oxide
HBTU	*O*-(benzotriazol-1-yl)-1,1,3,3-tetramethyluronium hexafluorophosphate
HOAt	1-hydroxy-7-azabenzotriazole
HOBt	1-hydroxybenzotriazole
HPLC	high performance liquid chromatography
HRMS	high resolution mass spectrometry
Lys	lysine
m	multiplet
MALDI	matrix assisted laser desorption ionization
MeOH	methanol

MHz	megahertz
MIC	minimum inhibitory concentration
mM	millimolar
mL	milliliter
NBA	3-nitrobenzyl alcohol
Nbs	2-nitrobenzenesulfonyl
NCA	*N*-carboxyanhydride
nm	nanometer
NMR	nuclear magnetic resonance
orn	ornithine
PAL	Peptide Amide Linker
PBS	phosphate buffered saline
PEG	polyethylene glycol
Pen-Strep	penicillin and streptomycin
*p*Nb	para-nitrobenzyl
PS	polystyrene
PyAOP	7-azabenzotriazol-1-yloxytris(pyrrolidino)phos-phonium hexa-fluorophosphates
s	singlet
SAR	structure-activity relationship
SDS	sodium dodecyl sulfate
SPPS	Solid-Phase Peptide Synthesis
t	triplet
TFA	trifluoroacetic Acid

TFE	trifluoroethanol
TFFH	tetramethylfluoroformamidinium hexafluorophosphate
THF	tetrahydrofuran
TIPS	triisopropylsilane
TMS	trimethylsilane
Z-OSu	*N*-(benzyloxycarbonyloxy)succinimide

Abstract

Peptides and peptide analogs are central to the understanding of biological and biochemical phenomena as well as in the development of new pharmaceutical agents. This research encompasses two classes of peptide mimetics: phosphonopeptides and short, amphipathic peptides rich in α,α-disubstituted amino acids (ααAA). The focus of the first part of the peptide analog project was on the preparation of sterically-hindered phosphonamide and thiophosphonamide dipeptides. Conditions were developed, based on our P(III) synthetic approach, for the preparation of the phosphonamide dipeptides, Cbz-CyhGly ψ [P (O) (O*p*Nb) NH] Trp-NH_2 and Cbz-CyhGly ψ [P (O) (O*p*Nb) NH] Trp-OMe, which were previously unattainable by P(V) methods. The use of reduced phosphorus intermediates also allowed preparation of the related thiophosphonamides, Cbz-CyhGly ψ [P (S) (O*p*Nb) NH] Trp-NH_2 and Cbz-CyhGly ψ [P (S) (O*p*Nb) NH] Trp-OMe. With the P(III) synthetic strategy we started from an amine-protected H-phosphinate amino acid ester and activated, in the presence of 2 equivalents of pyridine, with dichlorotriphenylphosphorane to generate a phosphonochloridite, which was treated with a diisopropylethylamine to form a proposed, very reactive, oxazaphospholine. The oxazaphospholine was coupled to an amine nucleophile followed by oxidation or sulfurization. This method was also used to prepare several simpler phosphonamide and thiophosphonamide dipeptides and thiophosphonates.

In the second part of this project a homologous series of 9-mer, ααAA-rich peptides (and their acetylated versions), which were designed to be amphipathic and 3_{10}-helical, were prepared using solid-phase synthetic techniques. The peptides were composed of 78% ααAAs (one 4-aminopiperidine-4-carboxylic acid (Api) and six

aminoisobutyric acid (Aib)). The *in situ* coupling agent, PyAOP, was used in the synthesis. The use of Fmoc-Aib-Aib-OH in the syntheses caused a significant improvement in the coupling and overall yields of the peptides. However, the monomer Aib had to be incorporated, along with double coupling, for the first two Aibs in each peptide's sequence.

The helix preference of each peptide in different solvent environments were investigated as well as each peptide's antimicrobial activity and cytotoxicity. Significant populations of both α- and 3_{10}-helices were observed for the non-acetylated peptides under the solvent conditions tested. The 3_{10}-helical, amphipathic design was observed best for the acetylated peptides. Most of the peptides exhibited modest activity against *E. coli* and no activity against *S. aureus*. The non-acetylated peptides (concentrations ≤ 100 μM) and the acetylated peptides (concentrations ≤ 200 μM) did not exhibit, based on a trypan blue stain procedure, any significant cytotoxicity to normal macrophages.

Chapter 1

Introduction

1.1 A Brief Overview of Peptides and Peptide Analogs

Peptides, which are relatively low-molecular weight polymers of amino acids (in contrast to high-molecular weight proteins), are present in most life forms. The amino acids are linked together by a covalent peptide bond between the carboxyl end of one amino acid and the α-amino end of another. Peptides play a key role in a diverse range of biological processes. Some examples of peptides found in the human body are enkephalins, bradykinin, vasopressin, oxytocin, and glutathione. Enkephalins are pentapeptides whose primary function is pain control; they lessen pain sensitivity by binding to receptors in certain brain cells.[1.1-1.2] Bradykinin, vasopressin, and oxytocin are peptide (nonapeptides) hormones that inhibit tissue inflammation, control blood pressure, and induce labor in pregnant women, respectively.[1.1] Glutathione is a tripeptide that destroys harmful oxidizing agents in the body.[1.1,1.3]

Unfortunately, peptides and proteins also play a pivotal role in many chronic and infectious diseases.[1.4-1.8] Insulin-dependent diabetes is a disease that is believed to be caused by otherwise innocent viral peptides.[1.4] They mimic peptides found in the human body and stimulate the immune system to attack these self-peptides.[1.4-1.5] Rheumatoid arthritis[1.6] and multiple sclerosis[1.7] are other autoimmune diseases where self-peptides are erroneously seen as foreign species. Furthermore, the aberrant functioning of proteases, which are an important class of enzymes that play key roles in a wide variety of biological processes, often lead to physical and mental ailments.[1.8]

Molecular recognition of a peptide by a macromolecular receptor is crucial to the processes or disorders mentioned above.[1.4-1.9] Therefore, peptides themselves seem to be the first obvious candidates to interfere with this action. However, it is often not advantageous to use peptides in drug therapy. In general, peptides have poor pharmacokinetic properties that limit their use as drugs. If given orally, they are prone to degradation by proteases in the stomach as well as poor absorption in the intestinal system.[1.10] Even if peptides are given intravenously, their activity is often short-lived because proteolytic enzymes in the blood and in other tissues rapidly degrade them.[1.11] The disadvantages of peptide drugs have stimulated an intense quest for peptide analogs.[1.12-1.15]

A peptide analog or a peptidomimetic is a compound that mimics the critical features (e.g., shape and functionality) of a parent peptide.[1.16-1.17] Peptidomimetics are often designed to be more stable and sometimes more active than peptides. For example, increased proteolytic stability can be achieved by replacing the amide bond by alkene bonds (as seen in a vinylogous peptide)[1.18] or placing the amino acid side-chain on the nitrogen atom (as seen in a peptoid).[1.19] It is also desirable for peptide analogs to have high-yielding coupling steps that are amenable to automation, which could lead to faster exploration of the space of chemical diversity for compounds with the desired properties.[1.11-1.12] Presented in Figure 1.1 are examples of several classes of peptide analogs; phosphonopeptides and α,α-dialkylated peptides are the foci of this dissertation. The general design of both of these peptide mimetics also allows for increased proteolytic stability as well as some bioactivity.

1.2 Importance of Phosphonopeptides

Phosphonopeptides (organophosphorus V derivatives) are a significant, stable class of biologically active peptide mimics.[1.20-1.21] In phosphonopeptides, as seen in Figure 1.1, the scissile peptide linkage is replaced with a tetrahedral phosphorus ester or

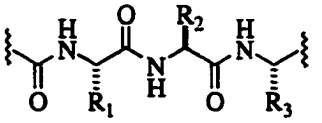

Peptide

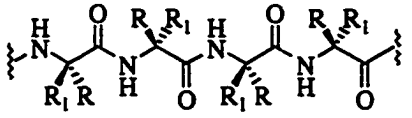

α,α–disubstituted amino acid-rich peptide

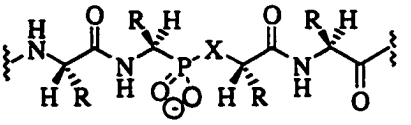

phosphono-peptide, X = O, NH

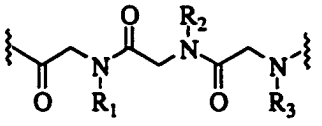

Peptoid [Oligo (N-substituted glycine)]

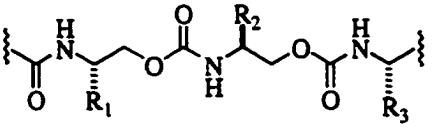

Oligocarbamate

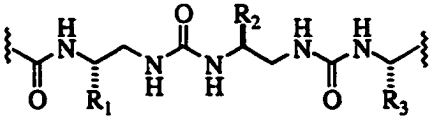

Oligourea

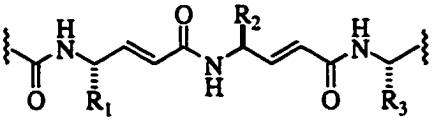

Vinylogous peptide

Figure 1.1 Classes of peptide analogs

amide moiety group. They emulate high-energy tetrahedral transition states that are common to many enzyme-catalyzed peptide hydrolysis reactions; hence, they are useful in the elucidation of enzyme mechanisms and as enzyme inhibitors.[1.22] Such transition-state analogs have been employed as effective inhibitors of serine (e.g., chymotrypsin and

human leukocyte elastase),[1.23-1.24] metallo (e.g., carboxypeptidase A and angiotensin-converting enzyme),[1.25-1.26] and aspartyl (e.g., pencillopepsin and HIV proteases),[1.15,1.27] proteases (Figure 1.2). Scheme 1.1 is an example of a metallo-protease catalyzing the hydrolysis of an amide bond in a model peptide or protein; the high-energy tetrahedral intermediate is bound more tightly than the substrate.[1.28-1.29] The inhibition of the metallo-protease by a model phosphonopeptide is also shown in Scheme 1.1; good potential inhibitors of the enzyme will bind more tightly than the substrates.[1.29]

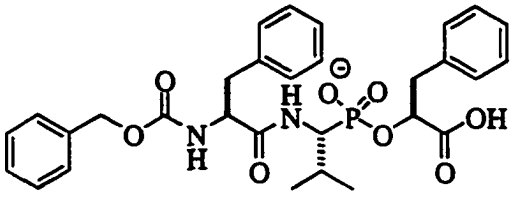

Z-Phe-Val ψ [(PO_2^-) O] Phe-OH
competitive inhibitor of
carboxypeptidase (Zn^{2+} protease)

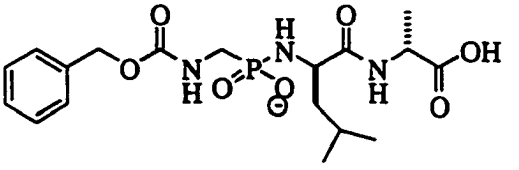

Z-Gly ψ [(PO_2^-)NH] Leu-Ala-OH
competitive inhibitor of
thermolysin (Zn^{2+} protease)

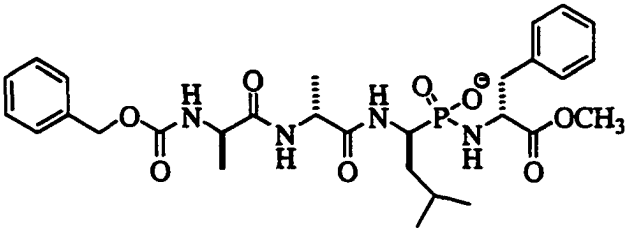

Z-Ala-Ala-Leu ψ [(PO_2^-) O] Phe-OCH_3
competitive inhibitor of
pencillopepsin (aspartyl protease)

Figure 1.2 Phosphonopeptide enzyme inhibitors

Several phosphonopeptides have also shown powerful antibacterial activity.[1.30-1.32] Allen et al. reported the design and synthesis of the first phosphono-based antibacterial agent, alafosfalin.[1.30] Several phosphonopeptide derivatives, based on alafosfalin, have since been reported.[1.32] They have been shown to have activity against several bacterial

species such as *Escherichia coli*, *Staphylococcus aureus*, *Bacillus subtilis*, and *Serratia marcescens*.[1.32]

More recently, phosphonopeptides have been applied to hapten design for generation of catalytic antibodies that possess peptide ligase activity.[1.33] It is possible to generate antibodies with enzymatic activity by choosing haptens that are analogous to the transition state of the substrate for a chemical reaction.[1.33-1.34] When a transition-state analogue is employed as a hapten, it induces an array of different antibodies that bind the hapten specifically.[1.34] Hirschmann et al. reported the antibody-catalyzed formation of a dipeptide; a phosphonate diester hapten was employed (Scheme 1.2).[1.33]

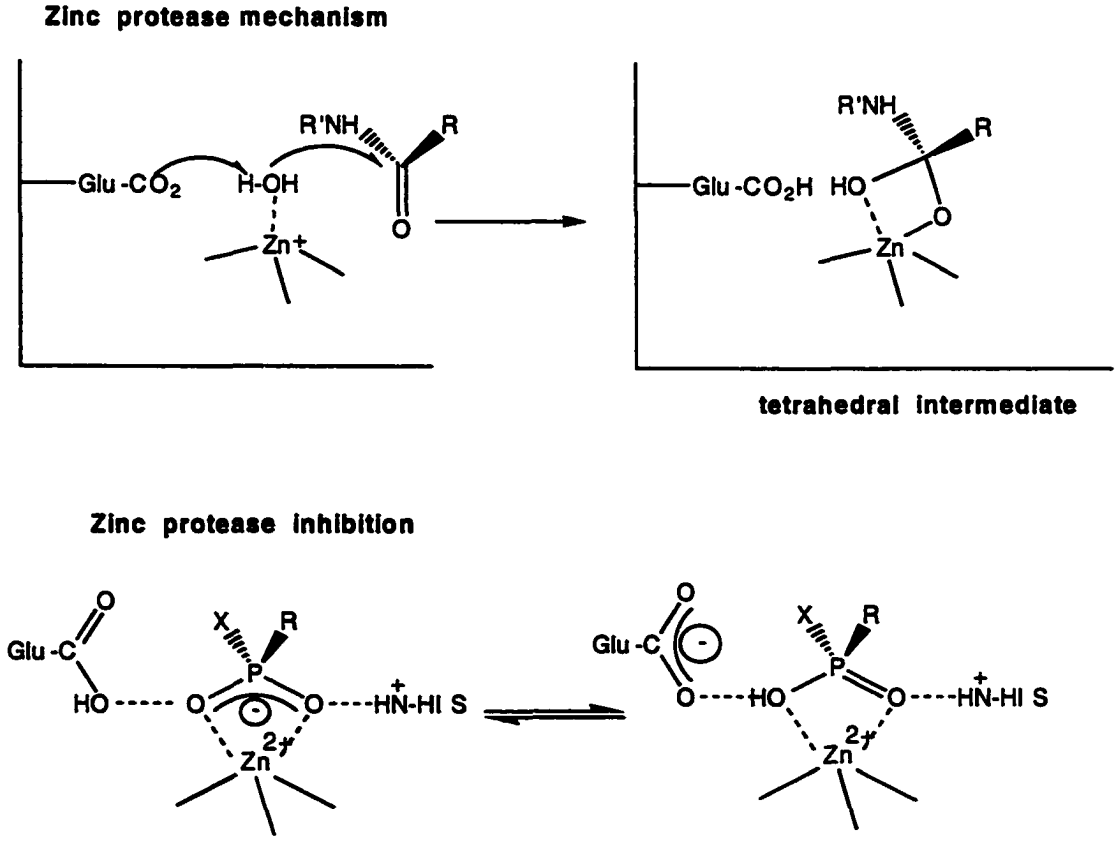

Scheme 1.1 Enzyme-catalyzed peptide hydrolysis (top) and enzyme inhibition (bottom)

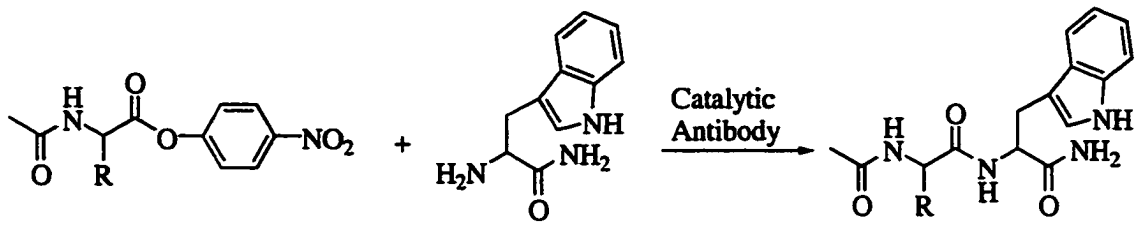

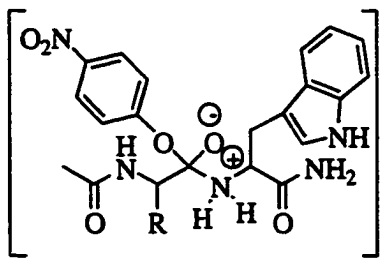

Proposed intermediate

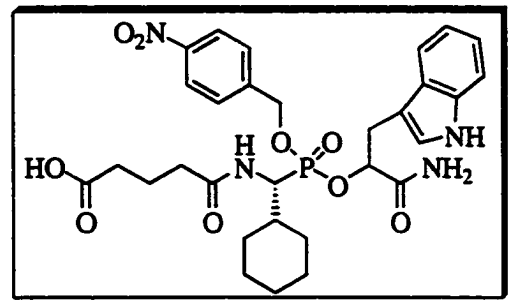

Hapten used to generate catalytic antibody

Scheme 1.2 Peptide synthesis catalyzed by an antibody

1.3 Synthetic Strategies for Phosphonate Esters and Amides

Generally, phosphonate and phosphonamide peptide analogs are prepared by coupling a phosphonochloridate (P (V) compound) with an alcohol or amine nucleophile, respectively (Scheme 1.3). Phosphonochloridates, for this purpose, have been obtained by the reaction of phosphonate diesters with phosphorus pentachloride,[1.35-1.37] by the treatment of phosphonate monoesters with thionyl chloride or oxalyl chloride,[1.15,1.28,1.38] and by oxidative activation of H-phosphinate esters with carbon tetrachloride.[1.39] These reactions, phosphonochloridates with alcohol or amine nucleophiles, are usually sluggish and low to moderate yielding, which are due, to some extent, to the slow nucleophilic attack on the phosphorus (V) center.[1.40] Moreover, for the amine nucleophiles, the amount of HCl that is produced in the reaction mixtures often interferes with the desired coupling process, even if excess base (e.g., Et_3N) is employed.[1.39]

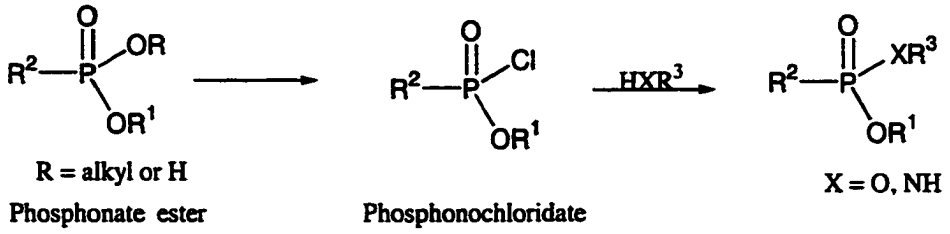

Scheme 1.3 Preparation of a phosphonopeptide via an activated P(V) species

Improved synthetic methods for preparing phosphonate diesters have been reported. Moderate to high and reproducible yields of diesters have been obtained under mild conditions with a modified Mitsunobu protocol in which the alcohol was the limiting reagent-for possible solid-phase synthetic application-and the modifications included an exogenous base and electron deficient phosphines.[1.41] Also, BOP-mediated activation of phosphonate monoesters is an efficient, racemization-free route for preparing phosphonate diesters; this procedure is complementary to Campbell's Mitsunobu methodology.[1.42]

Phosphonamides are, in general, more difficult to prepare than phosphonate diesters. Nevertheless, Moroder and coworkers[1.43] made significant improvements in the synthesis of phosphonamidate peptides. They optimized the preparation of phosphonochloridates with oxalyl chloride in the presence of catalytic amounts of DMF, which were then either employed under AgCN catalysis or converted into the 7-aza-1-hydroxybenzotriazole ester for phosphonamide bond formation. However, long reaction times (≈14 hrs.) and moderate yields (for some of the desired compounds) were still observed.[1.43] Besides their suggested acid-lability,[1.22,1.36-1.37] phosphonamidates' poor synthetic accessibility is severely limiting the use of this interesting class of compounds as tools in enzyme chemistry.[1.43]

Hirschmann and co-workers attempted the preparation of the phosphonamide hapten precursor (X = NH) in Scheme 1.4.[1.33-1.34] Unfortunately, their earnest attempts to couple D-tryptophanamide with the phosphonochloridate failed to yield the expected phosphonamide even in the presence of AgCN (catalyst). Furthermore, efforts made to try to couple the phosphonate monoester with D-tryptophanamide using several different kinds of condensing agents such as diphenyl phosphorylazide and BOP reagents were unsuccessful. Nevertheless, they were able to couple, under AgCN catalysis, the phosphonochloridate with (R)-(+)-β-indolyllactamide to obtain the phosphonate diester in yields that were initially variable (0-32%).[1.44] Preparation of the phosphonate diester in a reproducible 40 % yield was later achieved by converting the phosphonochloridate into a phosphonyltriethylammonium salt prior to the addition of AgCN and (R)-(+)-β-indolyllactamide (Scheme 1.5). The phosphonate diester was subsequently converted into a hapten, which was used to induce antibodies that possess peptide ligase activity.[1.33] However, the synthesis of the phosphonamide hapten precursor remained elusive.

1.4 Phosphorus (III) Synthetic Approach

The synthesis of phosphonate esters and amides from H-phosphinates by a novel one-pot activation-coupling-oxidation/sulfurization protocol was developed in Hammer's laboratory.[1.45] In this approach phosphonochloridites, activated P(III) species, were used in the key coupling step instead of phosphonochloridates, P(V) compounds (Scheme 1.6). Since nucleophilic displacement is much faster at a P(III) center than at a P(V) center,[1.40] this new synthetic approach has the potential of increasing the yield and efficacy of production of phosphonopeptides. This P(III) approach also permits facile design and

preparation of phosphonates with a variety of heteroatoms around the phosphorus center (e.g., X = NR, Y = O, Z = S or X = O, Y = S, Z = S) (Scheme 1.6).[1.45]

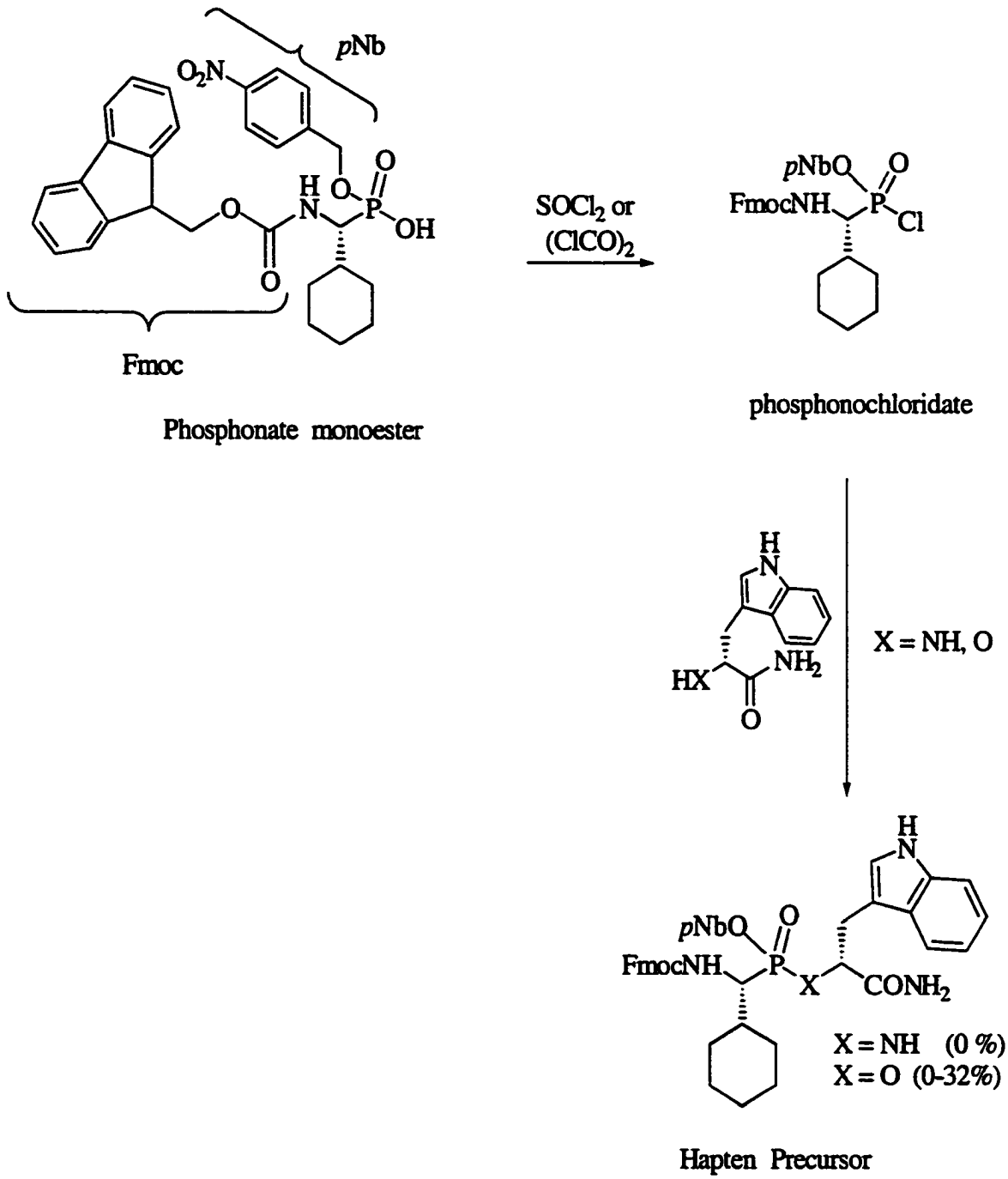

Scheme 1.4 Synthesis of hapten precursor via P(V) coupling method

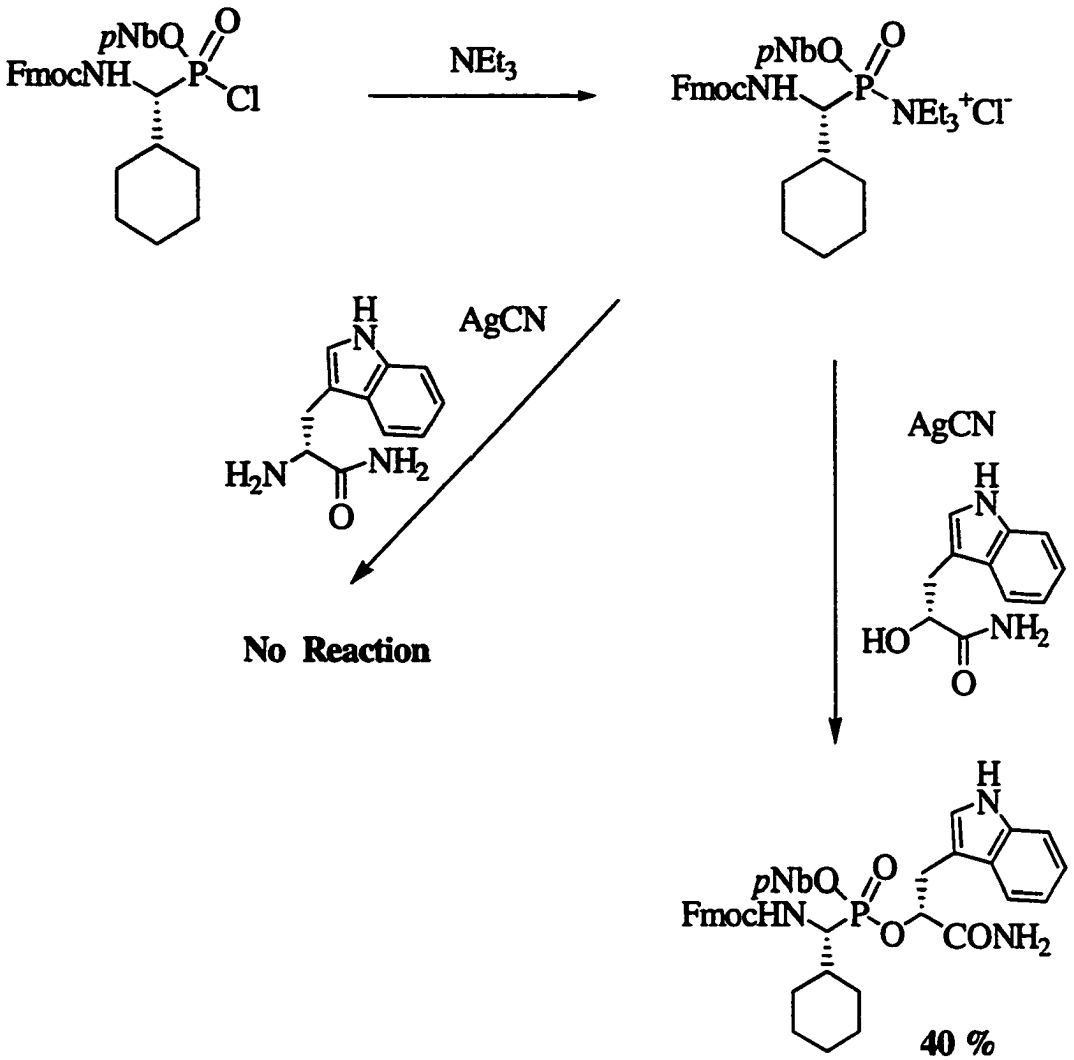

Scheme 1.5 Modified P(V) approach for attempted synthesis of hapten precursors

Because of their air-stability, the H-phosphinates were envisioned as the ideal precursors to the P(III)-based phosphonate synthesis. They could be easily converted to the P(III) species with the commercially available dichlorotriphenylphosphorane (Ph_3PCl_2). Following activation, the phosphonochloridite could be coupled, in the presence of base, to an amine or alcohol nucleophile and then oxidized or sulfurized. Using this protocol, Fernandez and co-workers were able to prepare about 12 dipeptide model compounds in moderate to good yields.[1,45]

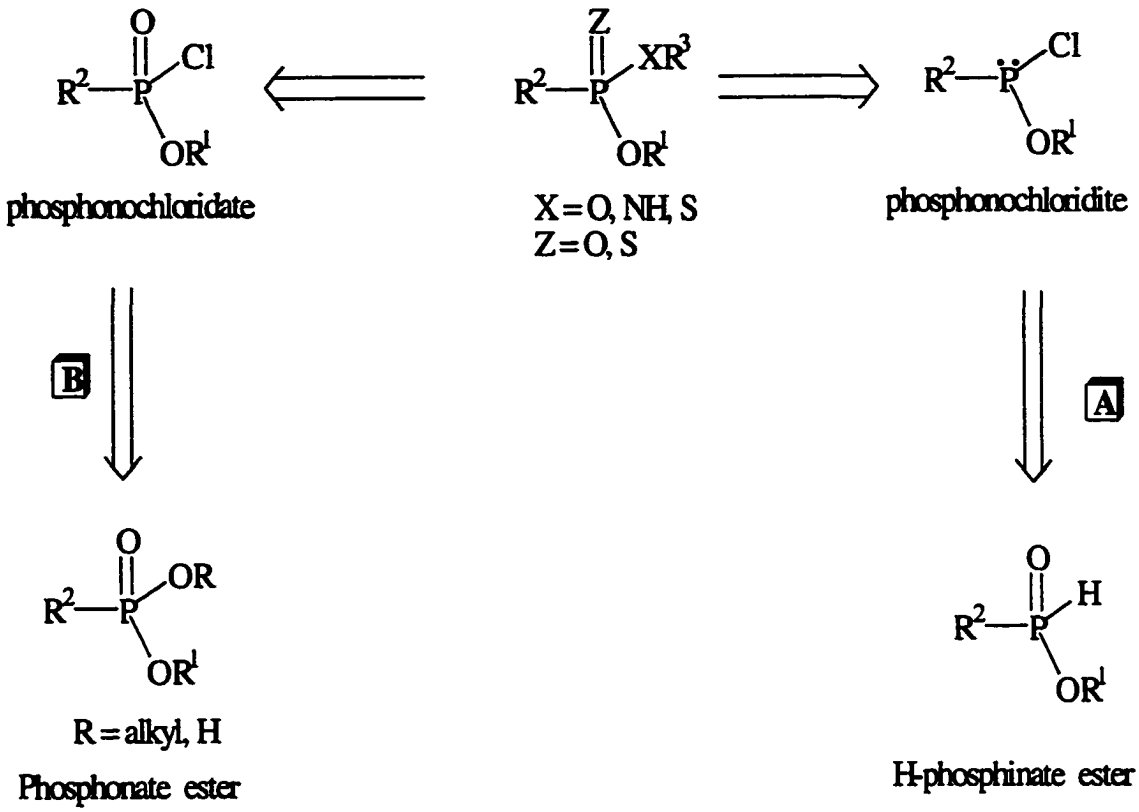

Scheme 1.6 Retrosynthetic analysis of phosphonopeptides

The goal of this part of the research was to develop general conditions, employing the P(III)-based protocol, for preparation of the phosphonamide hapten precursor[1.44] (described by Hirschmann and coworkers) and related sterically-hindered phosphonamide and thiophosphonamide derivatives. Since the P(III) strategy was successful for preparation of dipeptide model systems, it was employed to try to increase the yield and efficacy of production of our target phosphonodipeptides, which exemplify the difficulties many laboratories have encountered in preparing phosphonamidate peptides.[1.33,1.17,1.46] We hoped that optimization of this protocol would result in a facile, general method (solution- or solid-phase) for preparing simple or complex phosphonopeptides so that they may be readily available for biological and medicinal applications.

1.5 Peptide Secondary Structure

The amino acid sequence of a peptide or protein is termed its primary structure; however, the local conformation or regular folding pattern of its backbone defines its secondary structure.[1.47] The pair of conformational angles, phi (ϕ) and psi (ψ), of each amino acid determines the conformation of the main chain of a protein (Figure 1.3).[1.48]

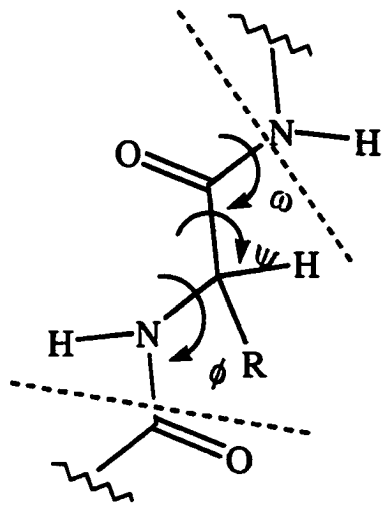

Figure 1.3 Torsional angles of a peptide backbone

The most common secondary structural elements found in proteins are the α-helix, β-pleated sheet, and turns or bends.[1.47] The α-helix and β-pleated sheet are periodic structures; they possess hydrogen-bonding patterns (main chain NH and C'O groups) that repeat at regular intervals.[1.47-1.48] The α-helix is rodlike and involves only one continuous peptide chain, but the β-pleated sheet, which can form a two-dimensional array, can include one or more polypeptide chains.[1.47-1.48] Besides hydrogen-bonding, the α-helix and β-pleated sheet are generally stabilized by hydrophobic effects, Van der Waals forces, and electrostatic forces.[1.49-1.51] The turns in a protein are the stretches or bends where the polypeptide chain abruptly changes direction; they often occur at the surface of

proteins.[1.47,1.50] Furthermore, incorporation of turns also allows α-helices and β- sheets to be folded back onto themselves.[1.50] Some polypeptides assume a random coil conformation, which is a non-repetitive structure that is flexible and statistically random.[1.47] Random coils, however, can form reproducibly in a peptide chain.[1.51]

The α-helix is the most prevalent helical structure found in proteins.[1.48-1.51] The consecutive residues in an α-helix all have the phi, psi angle pair at approximately -60° and -50°.[1.48] In the α-helix there are 3.6 residues per turn with hydrogen bonds between the carbonyl oxygen of residue *i* and the amide proton of residue *i* + 4, forming a 13-membered ring (Figure 1.4).[1.50-1.51] The rise per residue of an α-helix is 1.5 Å along the helical axis, which corresponds to a rise of 5.4 Å per turn.[1.48] Theoretically, an α-helix can be either right-handed or left-handed depending on the screw direction of the chain. However, right-handed α-helices, which are promoted by L amino acids, are almost always observed in proteins.[1.48,1.50-1.51] A left-handed α-helix is not allowed for L amino acids due to the proximity of the side chains and the carbonyl group.[1.48]

The 3_{10}-helix, though less common than the α-helix, accounts for approximately 10 % of helical structures in proteins.[1.52-1.53] The phi, psi angle pair for consecutive residues in a 3_{10}-helix is approximately -30° and -50°.[1.54] In 3_{10}-helices there are 3 residues per turn with hydrogen bonds between the carbonyl oxygen of residue *i* and amide proton of residue *i* + 3, forming a 10-membered ring (Figure 1.4).[1.53-1.54] The rise per turn in a 3_{10}-helix is 5.8 Å, which corresponds to a rise of 1.94 Å per residue. A 3_{10}-helix is therefore slightly longer and tighter than an α-helix.[1.54]

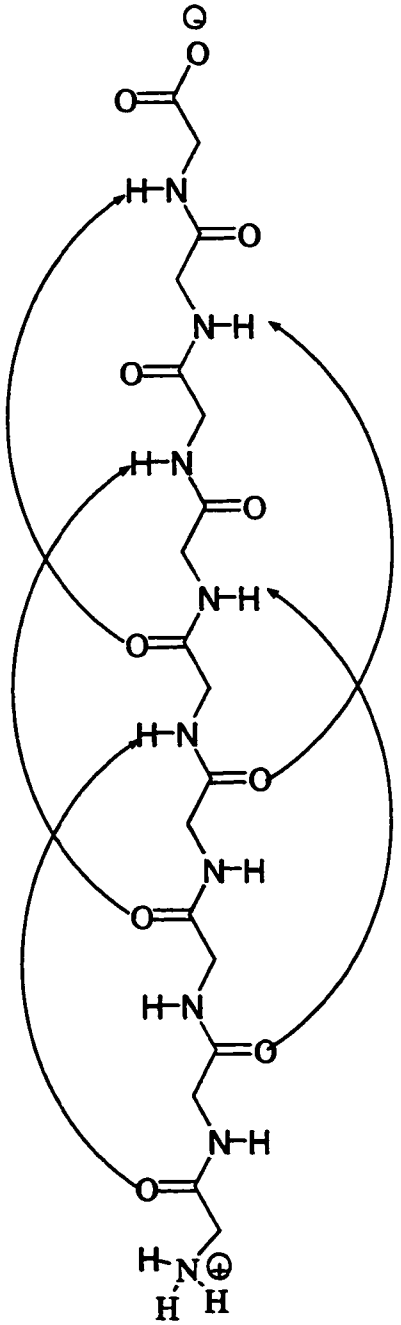

α-helix

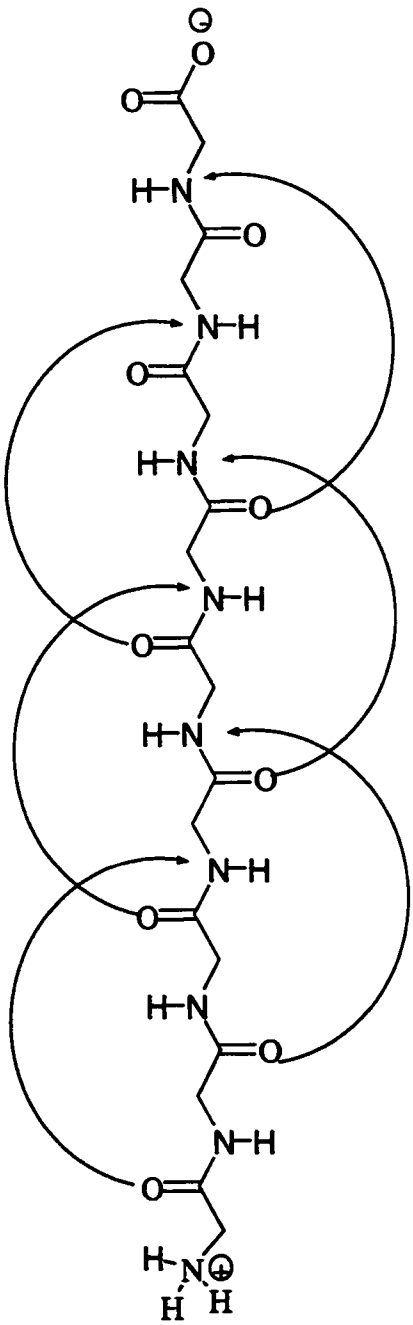

3_{10}-helix

Figure 1.4 Hydrogen bonding pattern of an α-helix and 3_{10}-helix.

1.6 Amphipathic α-Helix

In an amphipathic helix one face, along the helix axis, is hydrophilic while the opposite face is hydrophobic.[1.48] The "Schiffer-Edmundson" helical wheel projection (two-dimensional) shown in Figure 1.5 is a convenient way to illustrate the amino acid sequence of an amphipathic α-helix. In the diagram, P represents the polar residues of the hydrophilic face, and N represents the non-polar residues of the hydrophobic face. The helical wheel is shown as if looking down the helix axis from the C-terminus to the N-terminus. Since one turn in an α-helix is 3.6 residues long, each amino acid can be plotted every 360/3.6 = 100° around a circle.[1.48] The structural arrangement of amphipathic α-helices allows them to develop a barrier between non-polar regions of a macromolecule or molecular assembly and a polar environment.[1.55] It also provides a means for protein-protein interactions via hydrophobic interactions between two amphipathic helices on different peptide chains.[1.55]

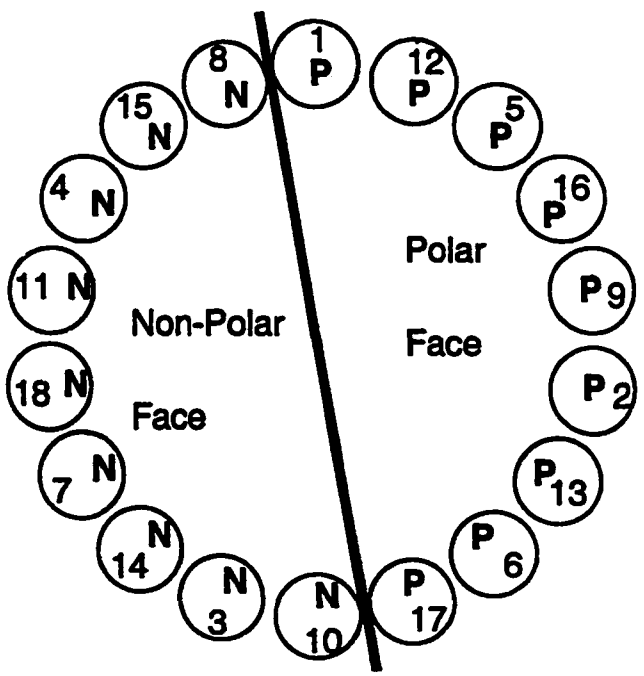

Figure 1.5 Helical wheel diagram of an amphipathic α-helix.

Amphipathic α-helices comprise about 50 % of the α-helices found in soluble globular proteins.[1.56-1.57] They are also found in fibrous proteins like myosin and tropomyosin, DNA-binding proteins, and smaller polypeptides such as hormones and venom.[1.57] Furthermore, amphipathic peptides are exploited as part of the host defense system of many organisms, ranging from prokaryotes to humans.[1.57-1.58] These antimicrobial peptides kill bacteria and other microbes presumably by disrupting the cell membrane.[1.57] Several studies have indicated that the amphipathic character of antimicrobial peptides plays a significant role in their biological activity.[1.57,1.59] In addition, even short, de novo peptides (10-16 residues of varying sequences) containing the amphipathic α-helix as the only consistent structural feature were shown to have comparable antimicrobial activities as longer or native peptides; they also tended to exhibit a higher degree of selectivity of bacterial killing over normal mammalian cells.[1.59]

Many naturally occurring antimicrobial peptides of broadly varying sequence have been isolated with amphipathic helical domains as a consistent structural feature.[1.59-1.60] Antimicrobial peptides usually contain approximately equal numbers of polar and non-polar amino acids within the amphipathic domains and a sufficient number of basic residues to provide the peptide an overall positive charge at physiological pH.[1.59] Some antimicrobial peptides display excellent selectivity in destroying bacteria over mammalian cells.[1.59] This selectivity has been ascribed to differences in the cell membranes of bacteria and mammals. Bacteria exterior membranes are negatively charged, but the exterior membranes of mammalian cells are essentially neutral. As stated previously, antimicrobial peptides have an overall positive charge; they might therefore preferentially bind to bacteria over mammalian cells. The cholesterol in the cell

membranes of mammals, which could possibly inhibit membrane disruption by antimicrobial peptides, and the lower membrane potential across mammalian cells have also been suggested as bases for selectivity of antimicrobial peptides.[1.59,1.61]

Some examples of natural antimicrobial peptides are melittin, cecropin A, magainin 2, and alamethicin.[1.62-1.63] Melittin, an amphipathic peptide composed of 26 residues, is extracted from the honey bee, *Apis mellifera*.[1.62] Melittin is positively charged (+ 6); its hydrophobic surface is more extensive than its narrower polar face. It exhibits broad spectrum antimicrobial activity at micromolar concentrations, but it is very cytotoxic.[1.59,1.62] Cecropin A is a 37-residue antimicrobial peptide isolated from the North American silk moth, *Hyalophora cecropia*. It contains two α-helical regions extending from residues 5 to 21 (amphipathic region) and 24-37 (largely hydrophobic) with the two helical regions lying in two planes that form an angle of 70° to 100°.[1.62] Cecropin A displays excellent antimicrobial activity at concentrations that are not cytotoxic toward mammalian cells.[1.59,1.62] Magainin 2 is a 23-residue antimicrobial peptide isolated from the skin of the frog, *Xenopus laevis*. Magainin 2, like Cecropin A, exhibits broad spectrum antimicrobial activity at concentrations not cytotoxic toward mammalian cells.[1.62] Furthermore, both Cecropin A and Magainin 2 are unstructured in aqueous solution but become α-helical in amphipathic media such as cell membranes and micelles. Alamethicin is 20-residue linear peptide of the fungus, *Trichoderma viride*.[1.54,1.63] It is a member of the peptaibol class of natural antiobiotics, but it is very toxic. It is characterized by an acetylated N-termini, a C-terminal alcohol (phenylalaninol), and a high percentage of α-aminoisobutyric acid (Aib) residues. It is

noteworthy that the short peptide, Alamethicin, is highly helical due to the presence of the high number (7) of Aib residues.[1.54,1.63]

1.7 Significance of α, α-Dialkylated Amino Acids in Short Peptides

The occurrence of Aib-rich sequences in natural peptide antibiotics and membrance-channel forming polypeptides has led to an upsurge of interest in the design and synthesis of short, Aib-rich peptides with predictive secondary structure.[1.64-1.69] Peptides containing Aib tend to favor a helical conformation. Although several proteinogenic amino acids are known for promoting helicity in proteins or peptides, the α, α-dialkylated amino acid, Aib, is rather unique because it effectively confers high helicity on short synthetic peptides of length 8-10, which is half the length required of most other sequences.[1.67] The allowable phi, psi angle pair for Aib occur in two very restricted regions, located in the area of (-57°, -47°) and (57°, 47°). These two regions correspond to a right-handed α- or 3_{10}-helix and a left-handed α- or 3_{10}-helix, respectively.[1.64,1.66] Since the Aib residue is achiral, either the L- or D- configuration is equally possible. Chiral residues that have the L- or D- configuration therefore determine the handedness of a helix comprised of Aib residues in the sequence.[1.64]

Backbone conformations of Aib-rich peptides may display a 3_{10}-, α-, or mixed 3_{10}-/α-helical pattern depending upon critical factors such as peptide length, Aib fraction, and amino acid sequence.[1.64-1.65] Karle and Balaram[1.64] compiled general conformational trends observed for 33 Aib-containing peptides (6-20 residues) in the crystalline state. The authors suggested from their study that, in general, a 3_{10}-helical structure is preferred for shorter peptides and an α-helical structure for longer peptides. A medium length of 8-10 was considered to be the 3_{10}/α transition length for peptides possessing 50 % Aib.

Peptides of a shorter length favor the 3_{10}-helix while longer ones favor the α-helix. Also, the study indicated that a large percent (> 50%) of Aib residues in a peptide induces a 3_{10}-helix. Similar findings were also found in other studies conducted on the crystal structure of various peptides containing many Aib residues.[1.64] Basu et al. reported that the amino acid sequence also affected the 3_{10}/α-helix equilibrium. Their study suggested that the α-helix is favored when two monosubstituted amino acids are next to each other, but the 3_{10}-helix, when no two monosubstituted amino acids are next to each other.[1.65]

Studies have also been investigated on the effect of the solvent on the 3_{10}/α-helix equilibrium of Aib-rich peptides. Several investigations (theoretical and empirical) suggested that solvents with low dielectric constant favor 3_{10}-helical structures, whereas solvents with high dielectric constant are inclined to favor α-helical structures.[1.64,1.67,1.69-1.72] Until recently, these studies were limited to spectroscopic measurements of hydrophobic peptides (e.g., oligomers of Aib) in organic solvents like chloroform and dimethylsulfoxide or X-ray structure determinations of peptides crystallized from organic solvents.[1.67,1.70] Yokum et al.[1.72] reported the design and synthesis of short, amphipathic α- and 3_{10}-helices that exhibited their designed structures in an aqueous, membrane-like media (25 mM SDS); their peptides contained 60% Aib content and the water-solubilizing α, α-disubstituted amino acid, 4-aminopiperidine-4-carboxylic acid (Api). They also reported that amphipathic design was primary in controlling the secondary structure (helical preference), overriding traditional key factors such as the number of α, α-amino acids (ααAA) and the order of the α-amino acids and ααAA in a sequence. Toniolo et al. reported the first pure-water-soluble 3_{10}-helical peptides, which were comprised mainly of ααAAs and the extremely water-solubilizing, azacrown-

functionalized α-amino acid, L-2-amino-3[1-(1,4,7-triazacyclononane)]propanoic (ATANP).[1.69,1.71]

1.8 Synthesis of Short, Helical Peptides

The incorporation of ααAAs into short *de novo* peptides promotes helical peptide structures and increases the peptides resistance to enzymatic hydrolysis,[1.73] but, until recently, the preparation of the peptides, especially peptides with sequential ααAAs, has proven to be a very difficult task.[1.74] The ααAA couplings are inherently more difficult because of the significantly greater steric bulk caused by the additional substituent on the α-carbon. The use of carbodiimides (e.g. dicyclohexyl carbodiimide (DCC) and diisopropyl carbodiimide (DIC)), which are traditional amino acid coupling agents, results in unsatisfactory yields for ααAA couplings.[1.75] Even longer reaction times or the use of additives such as 1-hydroxybenzotriazole (HOBt) rarely result in good yields for the carbodiimide-mediated ααAA couplings. Employing first-generation uranium salts (e.g., *O*-(benzotriazol-1-yl)-1,1,3,3-tetramethyluronium hexafluorophosphate (HBTU)) and phosphonium salts (e.g., benzotriazol-1-yloxy-tris(dimethylamine) phosphonium hexafluorophosphate (BOP)) along with extended reaction times or application of heat also usually yielded only moderate results for ααAA couplings.[1.72,1.76]

Alternate coupling protocols or reagents have been employed in an attempt to improve the unsatisfactory results often observed in ααAA couplings. Some of the methods or reagents employed are the following: fluorenylmethyloxycarbonyl-*N*-carboxyanhydrides (Fmoc-NCAs), azirine method (e.g., 2-(dimethylamino) 3,3-dimethyl-azirine), and acid chlorides. All of these methods have the potential of producing improved synthetic results for ααAA couplings, but their use have been limited because

of specific drawbacks. The use of Fmoc-NCAs often result in side-product formation and moderate to low yields.[1.76] The azirine method is limited because of the post coupling acid hydrolysis, which is detrimental to peptides containing acid labile protecting groups, often required for the resulting C-terminal amide.[1.65] The use of acid chlorides is very effective for coupling ααAAs, but the harsh, acidic conditions employed for the formation of acid chlorides also often limit them to amino acids containing no acid labile protecting groups.[1.77] Also, the formation of oxazalones, which could lead to racemization, is often associated with acid chlorides. Overall, none of these alternate or traditional methods are capable of producing sequential ααAA couplings in high yields under general, mild conditions, such as that required for high-purity sequences in solid-phase peptide synthesis (SPPS).[1.54]

New and improved methods have been developed for efficient coupling of sequential ααAAs. Carpino's acid fluoride coupling was the first method to give high yield couplings of sequential ααAAs under mild conditions both in solution and solid phase.[1.77-1.78] In contrast to acid chlorides, a wide range of protection schemes can be employed with the mild, acid fluoride method. An Acid fluoride synthesis is usually accomplished by coupling a preformed amino acid fluoride (4 equivalents) with the free amine of an amino acid in the presence of 2 equivalents of base like *N,N*-diisopropylethylamine (DIEA). Acid fluoride itself is prepared by treating an amine-protected amino acid with cyanuric fluoride (2 equivalent) and pyridine (1 equivalent).[1.79] In addition, a method for the *in situ* generation of an amino acid fluoride with tetramethylfluoroformamidinium hexafluorophosphate (TFFH) and subsequent coupling conditions has been developed; good, comparable results have been observed.[1.80]

More recently, uronium salts based on 1-hydroxy-7-azabenzotriazole (HOAt) such as {*N*-[(dimethylamino)-1H-1,2,3-triazolo[4,5-b]pyridin-1-ylmethylene]-N-methyl-methanaminium hexafluorophosphate *N*-oxide (HATU) have exhibited significant advantages for the coupling of sterically hindered amino acids in terms of improved coupling yields and acylation rates and decreased racemization.[1.81-1.82] Also, the phosphonium-based analog of HATU, 7-azabenzotriazol-1-yloxytris(pyrrolidino)phosphonium hexa-fluorophosphate (PyAOP) have also been reported to be very useful for the solid-phase preparation of peptides incorporating hindered amino acids.[1.83] Overall, both the second generation uranium salt (HATU) and phosphonium salt (PyAOP) are excellent reagents for ααAA couplings. However, PyAOP, relative to HATU, is more advantageous because of the formation a less toxic side-product (phosphoramide) and because excess PyAOP (in contrast to HATU) doesn't participate in any chain-terminating side reactions at the amino terminus.[1.83]

1.9 Circular Dichroism Spectroscopy

Several methods such as X-ray crystallography, NMR, electron spin resonance, and circular dichroism (CD) spectroscopy have been employed in peptide secondary structure determination.[1.84] However, due to its convenience and reliability, CD has become the method of choice for identifying global peptide secondary structure.[1.85] CD spectroscopy is a technique that measures the difference in absorbance of right- and left-circularly polarized light by an asymmetric substance.[1.86] Peptide secondary structure can be determined by CD in the "far-UV" spectral region (180-250 nm); at these wavelengths the chromophore is the peptide bond.[1.85-1.87] As seen in Figure 1.6, the major categories of peptide conformations (random coil, β-sheet, and helices) are distinctly different.[1.88]

The random coil displays a minimum near 195 nm and a maximum near 217 nm, whereas the β-sheet is distinguished by a positive band around 195 nm and a negative band centered about 217 nm. Both 3_{10} and α-helical peptides give rise to negative CD bands around 222 nm ($n \rightarrow \pi^*$) and 207 nm ($\pi \rightarrow \pi^*$). A positive band around 191 nm ($\pi \rightarrow \pi^*$) is also characteristic of both types of helical peptides, although it is usually much weaker in 3_{10} helical peptides.[1.89] The ratio R of the intensity of the negative bands, where $R = [\theta]_{n \rightarrow \pi^*}/[\theta]_{\pi \rightarrow \pi^*}$, is a generally accepted parameter used to distinguish a 3_{10}-helix from an α-helix. For an α-helix $R \approx 1$, but for a 3_{10} helix $R \approx \leq 0.4$.[1.89]

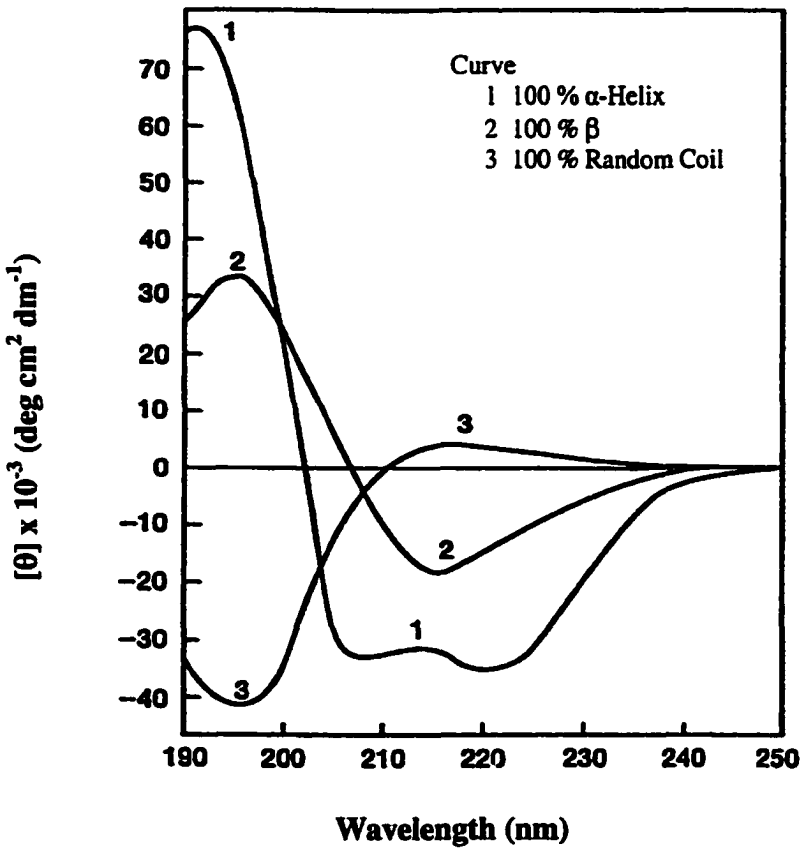

Figure 1.6 CD spectra of poly-L-lysine in the α-helical, β, and random conformations.

CD spectroscopy played an integral role in the general goal for this part of our research on peptide analogs. We were primarily interested in the design and efficient synthesis of

short, amphipathic 3_{10}-helical peptides that are able to retain good antimicrobial activity and low cytotoxicity. With CD, we could analyze the solvent (aqueous-organic) effects on the 3_{10}-/α- helix equilibrium on our designed, amphipathic 3_{10}-helical peptides, as well as correlate observed secondary structure in various media (e.g., SDS and pure water) with bioactivity.

1.10 References

1.1 Bruice, P. Y. In *Organic Chemistry*; 2nd ed.; Simon & Schuster: New Jersey, **1998**; pp. 927 - 928.

1.2 Campbell, M. K. In *Biochemistry*; 2nd ed.; Saunders College Publishing: Florida, **1995**; pp. 81 –82.

1.3 Zubay, G. L.; Parson, W. W.; Vance, D. E. In *Principles of Biochemistry*; 1st ed; William C. Brown Communications: Iowa, **1995**; pp. 526-528.

1.4 Wucherpfennig, K. W.; Strominger, J. L. *Cell* **1995**, 80, 695.

1.5 Barnett, L. A.; Fujinami, R.S. *FASEB J* **1992**, 6, 840.

1.6 Wendling, U.; Paul, L.; Van der Zee, R.; Prakhen, B.; Singh, M.; Van Eden, W. *J. Immunol.* **2000**, 164, 2711.

1.7 Trotter, J. L.; Damico, C. A.; Cross, A. H.; Pelfrey, C. M.; Karr, R.W.; Fu, X.T.; McFarland, H.F. *J. Neuroimmunol* **1997**, 75, 95.

1.8 Lee, K. J.; Kim, D. H. *Bioorg. Med. Chem.* **1998**, 6, 1613.

1.9 Wrighton, N. C.; Farrell, F. X.; Chang, R.; Kashyap, A. K.; Barbon, F.A.; Mulcalry, L. S.; Johnson, D. L.; Barrett, R. W.; Jollefe, L. K.; Dower, W.J. *Science* **1996**, 273, 5274.

1.10 Powel, M. F. In *Methods in Molecular Biology;* Shafer, W. M., Ed.; Humana Press: New Jersey, 1997; pp. 100-116.

1.11 Thompson, L. A.; Ellman, J. A.; *Chem. Rev.* **1996**, 96, 555.

1.12 Cho, C. Y.; Moran, E. J.; Cherry, S. R.; Stephans, J. C.; Fordor, S. P. A.; Adams, C. L. *Science* **1993**, 261, 1303.

1.13 Miller, S. M.; Simon, R. J.; Ng, S.; Zuckermann, R. N.; Kerr, J. M.; Moos, W. H. *Drug Dev. Res.* **1995**, 35, 20.

1.14 Moran, E. J.; Wilson, T. E.; Cho, C.Y.; Cherry, S.R.; Schulz, P. G. *Biopolymers (Pept. Sci.)* **1995**, 37, 213.

1.15 Ikeda, S.; Ashley, J. A.; Wirsching, P.; Janda, K. D. *J. Am. Chem. Soc.* **1992**, 114, 7604.

1.16 Smith, A. B.; Hirschmann, R.; Pasternak, A.; Guzman, M. C.; Yokoyama, A.; Sprengeler, P. A.; Darke, P. L.; Emini, E. A; Schleif, W. A. *J. Am. Chem. Soc.* **1995**, 117, 11113.

1.17 Mucha, A.; Kafarski, P. *Tetrahedron* **1994**, 50, 12743.

1.18 Hagihara, M.; Anthony, N. J.; Stout, T. J.; Clardy, J.; Schreiber, S. T. *J. Am. Chem. Soc.* **1992**, 114, 65.

1.19 Simon, R. J.; Kania, R. S.; Zuckerman, R. N.; Huebner, V. D.; Deutel, D.A.; Bamille, S.; Wang, L.; Roseburg, S.; Marlowe, C.K.; Spellmeyer, D. C.; Tan, R.; Erenkel, A. D.; Santi, D. V.; Cohen, F. F.; Bartlett, P. A. *Proc. Natl. Acad. Sci. U.S.A.* **1992**, 89, 9367.

1.20 Kaplan, A. P.; Bartlett, P. A. *Biochemistry* **1991**, 30, 8165.

1.21 Bertenshaw, S. R.; Rogers, R. S.; Stern, M. K.; Norman, B. H. *J. Med. Chem.* **1993**, 36, 173-176.

1.22 Jacobsen, N. E.; Bartlett, P. A. *J. Am. Chem. Soc.* **1981**, 103, 654.

1.23 Bartlett, P. A.; Lamden, L. A. *Bioorg. Chem.* **1986**, 14, 356.

1.24 Sampson, N. S.; Bartlett, P. A. *Biochemistry*, **1991**, 30, 2255.

1.25 Giannousis, P. P.; Bartlett, P. A. *J. Med. Chem.* **1987**, 26, 1603.

1.26 Barelli, H.; Dive, V.; Yiotakis, A.; Vincent, J. P.; Checler, F. *Biochem. J.* **1992**, 287, 621.

1.27 Bartlett, P. A., Hanson, J. E., Giannousis, P. P. *J. Org. Chem.* **1990**, 55, 6268.

1.28 Bartlett, P. A.; Hanson, J. E.; Giannousis, P. P. *J. Org. Chem.* **1990**, 55, 6268

1.29 Radkiewicz, J. L.; McAllister, M. A.; Goldstein, E.; Houk, K. N. *J. Org. Chem.* **1998**, 63 1419.

1.30 Allen, J. G.; Atherton, F. R.; Hall, M. J.; Hassall, C. H.; Holmes, S. W.; Lambert, R. W.; Nisbet, L. J.; Ringrose, P. S. *Nature* **1978**, 272, 56.

1.31 Kametani, T.; Kisagawa, K.; Hiiragi, M.; Wakisaka, G.; Haga, S.; Sugi, H.; Tanigawa, K.; Suzuki, Y.; Fukawa, K.; Irino, O.; Saito, O; Yamabe, S. *Heterocycles*, **1981**, 16, 1205.

1.32 Lejczak, B.; Kafarski, P.; Sztajer, H.; Mastalerz, P. *J. Med. Chem.* **1986**, 29, 2212.

1.33 Hirschmann, R.; Smith, A. B., III; Taylor, C. M.; Benkovic, P. A.; Taylor, S. D.; Yager, K. M.; Sprengeler, P. A.; Benkovic, S. J. *Science* **1994**, 265, 234.

1.34 Branden, C.; Tooze, J. In *Introduction to Protein Structure*; Garland Publishing: New York, 1991; p 189.

1.35 Dive, V.; Viotakis, A.; Nicolaou, A.; Toma, F. *Eur. J. Biochem.* **1990**, 190, 685.

1.36 Thorsett, E. D.; Harris, E. E.; Peterson, E. R.; Greenlee, W. J.; Patchett, A. A.; Ulm, E. H.; Vassil, T. C. *Proc. Natl. Acad. Sci. U.S.A.* **1982**, 79, 2176.

1.37 Elliot, R. L.; Marks, N.; Berg, M. J.; Portoghese, P. S. *J. Med. Chem.* **1985**, 28, 1208.

1.38 Malachewski, W. P.; Coward, J. K. *J. Org. Chem.* **1994**, 59, 7625.

1.39 Sampson, N. S., Bartlett, P. A. *J. Org. Chem.* **1988**, 53, 4500.

1.40 Letsinger, R. L.; Lunsford, W. B. *J. Am. Chem. Soc.* **1976**, 98, 3655.

1.41 Campbell, D. A.; Bermak, J. C. *J. Org. Chem.* **1994**, 59, 658.

1.42 Campagne, J.; Coste, J.; Jouin, P. *Tetrahedron Lett.* **1993**, 34, 6743.

1.43 Musiol, H. J.; Grams, F.; Rudolph-Bohner, S.; Moroder, L. *J. Org. Chem.* **1994**, 59, 6144.

1.44 Hirschmann, R.; Yager, K. M.; Taylor, C. M.; Witherington, J.; Sprengeler, P. A.; Phillips, B. W.; Moore, W.; Smith, A. B., III. *J. Am. Chem. Soc.* **1997**, 119, 8177.

1.45 Fernandez, M. d. F.; Vlaar, C. P.; Fan, H.; Liu, Y.-H.; Fronczek, F. R.; Hammer, R. P. *J. Org. Chem.* **1995**, 60, 7390.

1.46 Yamauchi, K.; Ohtsuki, S.; Kinoshia, M. *J. Org. Chem.* **1984**, 49, 1158.

1.47 Solomon, T.W.G In *Organic Chemistry*; 5th ed.; John Wiley and Sons, Inc.: New York, **1992**; p. 1118.

1.48 Branden, C.; Tooze, J. In *Introduction to Protein Structure*; Garland Publishing: New York, 1991; p 18.

1.49 Zubay, G. L.; Parson, W. W.; Vance, D. E. In *Principles of Biochemistry*; 1st ed; William C. Brown Communications: Iowa, **1995**; pp. 86-89.

1.50 Creighton, T. E. *Proteins: Structure and Molecular Properties*; 2nd *ed.*; W. H. Freeman and Co.: New York; 1993.

1.51 Walton, A.G. *Polypeptides and Protein Structure*; Elsevier: New York; 1981.

1.52 Barlow, D. J.; Thornton, J. M. *J. Mol. Biol.* **1988**, 201, 601.

1.53 Smythe, M. L.; Huston, S. E.; Marsha, G. R. *J. Am. Chem. Soc.* **1995**, 117,5445.

1.54 Wysong, C. L.; Yokum, T. S.; McLauglin, M. L.; Hammer, R. P. *Chem. Tech.* **1997**, 27, 26.

1.55 Stewart, J. M. In *Amphipathic Helix*; Epand, R. M., Ed.; CRC Press: Florida, 1993; pp 21-37.

1.56 Cornette, J. L.; Cease, K. B.; Maragalet, H.; Spouge, J. L.; Berzofsky, J. A.; Delisi, C. D. *J. Mol. Biol.* **1987**, 195, 659.

1.57 Barkley, M. D.; Javadpour, M. M. *Biochemistry* **1997**, 36, 9540.

1.58 Zasloff, M. *Proc. Natl. Acad. Sci. U.S.A.* **1987**, 84, 5449.

1.59 Javadpour, M. M.; Juban, M. M.; Lo, W. J.; Bishop, S. M.; Alberty, J. B.; Cowell, S. M.; Becker, C. L.; McLauglin, M. L. *J. Med. Chem.* **1996**, 39, 3, 107.

1.60 Saberwal, G.; Nayaraj, R. *Biochim. Biophys. Acta* **1994**, 1197, 109.

1.61 Tytler, E. M.; Anantharamaiah, G. M.; Walker, D. E.; Mishra, U. K.; Palgunachari, M. N.; Segrest, S. P. *Biochemistry* **1995**, 34, 4393.

1.62 Opella, S. J.; Gesell, J.; Bechinger, B. In *Amphipathic Helix*; Epand, R. M., Ed.; CRC Press: Florida, 1993; pp 88-104.

1.63 Fox, R. O.; Richards, F. M. *Nature* **1982**, 300, 325.

1.64 Karle, I. L.; Balaram, P. *Biochem.* **1990**, 29, 6747.

1.65 Basu, G.; Bagchi, K.; Kubi, A. *Biopolymers* **1991**, 31, 1763.

1.66 Aleman, C.; Subirana, J. A.; Perez, J. *Biopolymers* **1992**, 32, 621.

1.67 Basu, G.; Kuki, A. *Biopolymers* **1993**, 33, 995.

1.68 Yokum, T. S.; Elzer, P. H.; McLaughlin, M. L. *J. Med. Chem.* **1996**, 39, 3603.

1.69 Formaggio, F.; Crisma, M.; Rossi, P.; Scrimin, P.; Kaptein, B.; Broxterman, Q. B.; Kamphuis, J.; Toniolo, C. *Chem. Eur. J.* **2000**, 6, 4498.

1.70 Kennedy, D. F.; Crisma, M.; Toniolo, C.; Chapman, B. *Biochemisty* **1991**, 30, 6541.

1.71 Toniolo, C.; Poles, A.; Formaggio, F.; Crisma, M.; Kamphuis, J. *J. Am. Chem. Soc.* **1996**, 118, 2744.

1.72 Yokum, T. S.; Gauthier, T. J.; Hammer, R. P.; McLaughlin, M. L. *J. Am. Chem. Soc.* **1997**, 119, 1167.

1.73 Spatola, A. *In Chemistry and Biochemistry of Amino Acids, Peptides, and Proteins*; Weinstein, B., Ed.; Marcel Dekker, Inc.: New York, **1983**; pp. 267-357.

1.74 Balaram, P. *Curr. Opin. Struct. Biol.* **1992**, 2, 845.

1.75 Ferot, E.; Coste, J.; Pantaloni, A.; Dufour, M.; Jouin, P. *Tetrahedron* **1991**, 47, 259.

1.76 Wenschuh, H.; Beyermann, M.; Krause, E.; Brudel, M.; Winter, R.; Schumann, M.; Carpino, L. A.; Bienert, M. *J. Org. Chem.* **1994**, 59, 3275.

1.77 Carpino, L. A.; Choa, H. G.; Beyermann, M.; Bienert, M. *J. Org. Chem.* **1991**, 56, 2635.

1.78 Wenschuh, H.; Beyermann, M.; Haber, H.; Seydel, J. K.; Krause, E.; Bienert, M.; Carpino, L. A.; El-Faham, A.; Albericio, F. *J. Org. Chem.* **1995**, 60, 405.

1.79 Carpino, L. A.; Mansour, E. M. E.; Sadat-Aalaee, D. *J. Org. Chem.* **1991**, 56, 2611.

1.80 Carpino, L. A.; El-Faham, A. *J. Am. Chem. Soc.* **1995**, 117, 5401.

1.81 Carpino, L. A.; *J. Am. Chem. Soc.* **1993**, 115, 4397.

1.82 Carpino, L. A.; El-Faham, A.; Albericio, F. *Tetrahedron Lett.* **1994**, 35, 2279.

1.83 Albericio, F.; Cases, M.; Alsina, J.; Triolo, S. A.; Carpino, L. A.; Kates, S. A. *Tetrahedron Lett.* **1997**, 38, 4853.

1.84 Millhauser, G. L. *Biochemistry* **1995**, 34, 3873.

1.85 Kritanai, C.; Johnson, W. C. *Analyt. Biochem.* **1997**, 253, 57.

1.86 Juban, M. M.; Javadpour, M. M.; Barkley, M. D. In *Methods in Molecular Biology*; Shafer, W. M., Ed.; Humana Press, Inc.: New Jersey, **1997**, 78, pp. 73-75.

1.87 Johnson, W. C. *Proteins: Structure, Function, and Genetics* **1990**, 7, 205.

1.88 Greenfield, N. J.; Fasman, G. D. *Biochemistry* **1969**, 8, 4108.

1.89 Manning, M.; Woody, R. W. *Biopolymers* **1991**, 31, 569.

Chapter 2

Synthesis of Phosphonamides and Thiophosphonamides by a One-Pot Activation-Coupling-Oxidation Procedure

2.1 Introduction

Phosphonopeptides are peptide mimics[2.1-2.2] that emulate high-energy tetrahedral transition states of enzyme-catalyzed peptide hydrolysis reactions. Thus, they are useful as mechanism-based inhibitors of asparty[2.3-2.4] and metallo-proteases.[2.5-2.6] Several phospho-nopeptides have also shown powerful antibacterial activity.[2.7-2.8] More recently, these types of compounds have been applied to hapten design for the generation of catalytic antibodies that possess peptide ligase activity.[2.9] In this chapter we report the synthesis of phosphonamide dipeptides **1a-d** (R = Cbz) (Scheme 2.1) in isolated yields up to 30 % using our P(III) one-pot activation-coupling-oxidation procedure.[2.10] Previous attempts to prepare the hapten precursor **1a** from P(V) phosphonochloridate **2** and D-tryptophamide under standard and optimized conditions were unsuccessful, due in part to the steric bulk of the amino acid side chains.[2.11-12] The problems of preparing the hapten precursor **1a**

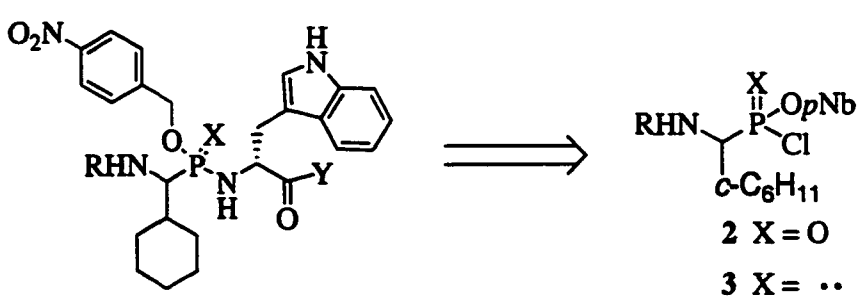

1a X = O, Y = NH_2
1b X = S, Y = NH_2
1c X = O, Y = OCH_3
1d X = S, Y = OCH_3
R = Fmoc or Cbz

Scheme 2.1 Retrosynthethic analysis of phosphonamides and thiophosphonamides **1a-d**

exemplify the difficulties many laboratories have encountered in preparing phosphonamidate peptides via P(V) coupling protocols.[2.13-16] The P(III) method detailed herein using phosphonochloridite **3** as the key intermediate may provide a general approach to preparing complex phosphonamide peptide analogs for a variety of applications.

2.2 Results and Discussion

The air-stable precursor used for generation of phosphonochloridite **3** is racemic, carbamate-protected H-phosphinate amino acid **4** (Scheme 2.2) as a diastereomeric mixture of para-nitrobenzyl (*p*Nb) esters. The H-phosphinate **4**, under certain conditions, was converted to the phosphonochloridite **3** with the commercially available dichlorotriphenylphosphorane (Ph_3PCl_2). Because the solvent pyridine and the solvent system CH_2Cl_2/Et_3N worked well in our model systems,[2.10] they were initially employed during activation of **4** with Ph_3PCl_2. However, only a small amount of the phosphonochloridite **3** (^{31}P = 200 ppm) admixed with several other as yet unidentified products formed. This may be due to the amide functionality in **4** being possibly sensitive to the combination of Ph_3PCl_2 with Et_3N or pyridine (when used as solvent). Ph_3PCl_2 in the presence of Et_3N is known to convert secondary amides to imidoyl chlorides.[2.17] Mechanistically, the formation of an isocyanate from the carbamate functionality with Ph_3PCl_2/ Et_3N is also possible. We therefore searched for alternative solvent conditions for the activation step.

In standard P(V) chemistry, successful conversion of a phosphonate monoester to the corresponding phosphonochloridate with thionyl or oxalyl chloride is often done in the absence of base.[2.11-2.12,2.18-2.20] Therefore, in an analogous attempt to improve the activation step of our P(III) protocol, treatment of **4** with Ph_3PCl_2 was carried out in the absence of base. Only two phosphorus signals, 193 ppm (activated P(III) species) and

40 ppm (Ph_3PO^+ HCl^-) resulted. After activation, we proceeded to the next step of coupling, followed by oxidation or sulfurization. Several attempts to isolate or purify the resulting dipeptides by column chromatography (silica and alumina under various solvent conditions) were generally unsuccessful.

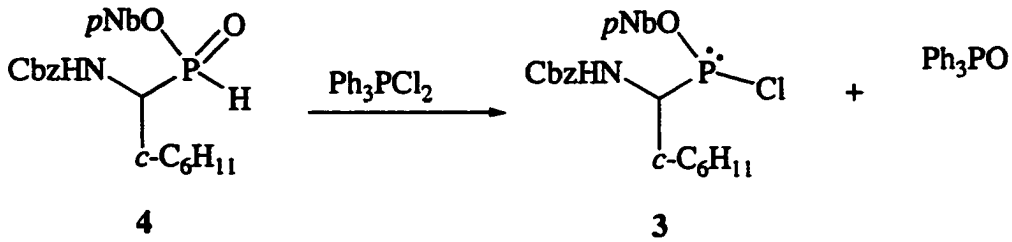

4 3

Scheme 2.2 Activation of H-phosphinate **4** to form phosphonochloridite **3**

The difficulty in isolation of the phosphonodipeptides from the silica column was initially attributed to the general acid lability of phosphonamides.[2.15,2.21-2.22] However, only about 0-3 % of the sulfurized species (^{31}P = 75-80 ppm) sometimes eluted from the alumina (basic or neutral) column. Furthermore, triphenylphosphine oxide tended to smear the columns; therefore, it was often observed in every collected fraction. Oftentimes Ph_3PO was the only substance to elute.

In an effort to find a solution to the synthetic or isolation problems associated with preparation of **1**, experiments (P (III) protocol) were conducted using **4** and less complex nucleophiles like benzyl alcohol, methyl-S-lactate, leucine methyl ester, and benzylamine. In the crude mass spectra (FAB) of these less complex phosphonate esters and amides, the parent ions minus the *p*Nb group were readily observed. Further examination of the FABMS of the crude reaction mixtures containing our synthetic targets **1a-d** also revealed that the major products appeared to be ones in which the *p*Nb group had been cleaved off. It was therefore postulated that the *p*Nb group of these

simple phosphonate derivatives as well as our targets **1** was possibly being cleaved during one of the three steps of the P (III)-based protocol.

2.2.1 Examination of Activation Reaction

Upon further inspection of ^{31}P NMR spectra from the activation step without any base, it was speculated that the activated species at 193 ppm was not the desired P (III) species **3**. In acidic medium the major side product, Ph_3PO, resonated at 40 ppm, but, upon addition of base, it shifts back upfield to 27 ppm, where it normally resonates in neutral or basic milieu. Conversely, the activated P (III) species at 193 ppm, upon addition of base, doesn't move to the downfield chemical shift of 200 ppm expected in basic media. From this simple ^{31}P spectra analysis and difficulties with isolation of **1a-d**, we proposed that activation in the absence of base forms **3** but quickly converts, after *p*Nb cleavage, to the respective phosphonodichloridite (^{31}P = 193 ppm); para-nitrobenzyl chloride (pNbCl) was also thought to form in this process (Scheme 2.3).

To validate the hypothesis of *p*Nb cleavage during activation, a study was conducted on the activation step using **4** and GC-MS analysis of the products. Reaction of **4** with Ph_3PCl_2 in CH_2Cl_2 in the absence of base produced an intense peak corresponding to 4-nitrobenzyl chloride (~1:1 ratio with Ph_3PO). In contrast, when this reaction was performed with pyridine present (~1.5 equiv.), the peak corresponding to 4-nitrobenzyl chloride was very weak (<5 % the intensity of Ph_3PO) (Figure 2.1). It was therefore concluded that in order to prevent *p*Nb cleavage, the presence of base to scavenge generated HCl during the activation reaction was essential.

The best solvent/base combination for activation of **4** with Ph_3PCl_2 was finally determined to be two equivalents of pyridine (~ 3%) in CH_2Cl_2. With one equivalent of

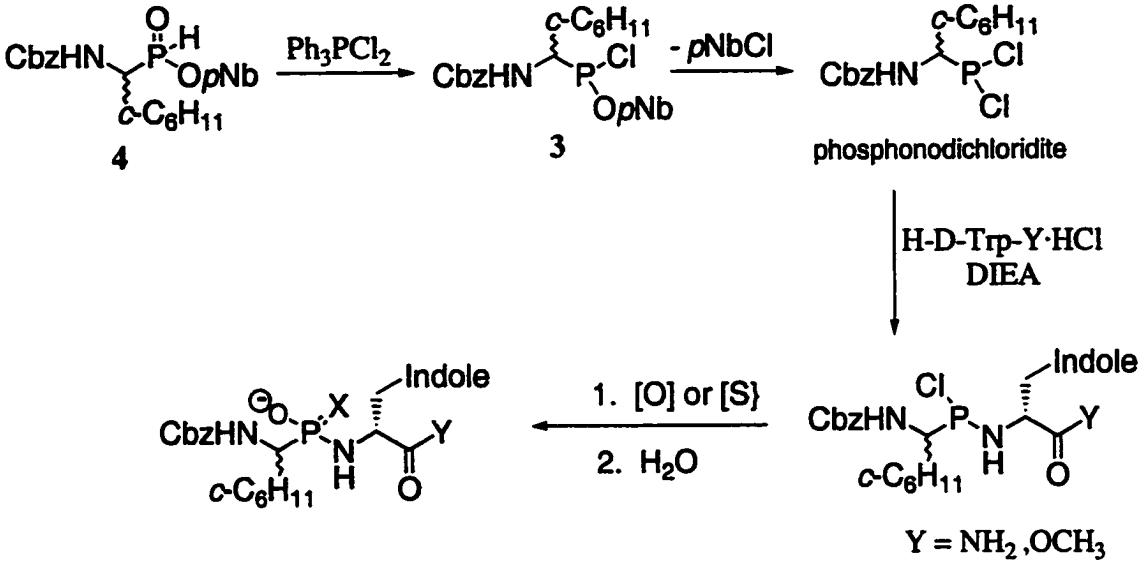

Scheme 2.3 Proposed route for phosphonate ester cleavage and phosphonamidate formation

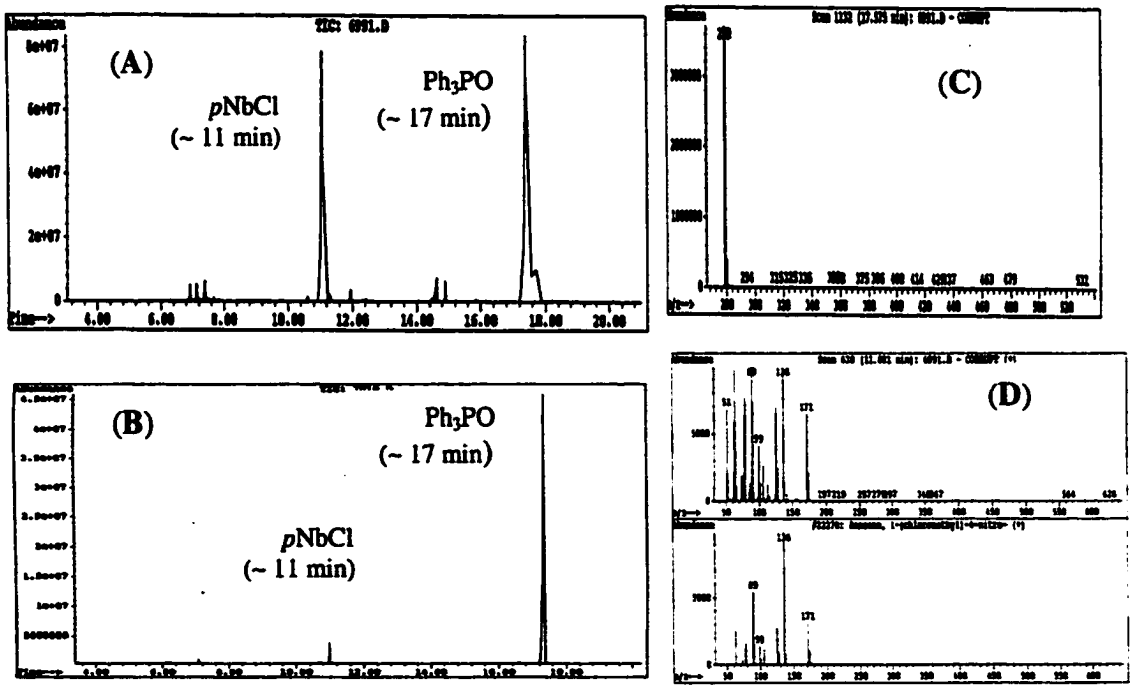

Figure 2.1 Comparative GC-MS study of activation step. **(A)** Sample from activation of 4 in the absence of base with extensive ester cleavage evidence by side-product, *p*NbCl. **(B)** Sample from activation of 4 in the presence of pyridine with minimum ester cleavage. **(C)** Mass Spectrum of peak ~ 17 min. (Ph_3PO). **(D)** Mass Spectrum of peak ~11 (*p*NbCl).

pyridine nearly equal amounts of **3** (^{31}P = 200 ppm) and the P(III) species (^{31}P = 193 ppm) that resulted from *p*Nb cleavage formed. Furthermore, as the number of equivalents of pyridine increased from 2 to huge excess (e.g., pyridide as solvent), the number and amount of side-products increased (Table 2.1). However, with the optimized solvent condition, very little or no side products were evident from ^{31}P NMR.

Table 2.1 Phosphonochloridite generation under various solvent and base conditions

Solvent	Ph_3PCl_2[a]	Base (equiv.)	^{31}P δ ppm (ratio)[c]
Pyridine	2.5[b]	Solvent	200 (0.25), 180 (0.05), 165 (0.04), 158 (0.15), 120 (0.18), 115 (0.05), 39-41 (0.08), 28 (1))
CH_2Cl_2	2.5[b]	NEt_3 (2)	same as above
CH_2Cl_2	2.0[b]	none	193 (0.4), 40[d] (1)
CH_2Cl_2	1.5[b]	pyridine (1)	200 (0.3), 193 (0.4), 28 (1)
CH_2Cl_2	1.2[b]	pyridine (2)	200 (0.85), 28 (1)

[a] Contains 10-20 % Ph_3PO
[b] Represent number of equivalents needed to consume **4**
[c] Represent intensity of each peak relative to Ph_3PO
[d] $Ph_3PO^+HCl^-$

2.2.2 Coupling Step

The next step of the one-pot procedure was the coupling of **3** to D-tryptophanamide **5a** or D-tryptophan methyl ester **5b** to form the phosphonamidite **6** (Scheme 2.4, Path A). The major problem initially encountered with the amine coupling of **5** to **3** was the formation of an unknown substance ($^{31}P \cong 180$ ppm) that competed with the formation of the phosphonamidite **6**. When **5** was added in one portion to the

phosphonochloridite **3**, only the ^{31}P signal around 180 ppm was observed. However, when **5** was added over 15-20 minutes, the intensity of the peak ~ 180 ppm and the four possible diastereomeric peaks (^{31}P, 123, 124, 126, 128 ppm) was nearly equal. We therefore directed our investigation toward elucidating the identity or properties of that unknown species ($^{31}P \equiv 180$ ppm).

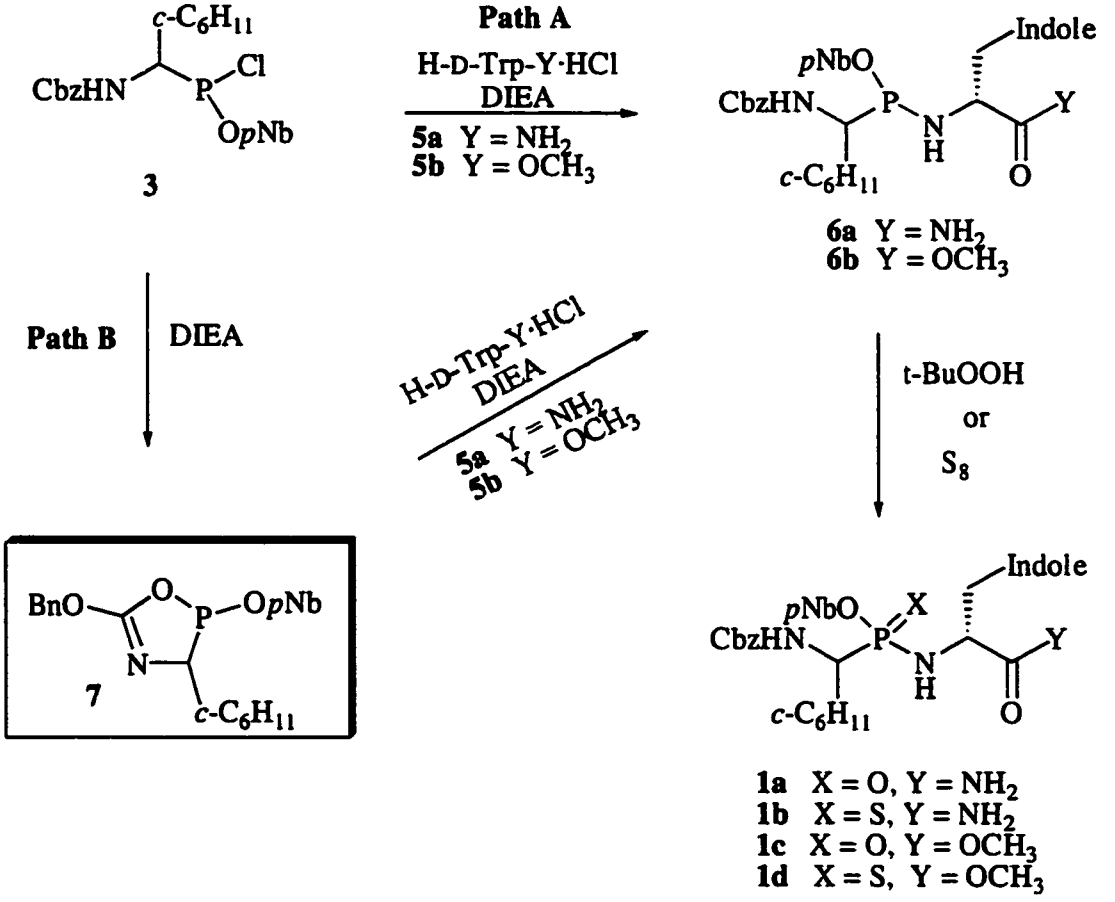

Scheme 2.4 Synthesis of **1a-d** via **Path A** or **Path B**

In the presence of tertiary amines urethane-protected amino acids and peptides are known to cyclize to form oxazolones,[2.23] which are themselves reactive acylating agents. We reasoned that similar cyclization could be occurring with our urethane-protected phosphonochloridite **3** to form an oxazaphospholine[2.19] ($^{31}P \equiv 180$ ppm). We generated the proposed oxazaphospholine **7** (Scheme 2.4, Path B) by adding 1.5 equivalents of the

tertiary base, diisopropylethylamine (DIEA), to **3**. To investigate the reactivity of **7**, the nucleophile **5a** or **5b** was added in one portion. After about 15 minutes, two phosphonamidite diastereomers preferentially formed, which, after sulfurization or oxidation, resulted in **1** as a mixture of two diastereomers (Figure 2.2, Figure 2.3, and Figure 2.4); they were isolated using reverse-phased HPLC (Figure 2.5 and Figure 2.6).

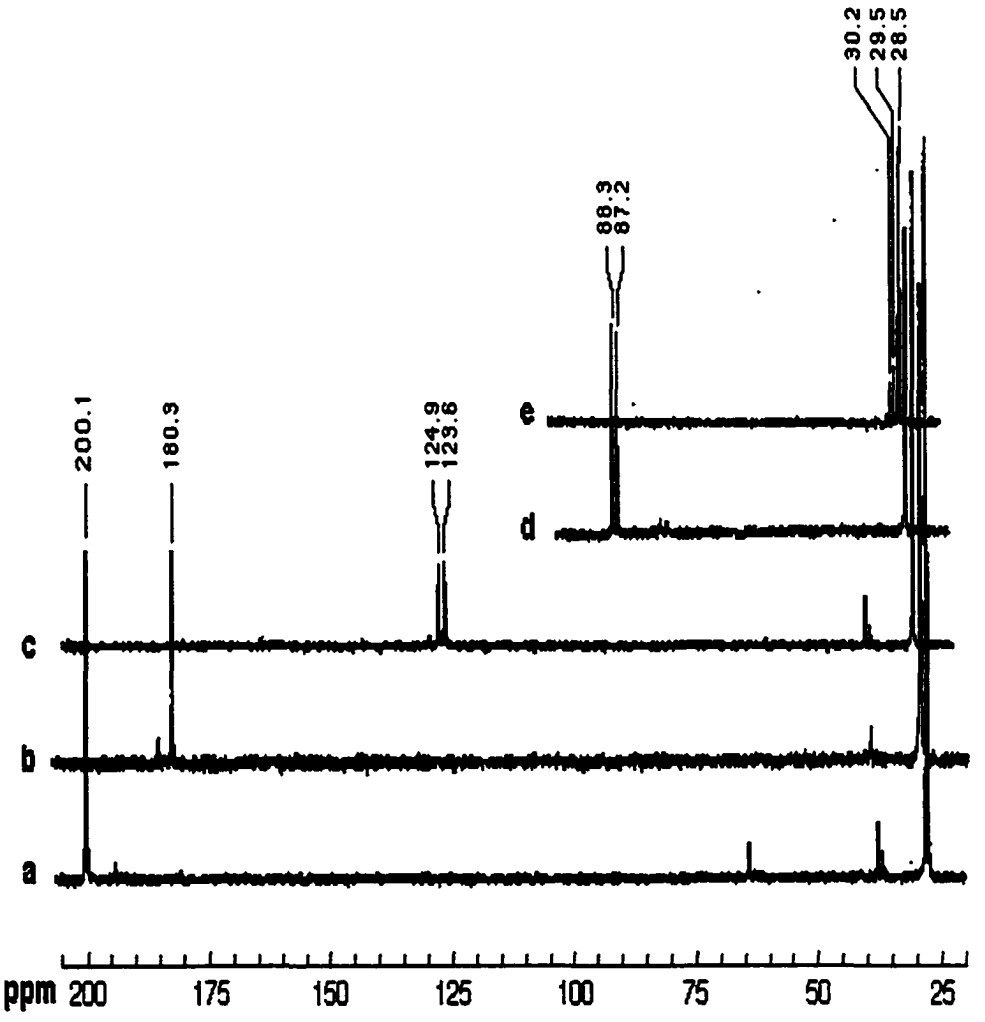

Figure 2.2 ^{31}P NMR spectra: **a.** Reaction of H-phosphinate **4** with Ph_3PCl_2 in presence of pyridine (2 equiv.) to form phosphonochloridite **3** (~200 ppm); unreacted **4** is ~ 36 and 37 ppm and Ph_3PCl_2 ~ 64 ppm; peak ~ 28 ppm is Ph_3PO in each spectrum **b.** Proposed oxazaphospholine **7** (~ 180 ppm). **c.** Species **6a** (~ 123.6 and 124.9 ppm). **d.** Target **1b** (87.2 and 88.3 ppm). **e.** Target **1a** (~ 29 and 30 ppm).

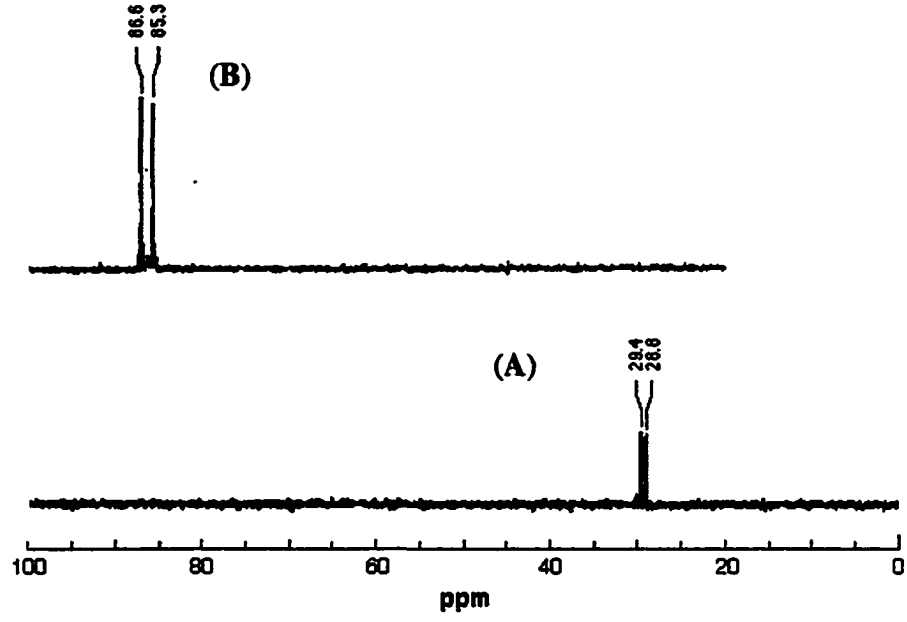

Figure 2.3. ^{31}P NMR Spectra of HPLC-purified **1a-1b.** (**A**). Cbz-CyhGly ψ [P (O) (O*p*Nb) NH] Trp-NH_2 **1a.** (**B**). Cbz-CyhGly ψ [P (S) (O*p*Nb) NH] Trp- NH_2 **1b.**

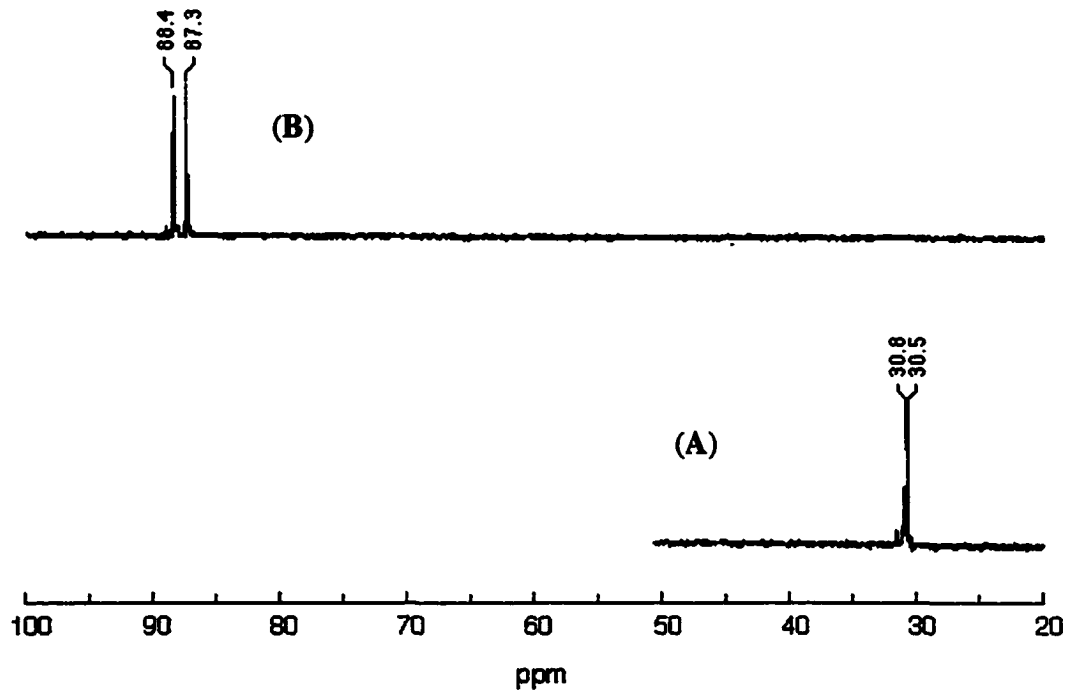

Figure 2.4 ^{31}P NMR spectra of HPLC-purified **1c-d.** (**A**). Cbz-CyhGly ψ[P (O) (O*p*Nb) NH] Trp-OCH_3 **1c.** (**B**). Cbz-CyhGly ψ[P (S) (O*p*Nb) NH] Trp- OCH_3 **1d.**

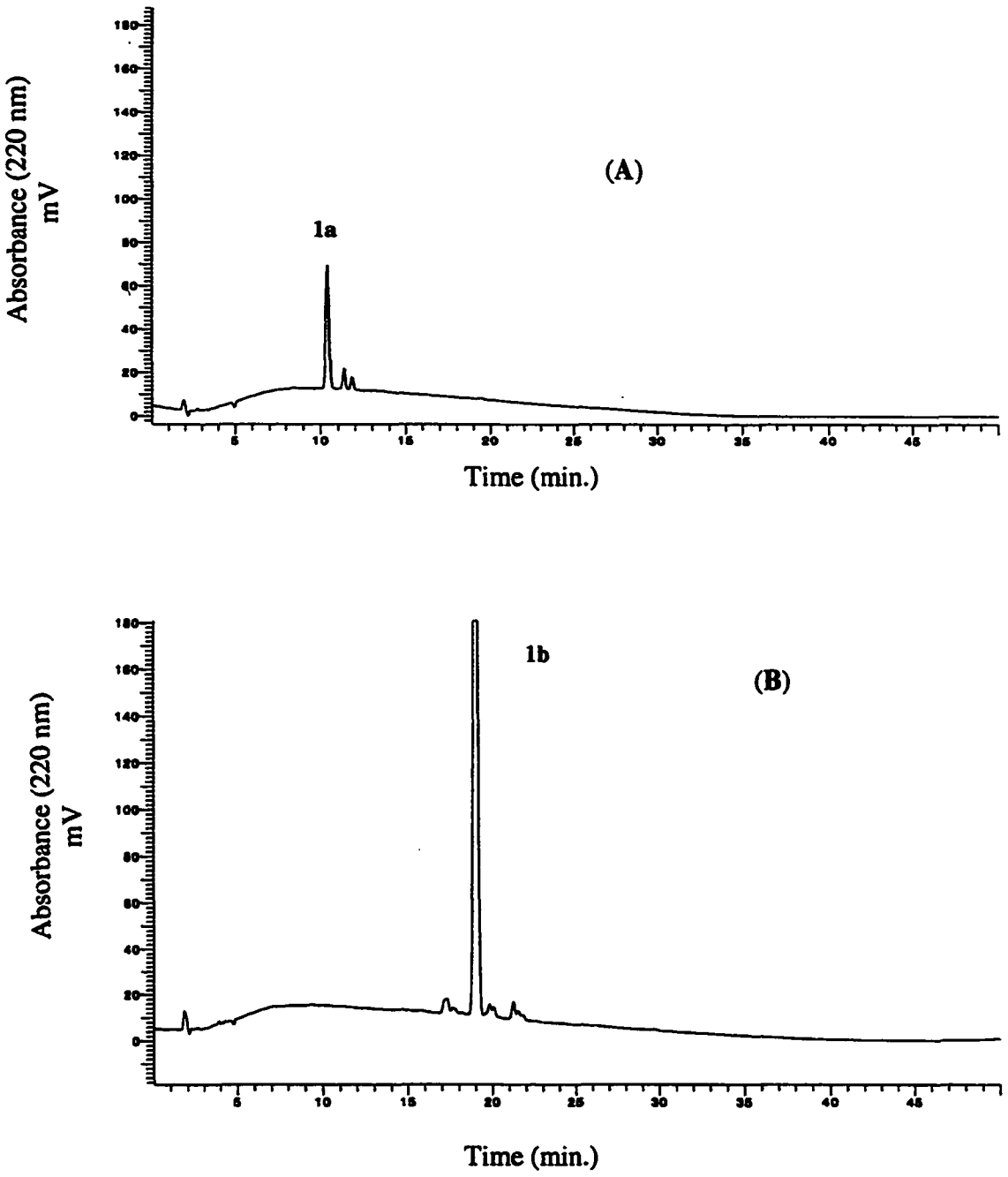

Figure 2.5. Analytical HPLC purity check of isolated **1a** and **1b**. HPLC was carried out on a Supelco 5 μm C-18 reversed-phase column (0.21 x 25 cm) using a mobile phase of 0.1 M TEAA buffer (pH = 7) and CH_3CN (10 % v/v, 0.05 M aqueous TEAA) with a gradient of 50-100 % of the organic phase over 50 min and a flow of 1 mL/min. **(A).** Cbz-Cyclohexyl ψ[P (O) (OPNB) NH] Trp-NH_2 **1a**; t_R = 10.7 min; purity 82 %. **(B).** Cbz-Cyclohexyl ψ[P (S) (OPNB) NH] Trp- NH_2 **1b**; t_R = 19.2 min; purity 95 %.

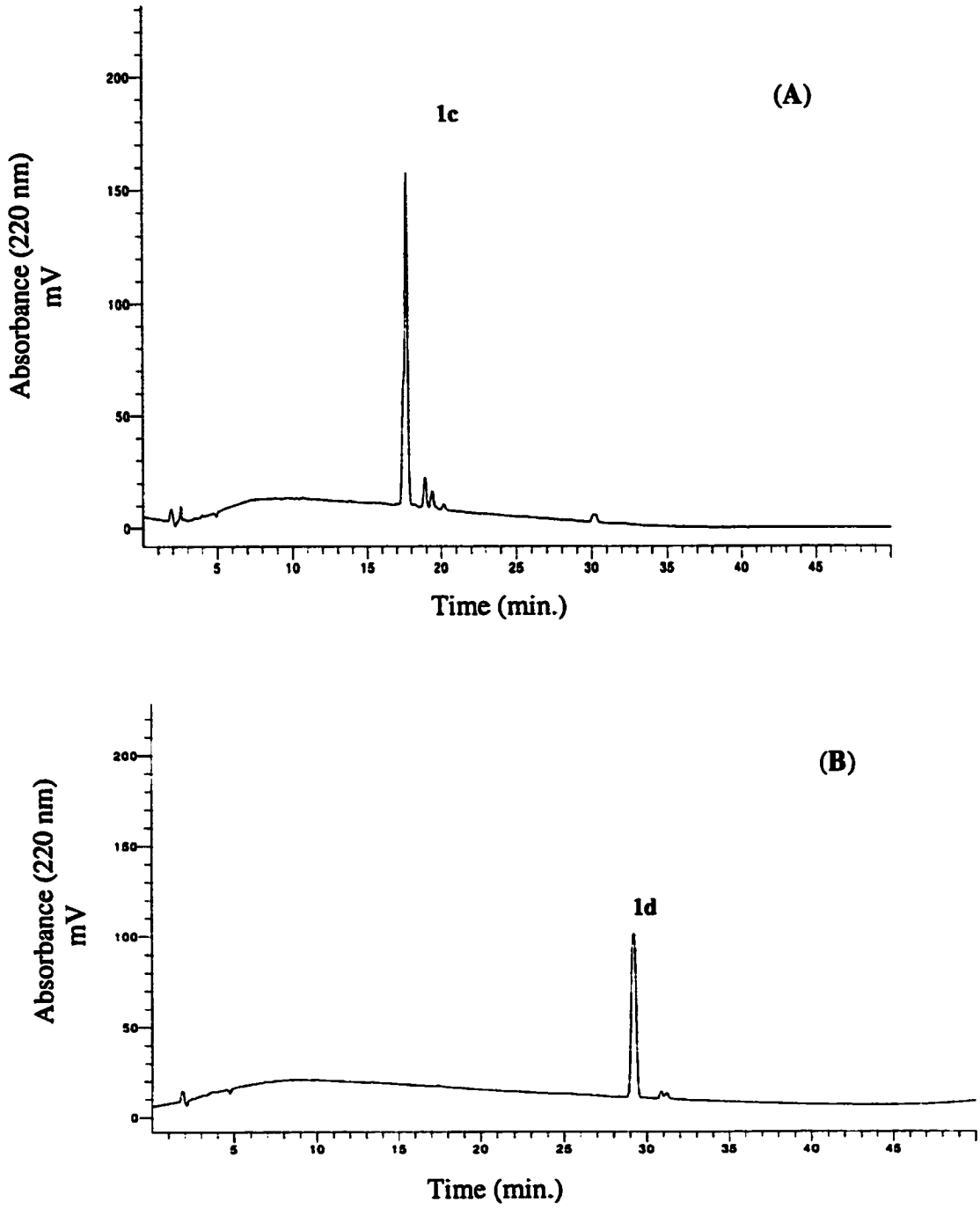

Figure 2.6. Analytical HPLC purity check of isolated **1c** and **1d**. HPLC was carried out on a Supelco 5 μm C-18 reversed-phase column (0.21 x 25 cm) using a mobile phase of 0.1 M TEAA buffer (pH = 7) and CH_3CN (10 % v/v, 0.05 M aqueous TEAA) with a gradient of 50-100 % of the organic phase over 50 min and a flow of 1 mL/min. (A). Cbz-CyhGly ψ[P (O) (O*p*Nb) NH] Trp-OMe **1c**; t_R = 17.7 min; purity 90 %. (B). Cbz-CyhGly ψ[P (S) (O*p*Nb) NH] Trp-OMe **1d**; t_R = 29.2 min; purity 95 %.

It is interesting to note that the activation of the H-phosphinate ester **4** (^{31}P = 36 and 37 ppm) resulted in the formation of only one peak (^{31}P ~ 200 ppm) for the resulting phosphonochloridite **3**. We proposed that the expected two diastereomers of **3** resonated at the same chemical shift. However, the formation of only two diastereomers of **1** instead of the expected four may be due in part to the formation of only the trans conformer (plus its enantiomer) of **7**: the observed, one peak (^{31}P ~ 180 ppm) of **7** could possibly correspond to one pair of enantiomers (e.g., *R*, *S* and *S*, *R*). The cis conformer (e.g., enantiomers *R*, *R* and *S*, *S*) appears to be more sterically crowded (Figure 2.7); therefore, its possible instability may have precluded its formation.

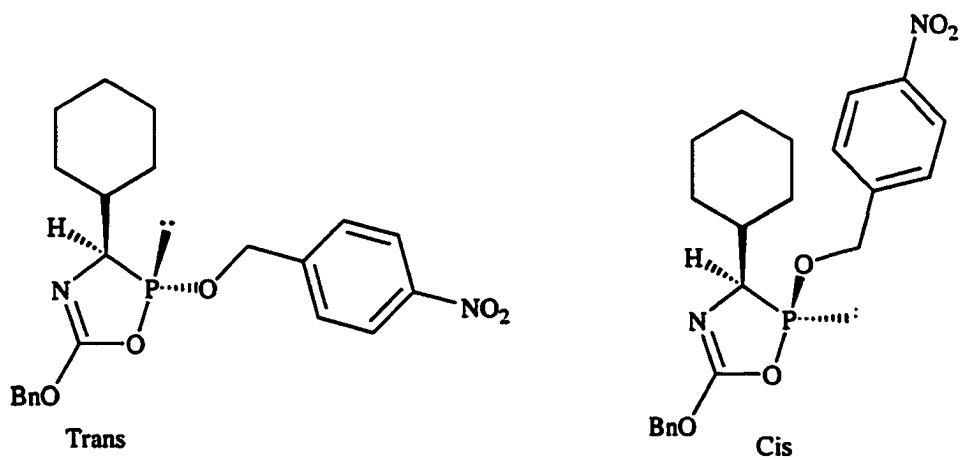

Figure 2.7 Trans and Cis conformer of oxazaphospholine **7**

The proposed oxazaphospholine **7** was also coupled to the amine nucleophiles, leucine methyl ester and glycine ethyl ester, and the alcohol nucleophiles, benzyl alcohol and methyl (*S*)-lactate. Coupling of **7** to leucine methyl ester **8** and glycine ethyl ester **9** resulted in the formation of the phosphonamidites **10** (^{31}P = 124.9, 126.1 ppm) and **11** (^{31}P = 126.5 ppm), repectively. Sulfurization of **10** and **11** formed the thiophosphonamides **12** (^{31}P = 86.9, 88.3 ppm) and **13** (^{31}P = 89.7 ppm), respectively; oxidation of **11**

formed the phosphonamide **14** (^{31}P = 39.2 ppm) (Scheme 2.5, Figure 2.8). Coupling of **7** to benzyl alcohol **15** and methyl-S-lactate **16** resulted in the formation of the phosphonates **17** (^{31}P = 178.7 ppm) and **18** (^{31}P = 179.8, 179.9 ppm), respectively. Sulfurization of **17** and **18** formed the thiophosphonamides **19** (^{31}P = 97.1 ppm) and **20** (^{31}P = 95.5, 96.9 ppm), respectively (Scheme 2.6, Figure 2.9).

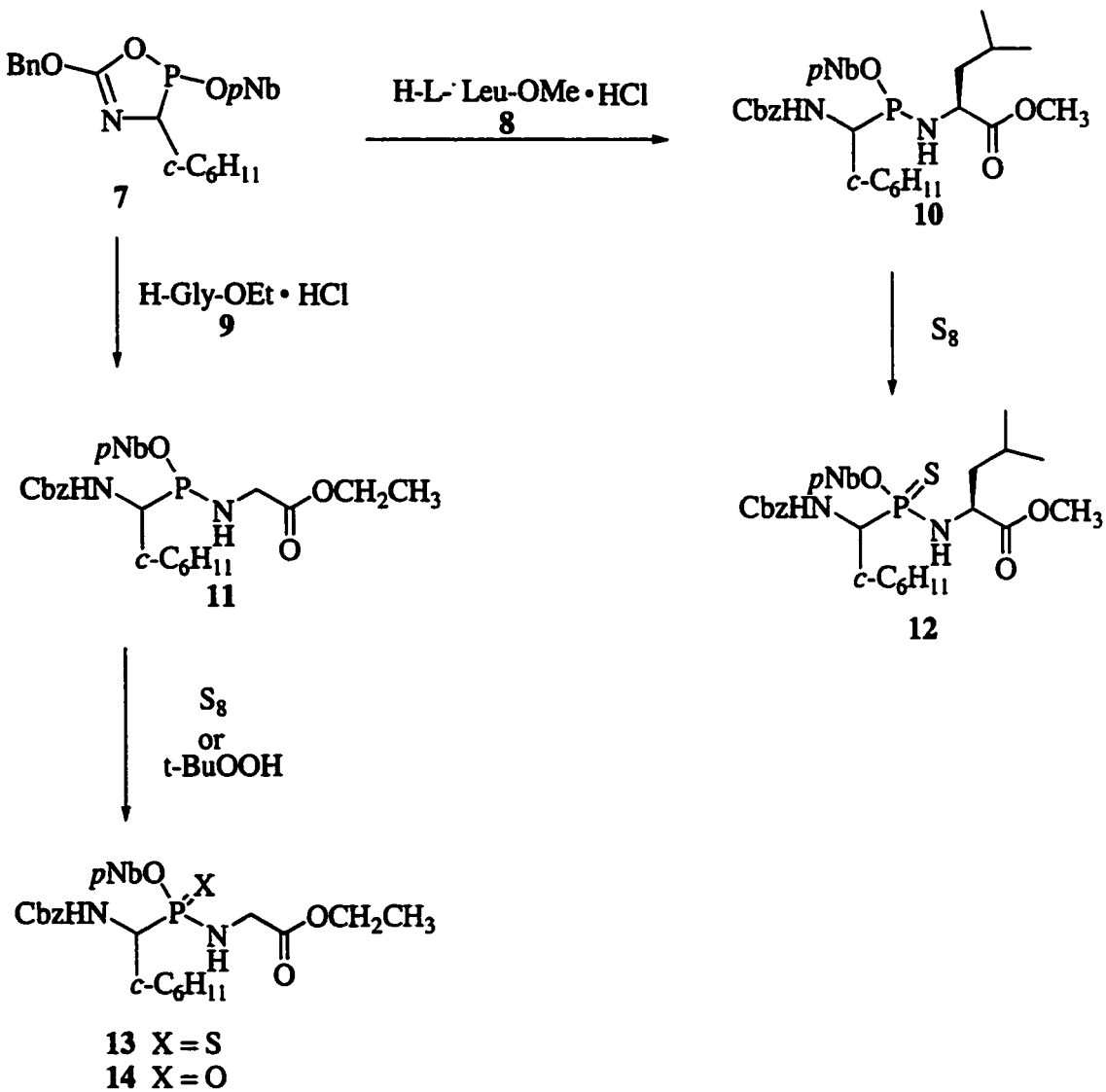

Scheme 2.5 Synthesis of Cbz-protected thiophosphonamides **12-13** and phosphonamide **14**.

An alternative structure was explored for the phosphitylating agent ($^{31}P \equiv 180$ ppm). We speculated that the observed reactive species could also possibly be analogous to the previously unrecognized phosphonyltrialkylammonium salts of Hirschmann and co- workers.[2.11-2.12] To test that hypothesis, we tried to generate the phosphitylating agent ($^{31}P = 180$ ppm) by adding the phosphonochloridite **3** to PS-DIEA resin (DIEA attached to a polystyrene resin). We reasoned that if a reactive phosphinyltrialkylammonium salt forms, then it would remain attach to the resin. However, after the reaction mixture was filtered from the resin, the newly formed phosphitylating agent was found in solution, not attached to the resin (Scheme 2.7, Path A vs. Path B). Therefore, we concluded that the reactive species that resonated around 180 ppm wasn't a phosphinyltrialkylammonium salt but possibly indeed the initially proposed oxazaphospholine **7**.

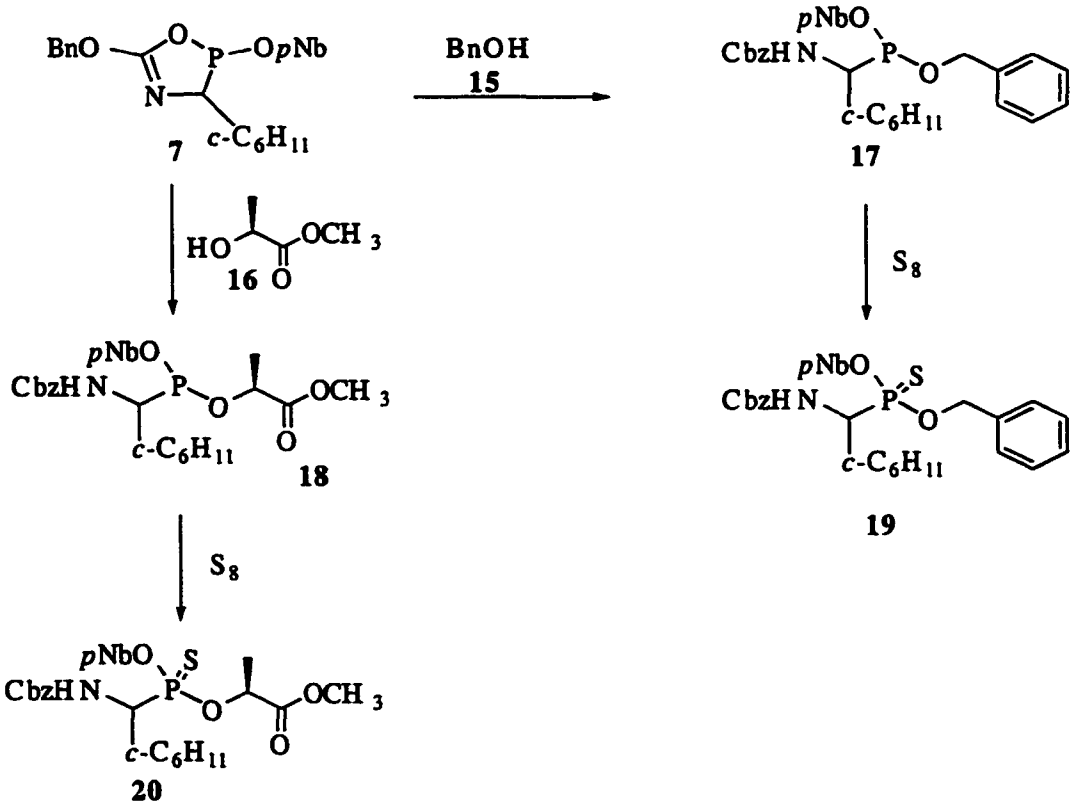

Scheme 2.6 Synthesis of thiophosphonate diesters **19-20**

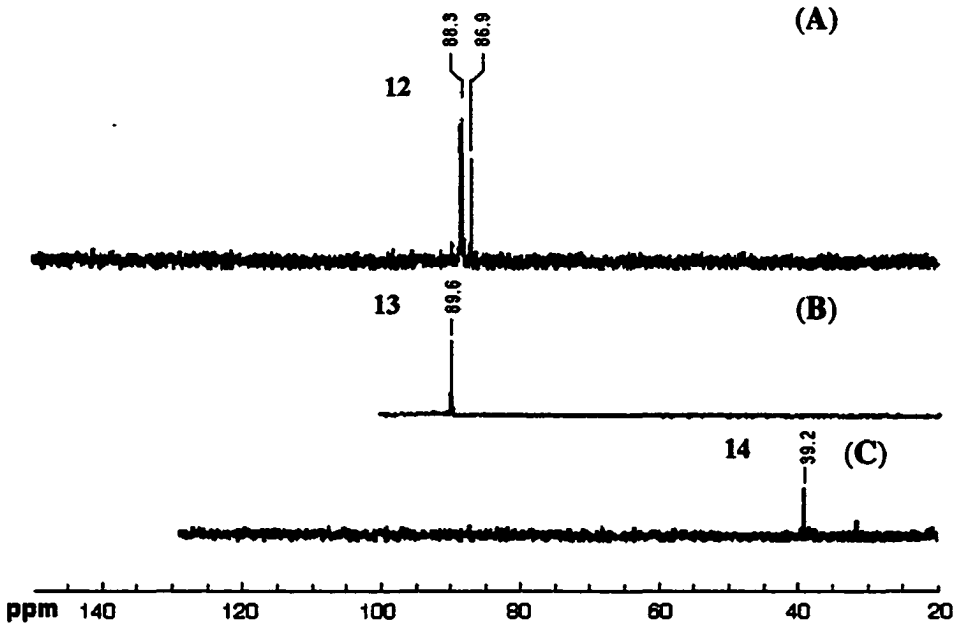

Figure 2.8 ^{31}P NMR spectra of thiophosphonamides **12-13** and phosphonamide **14** after isolation. **(A)** Compound **12** after isolation by pressure alumina chromatography. **(B)** Compound **13** after isolation by reverse-phase chromatography. **(C)** Compound **14** after isolation by reverse-phase chromatography.

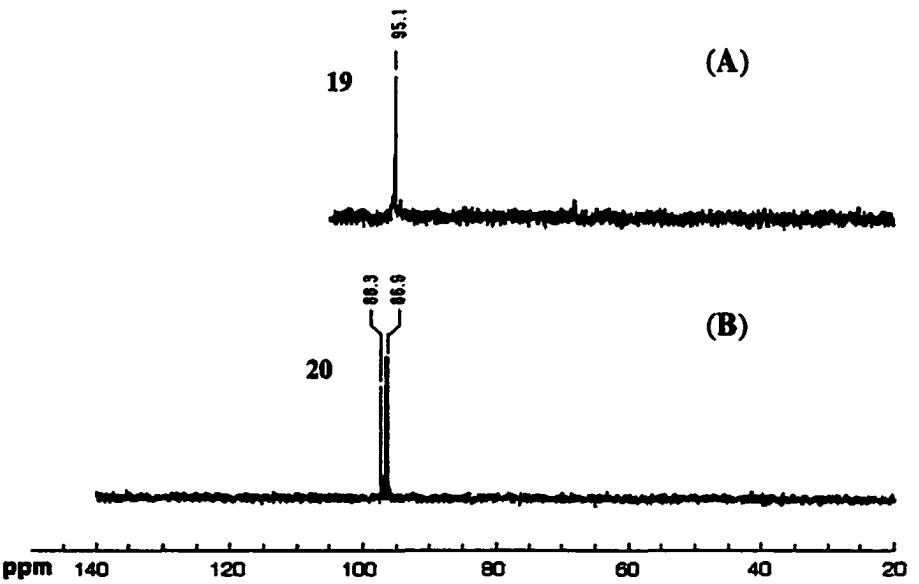

Figure 2.9 ^{31}P NMR spectra of phosphonates **19-20** after isolation. **(A)** Compound **19** after isolation by normal-phase chromatography. **(B)** Compound **20** after isolation by reverse-phase chromatography.

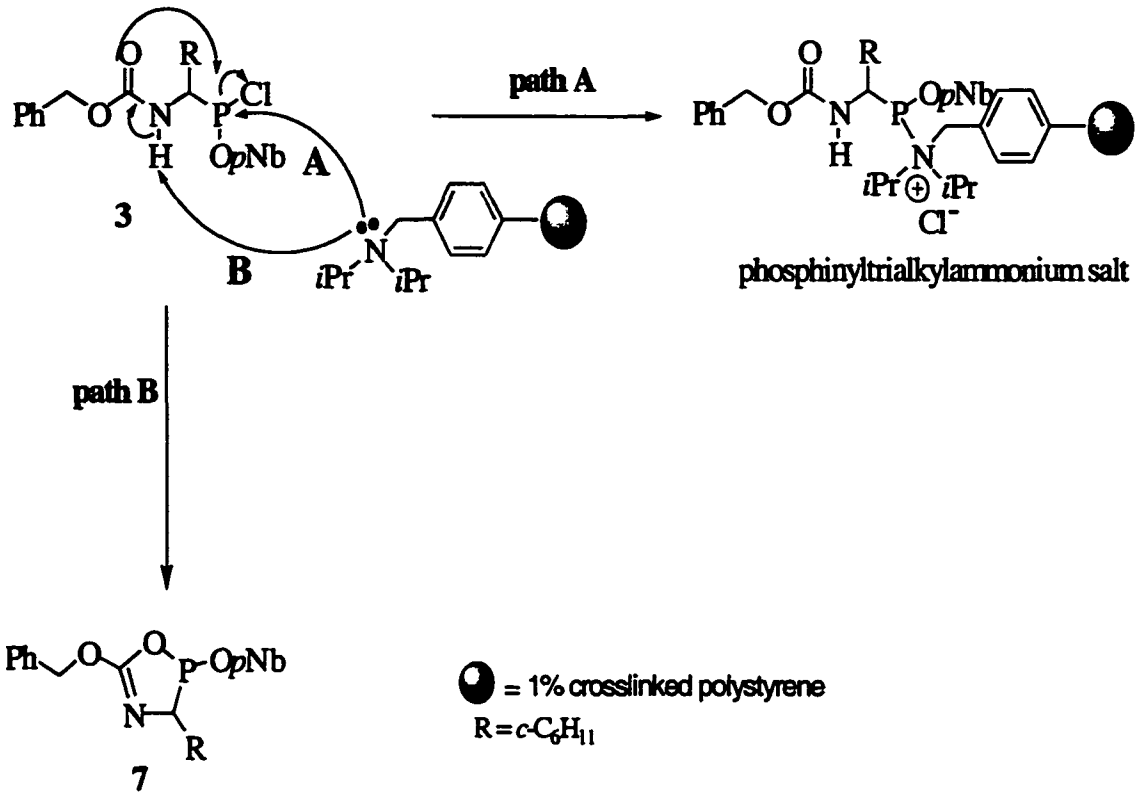

Scheme 2.7 Synthesis of oxazaphospholine **7** via PS-DIEA resin.

To prepare the final products **1a-d**, **12-14**, and **19-20** in Table 2.2, we first generated the proposed phosphitylating agent **7** from the phosphonochloridite **3** and two equivalents of DIEA. Then an amine or alcohol nucleophile was coupled to **7** to form a phosphonamidite or phosphonite followed by sulfurization or oxidation with elemental sulfur or t-butylhydroperoxide, respectively. Alternatively, we found that by adding two equivalents of **5** with 4 equivalents of DIEA to the phosphonochloridite **3** followed by oxidation or sulfurization also results in the formation of **1**, but, as a mixture of four diastereomers instead of two (Figure 2.10). With this method, the proposed oxaza-phospholine wasn't observed; however, we strongly believe it still partially formed during the coupling step but quickly reacted with **5** to aid in forming the resulting diastereomers of **1a-d**.

Table 2.2 Synthesis of phosphonamides and thiophosphonamides

Entry	Nucleophile	X	Product	% yield[e]	^{31}P
1	**5a**	O	**1a**[a,b]	18	28.8, 29.4
2	**5a**	S	**1b**[a,b]	14	85.3, 86.6
3	**5b**	O	**1c**[a,b]	15	30.5, 30.8
4	**5b**	S	**1d**[a,b]	30	88.4, 87.3
5	**8**	S	**12**[b,c]	28	86.9, 88.3
6	**9**	S	**13**[a,b]	26	89.7
7	**9**	O	**14**[a,b]	21	39.2
8	**15**	S	**19**[b,d]	15	97.1
9	**16**	S	**20**[a,b]	30	95.5, 96.9

[a] Isolated using reversed-phase HPLC [b] characterized by ^{31}P NMR, ^{1}H NMR, and MS (FAB). [c] Purified by pressure alumina chromatography. [d] Purified by flash (silica) chromatography. [e] Isolated yield.

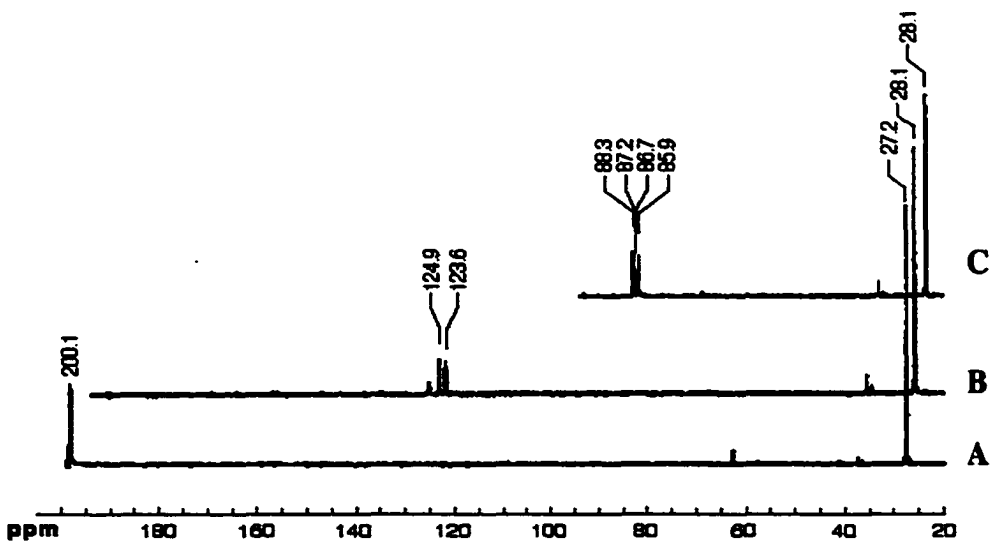

Figure 2.10 ^{31}P NMR of alternate procedure for preparation of **1d**. **A.** Reaction of H-phosphinate **4** with Ph_3PCl_2 in presence of pyridine (2 equiv.) to form phosphonochloridite **3** (~200 ppm); unreacted **4** is ~ 36 and 37 ppm and Ph_3PCl_2 ~ 64 ppm; peak ~ 28 ppm is Ph_3PO in each spectrum. **B.** Coupling of **5b** directly to **3** to form phosphonamidites **6b** as mixture of diastereomers. **C.** Sulfurization of **6b** to form **1d** as a mixture of four diastereomers (85.9, 86.7, 87.2, and 88.3 ppm).

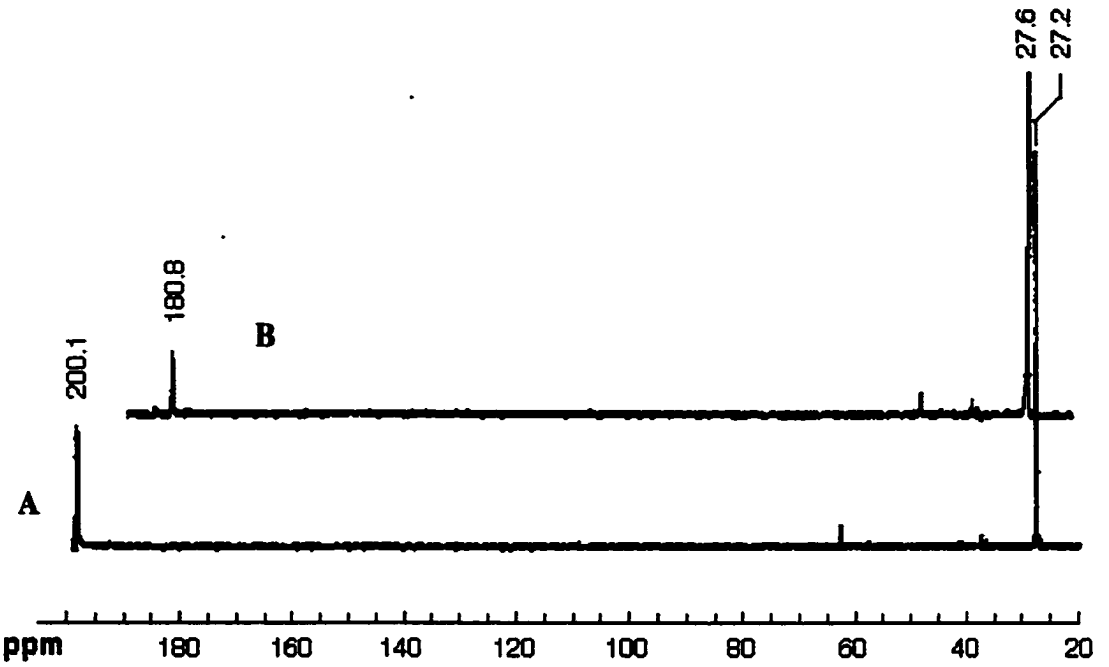

Figure 2.11 Generation of oxazaphospholine **7** via PS-DIEA resin. **A.** Reaction of H-phosphinate **4** with Ph_3PCl_2 in presence of pyridine (2 equiv.) to form phosphonochloridite **3** (~200 ppm); unreacted **4** is ~ 36 and 37 ppm and Ph_3PCl_2 ~ 64 ppm; peak ~ 28 ppm is Ph_3PO in each spectrum. **B.** Reaction of PS-DIEA resin (3.68 mmol/g, 2 equivalent) with **3** to form **7** in solution; no ^{31}P signal observed on resin after reaction.

2.2.3 Role of Amine-Protecting Group

If oxazaphospholine formation is undesired (e.g., result in low coupling efficiency or racemization of products) in a phosphonopeptide synthesis, the use of a different kind of amine-protecting group may be a logical solution. We investigated the non-urethane protecting groups 2-nitrobenzenesulfonyl (Nbs) and 5,5-dimethyl-2-acetyl-1,3-cyclohexanedione (Dde) (Figure 2.12). According to Miller and Scanlan,[2.24] Nbs-protected amino acid chlorides are not capable of oxazolone formation. Bycroft *et al.*[2.25-2.26] concluded that the Dde-protecting group precludes racemization via the common oxazolone mechanism observed with urethane amine-protecting groups. Both amine-protecting groups (Nbs and Dde) can be removed under relatively mild conditions. The removal of the Nbs group[2.24,2.27] can be accomplished with $PhSH/K_2CO_3$ in DMF and the

removal of the Dde[2.25-2.26] group with 2% hydrazine in DMF. Furthermore, the Dde group can be used orthogonally with both Fmoc and Boc protection in solution and solid-phase peptide synthesis. We prepared the Nbs- and Dde-protected H-phosphinate amino acid esters **21** and **22** and activated them with Ph_3PCl_2 (Scheme 2.8). As with the Cbz-protected phosphonochloridite, we also treated the Nbs- and Dde-protected phosphonochloridite **23** and **24**, respectively, with DIEA. With the Nbs species, a tiny peak around 180 ppm along with a myriad of other small peaks (downfield and upfield) is usually observed. In this case we believe that deprotonation of the sulfonamide proton is occurring which could lead to a variety of other possible side reactions such as cyclization to a five- or three-membered ring or possibly some type of polymerization reaction (Scheme 2.9). In the case of the Dde-species, no peak was observed around 180 ppm, but several upfield peaks were observed. We believe that the Dde group may have been prematurely cleaved by DIEA, which is a stronger base hydrazine (used to cleave Dde) (see Scheme 2.10 and Scheme 2.11). Self-condensation is one side-reaction that may have occurred as a result of Dde cleavage.

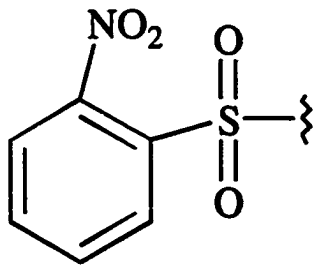

Nbs

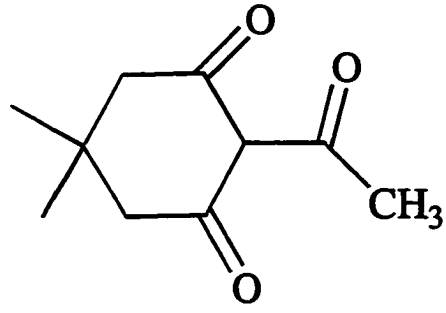

Dde

Figure 2.12 Non-urethane amine-protecting groups

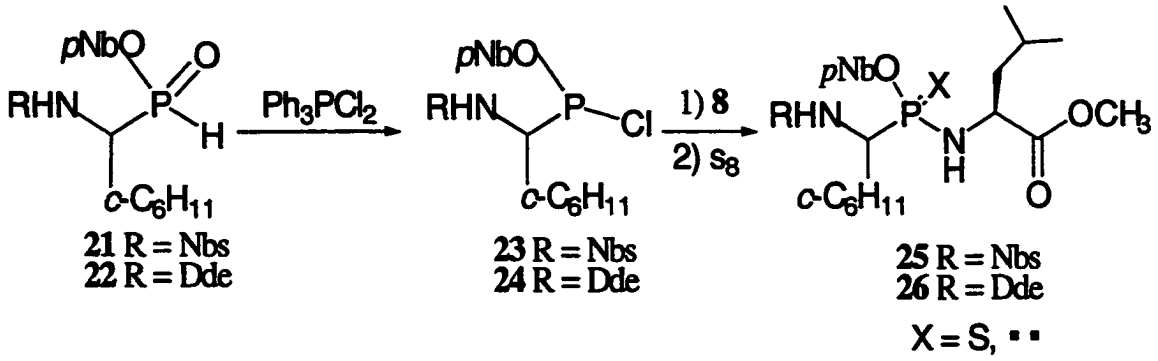

Scheme 2.8 Use of non-urethane amine-protecting groups in phosphonopeptide synthesis

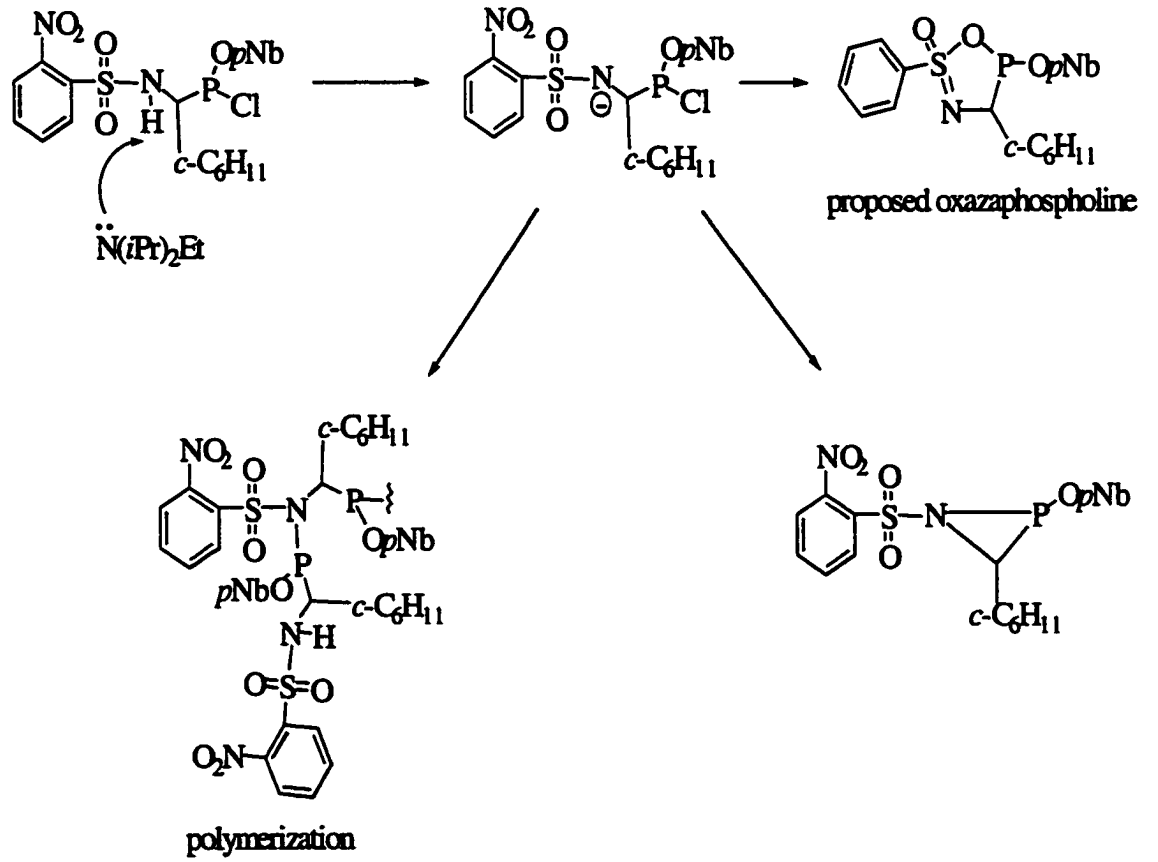

Scheme 2.9 Proposed intermediates after deprotonation of Nbs-protected phosphonochloridite

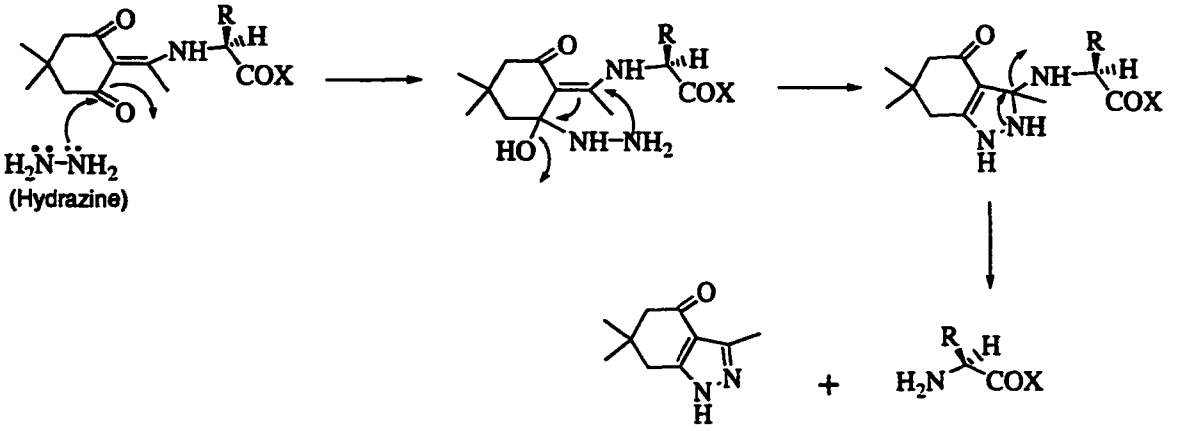

Scheme 2.10 Cleavage mechanism for Dde-protected amino acid or peptide.

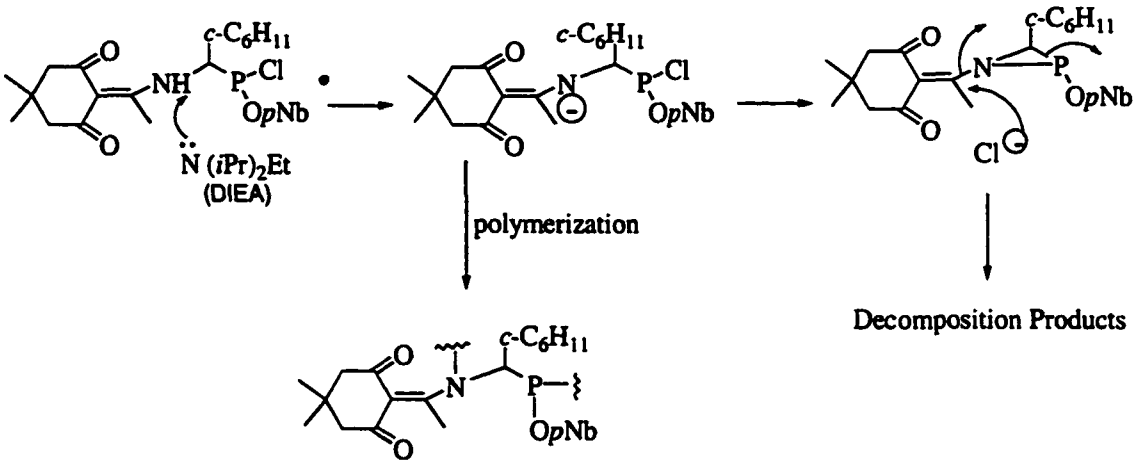

Scheme 2.11 Proposed cleavage mechanisms for Dde-protected phosphonochloridite

However, coupling **8** (2 equiv. **8** with 2 equiv. DIEA) to the Nbs-protected phosphonochloridite resulted in the expectant diastereomeric mixture of phosphonamidites **25** (X = ⁻) (Figure 2.13) along with a small peak around 180 ppm (proposed oxazaphospholine); the intensity of the latter peak was much less than the intensity of the same peak that resulted from the cyclization of the Cbz-protected phosphonochloridite. The formation of the oxazaphospholine could be further reduced by the slow addition (~15-20 min.) of the nucleophile to Nbs-protected phosphonochloridite. With the Dde-protected phosphonochloridite, the peak at 180 ppm

wasn't observed during coupling of **8**, but the overall coupling reaction (Figure 2.14) didn't proceed as well as the reaction with the Nbs phosphonochloridite.

Although cyclization wasn't expected with the Nbs-protected phosphonochloridite **23**, we do believe that it formed to a small extent (evident by ^{31}P ~180 ppm) during the coupling of **8** to **23** in the presence of DIEA. Interestingly, in contrast to Cbz-protected phosphonochloridite **3**, cyclization to the proposed oxazaphospholine doesn't occur to a great extent with the Nbs-protected phosphonochloridite upon addition of two equivalents of DIEA (before coupling). Since very minimal cyclization is observed with **23** in the presence of DIEA, the Nbs group could be employed in phosphonopeptide synthesis with potentially very little racemization.

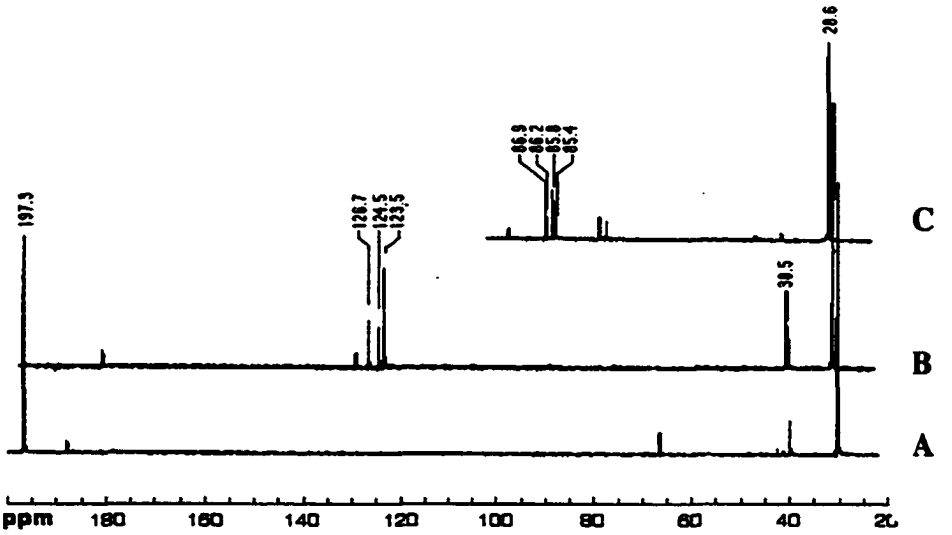

Figure 2.13 ^{31}P NMR spectra of one-pot procedure with Nbs-protected H-phosphinate **21**. **A.** Reaction of **21** with Ph_3PCl_2 in presence of pyridine (2 equiv.) to form a Nbs-protected phosphonochloridite (~197 ppm); peak ~ 28 ppm is Ph_3PO in each spectrum **B.** Coupling of **8** (2 equiv)/DIEA (2 equiv) to Nbs-protected phosphonochloridite to form four phosphonamidites (~ 123-127 ppm);peak ~ 180 ppm corresponds to a proposed oxazaphospholine. **C.** Sulfurization of phosphonamidites to form thiophosphonamides (85.4, 85.8, 86.2, 86.9 ppm); peaks at 75.5 and 76.5 ppm are thiophosphonate acid esters that are form from sulfurization of unreacted ester **21** in the mixture.

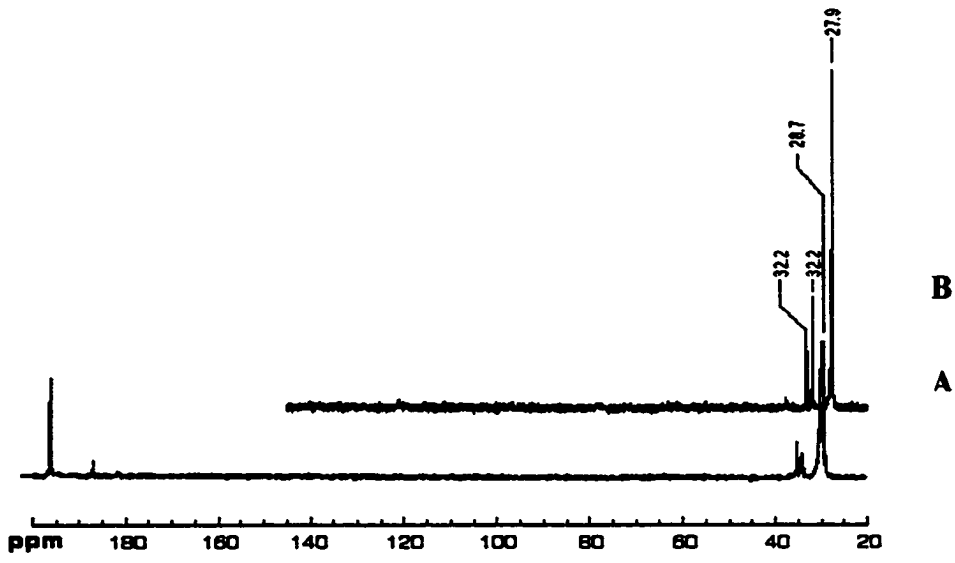

Figure 2.14 ^{31}P NMR spectra of activation and coupling step of one-pot procedure with Dde-protected H-phosphinate **22**. A. Reaction of **22** with Ph_3PCl_2 in presence of pyridine (2 equiv.) to form a Dde-protected phosphonochloridite (~196 ppm); peak ~ 28 ppm is Ph_3PO in each spectrum **B**. Very poor coupling of **8** (2 equiv)/DIEA (2 equiv) to Dde-protected phosphonochloridite to form barely noticeable coupling species ~ 123 ppm.

The ^{31}P spectra in Figures 2.10 and 2.13 resemble each other. In Figure 2.10, the oxazaphospholine 7 wasn't purposely generated, like in Figure 2.2, before amine-coupling. However, we strongly believe that it still partially formed during coupling (2 equiv. of **5b** with 4 equiv. of DIEA) but quickly reacted with the amine nucleophile to form the diastereomeric mixture of phosphonamidites. This is based on the following observation: when two equivalents of **5b** along with only two equivalents of DIEA was allowed to react with the phosphonochloridite **3**, ^{31}P peaks corresponding to both the oxazaphospholine **7** and the expected diastereomeric mixture of phosphonamidites formed to a substantial extent. Conversely, based on data explained above, the formation of an oxazaphospholine plays a very minimal, if any, role during the coupling step of a Nbs-protected phosphonochloridite. Nevertheless, in both Figure 2.10 and Figure 2.13, thiophosphonamides, as a mixture of four diastereomers, is observed.

2.2.4 Use of Resin-bound Ph_3PCl_2

We investigated the potential of a triphenylphosphine-polystyrene resin, on which the activating agent Ph_3PCl_2 can be generated, in the synthesis of our compounds. We were attracted to the resin-bound Ph_3PCl_2 because one of the major contaminants, Ph_3PO, of our one-pot procedure would remain attached to the resin after filtration. The resin-bound Ph_3PCl_2[2.28] was prepared by treating the PS-PPh_3 resin (in glovebox) with one-half equivalent of triphosgene (Figure 2.15). As with our solution-phase synthesis, we initially used two equivalents of pyridine with the H-phosphinate ester **4** during activation with the resin. However, only a tiny activation peak along with other peaks around 19, 35-40, and 165 ppm were observed. Basically, the same types of spectra were observed when 1-1.5 equivalents of base were used during activation. Because the reactions were performed in a glovebox under argon pressure, we reasoned that much less base is probably required during activation because of possible removal of some of the generated HCl by the continuous flow of argon. The activation reaction was then tried with only 0.5 equivalent of pyridine. One peak at 195 ppm resulted. D-Tryptophan methyl ester was added to the filtered solution containing the activated species (^{31}P, 195 ppm). Two coupling peaks (~135 and 136 ppm) resulted (noisy baseline). After sulfurization, a tiny peak (~80 ppm) corresponding to the sulfurized species along with several upfield peaks were observed (Figure 2.16 and Scheme 2.12). FABMS of the crude reaction mixture indicated a tiny m/e peak corresponding to the desired compound minus the *p*Nb group. Therefore, ester cleavage must have occurred during the activation step. Nevertheless, the use of this resin appears to be very promising for the facilitation of the synthesis and

partial purification of phosphonopeptides once the activation conditions has been clearly determined or optimized.

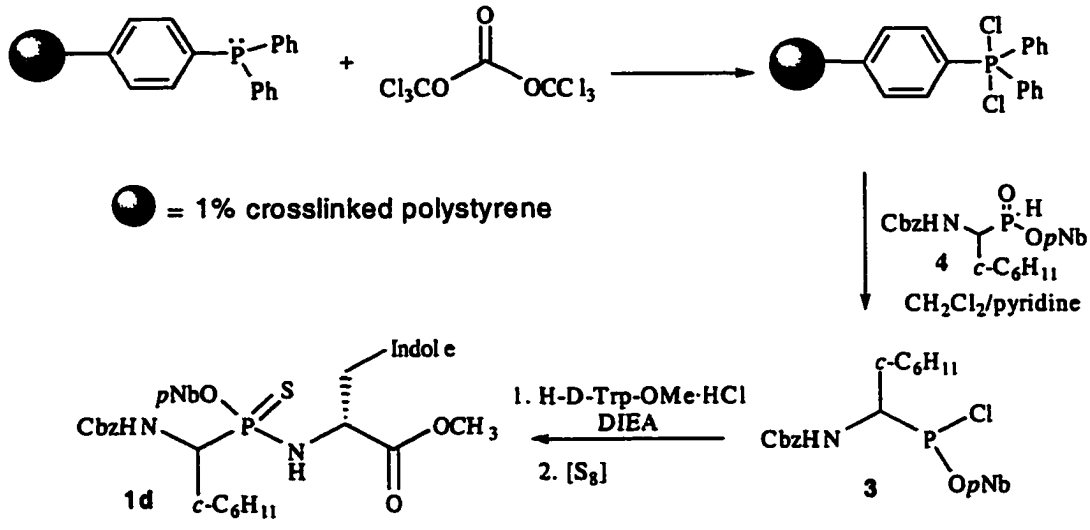

Scheme 2.12 Use of triphenylphosphine-polystyrene resin in preparation of **1d**

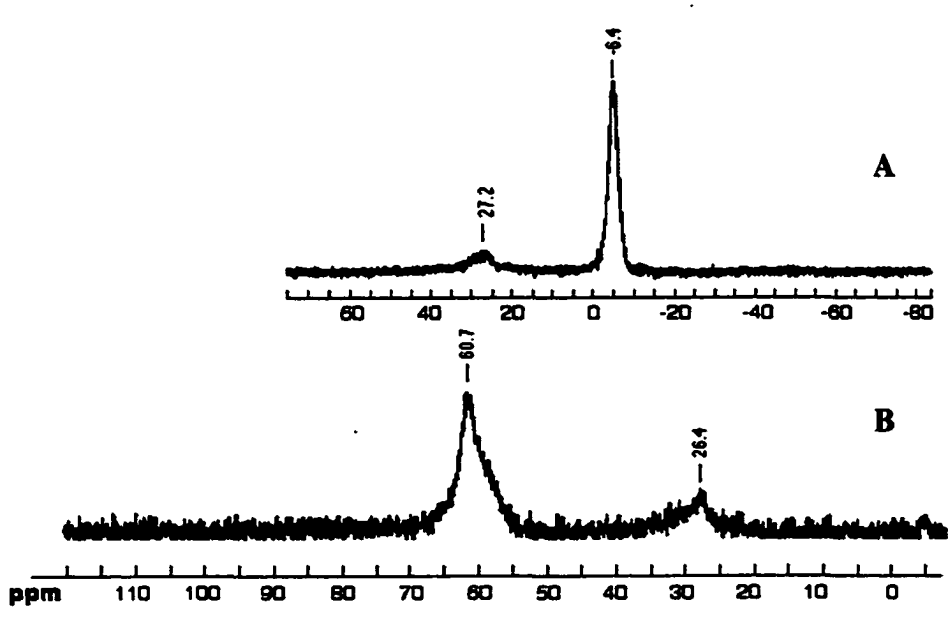

Figure 2.15 Generation of resin-bound Ph_3PCl_2. **A.** Triphenylphosphine (-6.4 ppm) polystyrene resin contaminated with small amount of Ph_3PO (27.2 ppm). **B.** Reaction of Ph_2P-PhPS with triphosgene to form resin-bound Ph_3PCl_2 (60.7 ppm).

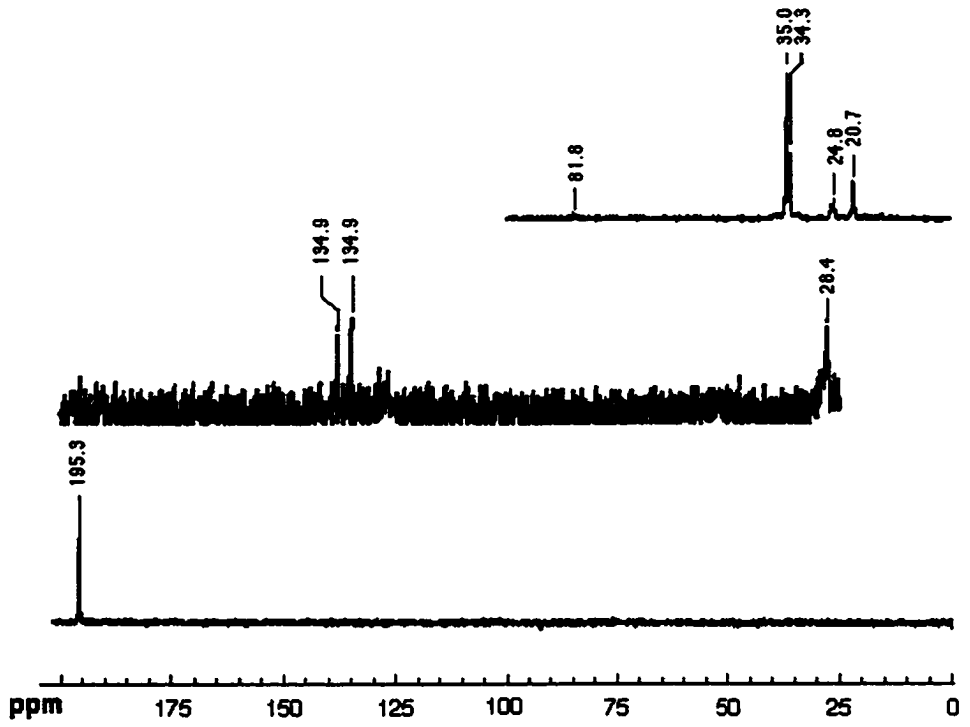

Figure 2.16 ^{31}P NMR spectra of one-pot procedure with resin-bound Ph_3PCl_2. **A.** Reaction of H-phosphinate ester **4** with Cl_2PPh_2-PhPS. **B.** Coupling products (~ 135 and 136 ppm) resulting from the addition of D-tryptophan methyl ester to the activated species (195 ppm); unidentified side-product (28 ppm). **C.** Sulfurized product (81.8 ppm), determined to be **1d** minus the *p*Nb group.

2.2.5 Synthesis of Protected α-Amino-Alkyl-H-Phosphinate Esters

The 1-aminoalkylphosphonous acid **29** was the starting point for the synthesis of the amine-protected H-phosphinate amino acid esters. Compound **29** was prepared according to a procedure adapted from Baylis et al.[2.29] Reaction of the hypophosphonite salt **27**, which is formed from a reaction of hypophosphorus with benzhydrylamine, with cyclohexane aldehyde produced the diphenylmethylaminoalkylphosphonous acid **28**. The latter acid was subsequently deprotected in refluxing HBr to afford **29** in 61% yield (Scheme 2.13).

Scheme 2.14 outlines the synthesis of Z- or Cbz-protected phosphonous acid **30** and Nbs-protected phosphonous acid **31**. A procedure developed by Dumy *et al*[2.30] was

employed. They were prepared primarily by adding a solution of N-(benzyloxy-carbonyl) succinimide or 2-nitrobenzenesulfonyl chloride in dioxane to a solution of **29** in water at a controlled pH (9-9.5 using 4 N NaOH). Compound **30** and **31** were obtained in 77% and 76% yield, respectively.

Dde-protected phosphonous acid **32** was prepared according to a procedure described by Bolin et al.[2.31] In general compound **29** and TMS-Cl were refluxed in CH_2Cl_2 for 2 hours and then, after cooling to 4 °C, 5,5-dimethyl-2-acetyl-1,3-cyclohexanedione and DIEA were added. Compound **32** was obtained in a 37% yield.

Esterification of the protected phosphonous acids **30** and **31** (Scheme 2.14) and **32** (Scheme 2.15) were prepared according to a procedure described by Sampson and Bartlett.[2.32] To a solution of **30**, **31**, or **32** in CH_2Cl_2 was added EDC. The H-phosphinates **4**, **21**, and **22** were formed as mixture of two diastereomers in yields of 82%, 94%, and 56%, respectively.

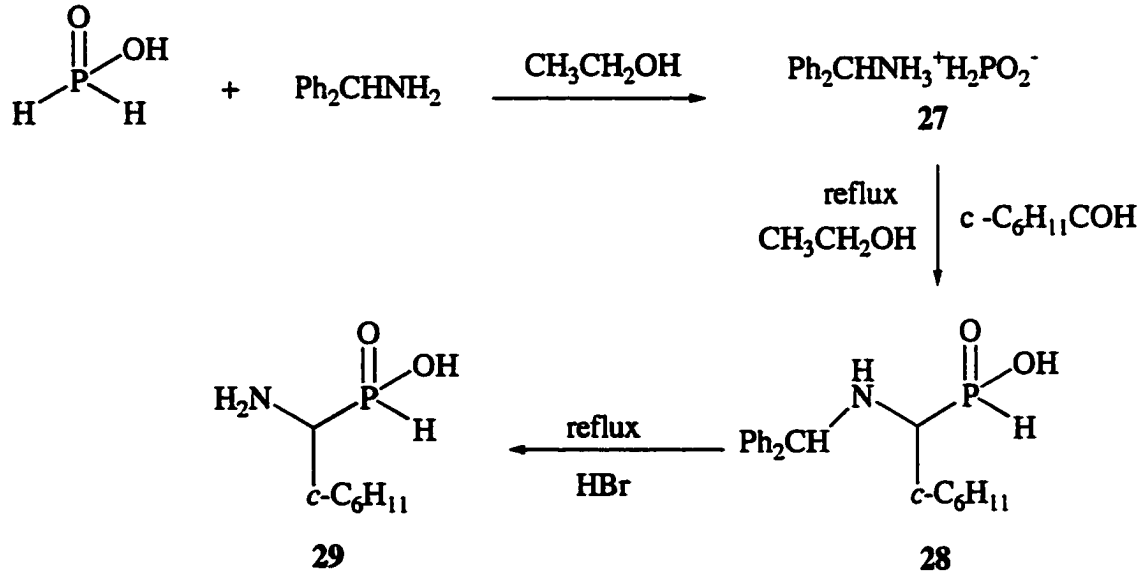

Scheme 2.13 Synthesis of 1-aminoalkylphosphonous acid **29**

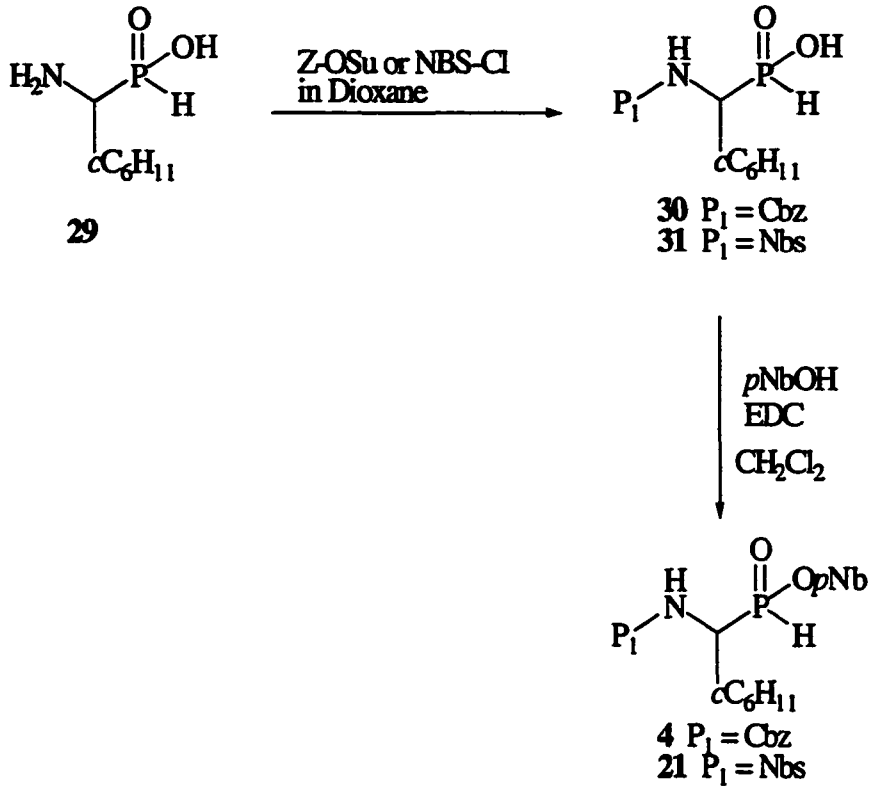

Scheme 2.14 Synthesis of Cbz- and Nbs-Protected H-Phosphinate Esters

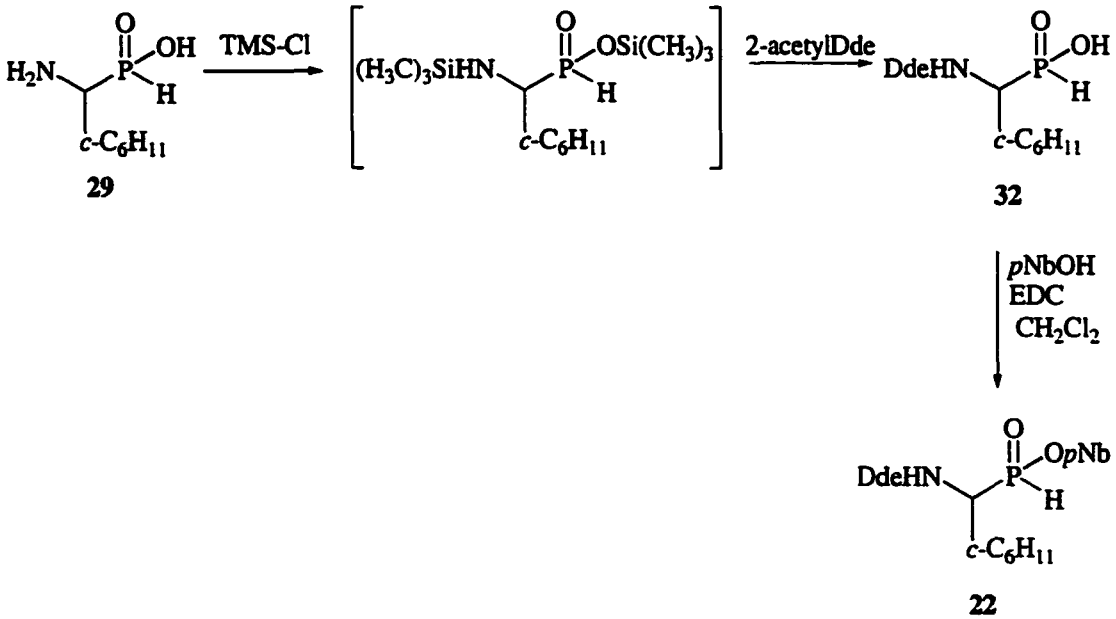

Scheme 2.15 Synthesis of Dde-protected H-phosphinate ester **22**

2.3 Conclusions

We developed conditions, based on a one-pot activation-coupling-oxidation/sulfurization protocol,[2.10] for preparation of sterically hindered phosphonamide and thiophosphonamide dipeptides. It was determined via a GC-MS Study that the presence of 2 equivalents of pyridine during activation of our H-phosphinate amino acid ester **4** with Ph_3PCl_2 was necessary to prevent ester cleavage; however, using excess base (more than 2 equivalents) or a base that is too strong (e.g., triethylamine) could result in the formation of several side-products (evident from ^{31}P NMR). We proposed that an oxazaphospholine was forming during the coupling step and was competing with the formation of the desired phosphonamidites. After discovering that it was a reactive phosphitylating agent, it was purposely generated by addition of DIEA to **3** before addition of a nucleophile. This coupling route generally led to the formation of two coupling, diastereomeric products instead of the possible four. This was attributed to, in part, to the formation of only the trans conformer (plus its enantiomer) of the oxazaphospholine **7**. Oxidation and sulfurization were easily accomplished with *t*-butylhydroperoxide and elemental sulfur, respectively. Using our developed conditions, we prepared the previously inaccessible phosphonamide **1a** (hapten precursor) and related derivatives **1b-d**. We also applied our method to the preparation of the thiophosphonates **19-20**, thiophosphonamides **12-13**, and phosphonamide **14**. Compound **12** and **19** were purified by flash chromatography, but the other products were purified by reverse-phase HPLC. All of the final products were characterized by ^{31}P NMR, ^{1}H NMR, and FABMS.

2.4 Experimental Material

2.4.1 Technical Information

Unless otherwise indicated, materials were purchased from commercial suppliers and used without further purification. All reactions were performed in dry glassware under an atmosphere of argon. Triethylamine was dried by refluxing over CaH_2 and distilling directly onto dry molecular sieves (3Å). Anhydrous dichloromethane, pyridine, and diisopropylethylamine were purchased from Aldrich. Dichlorotriphenylphosphine (95 % purity, Aldrich) was stored and manipulated in a dry box. NMR spectra were obtained either on a Bruker AC-250 (^1H, ^{31}P) or AC-400 (^1H, ^{31}P) spectrometer. All ^{31}P NMR spectra were externally referenced against 85 % H_3PO_4. Gas chromatography was performed on a Hewlett Packard 5971A instrument with a crosslinked capillary column (10m x 0.53mm, 2.0 um film thickness) and the following temperature programming: $T_{initial}$ 40 °C for 2 minutes then 35 °C/min. up to T_{final} 270 °C. Preparative HPLC was carried out on a Waters 15-μm Deltapak C_4 column (25 x 100 cm) using a mobile phase of acetonitrile (10 %, v/v, 0.05 M aqueous triethylammonium acetate) and 0.1 M ammonium acetate buffer and a gradient of 50-100 % of the organic phase over 1 hour. Mass spectrometry (FABMS) was performed at Louisiana State University and University of Nebraska-Lincoln Mass Spectrometry facilities. Elemental analyses were performed by MHW Laboratories (Phoenix, AZ).

2.4.2 General Procedure

At room temperature, a solution of dichlorotriphenylphosphorane (60 mg, 0.18 mmol) in dichloromethane (0.28 mL) was added to a solution of the H-phosphinate amino acid ester **4** (0.15 mmol) in CH_2Cl_2 (0.7 mL) and pyridine (0.023 mL, 0.29 mmol).

After 30 minutes, diisopropylethylamine (0.22 mmol) was added to the reaction mixture followed, after 15 minutes, by the addition of the nucleophile (0.29 mmol for amines, 0.22 mmol for alcohols) in one portion. After an additional 15 minutes, elemental sulfur (5 mg, 0.15 mmol) or anhydrous t-butyl peroxide (5.5 M in decane, 0.04 mL, 0.22 mmol) was added. About 30 minutes later the reaction mixture was concentrated, and the resulting residue was triturated with ethyl acetate (3 x 2 mL). The combined ethyl acetate fractions were washed with $NaHCO_3$ (2 x 3 mL) and brine (6 mL), dried with Na_2SO_4, and then evaporated to give an oily residue. The compounds were isolated using reversed-phase HPLC (except were noted) and characterized by ^{31}P NMR, ^{1}H NMR, and FABMS.

2.4.3 Synthesis and Characterization of 1-Amino-1-Cyclohexylmethane-phosphonous acid

The following compounds were obtained and used in the preparation of compound **29**.

_N_-(diphenylmethyl) ammonium phosphonite (27)[2.28]

Anhydrous hypophosphorus acid (5.94 g, 90 mmol) was dissolved in ethanol (225 mL). Benzhydrylamine (15.5 mL, 90 mmol) was then added to the reaction flask and stirred for 30 minutes. The solvent was removed with rotary evaporation, and the white phosphonite crystals were dried under high vacuum. Yield: 22 g (98%). ^{31}P NMR (101 MHz, EtOH) 1.06 ppm.

1-benzhydrylamino-1-cyclohexylmethanephosphonous acid (28)

The phosphonite salt **27** (4.95 g, 19.79 mmol) and cylcohexane carboaldehyde (2.40 mL, 19.79 mmol) were dissolved in absolute ethanol, and the reaction mixture was heated at reflux for 4 hours. A precipitate of the diphenylmethylaminophosphonous acid

formed upon cooling of the solution. The precipitate was collected by filtration, washed with ethanol and ether, and dried under high vacuum. Yield: 3.73 g (55%). ^{31}P NMR (101 MHz, DMSO) 27 ppm.

1-amino-1-cyclohexylmethanephosphonous acid (29)

An excess of 48% HBr (19 mL) was added to a flask containing the phosphonous acid **28** (3.73 g, 10.89 mmol). The mixture was refluxed for 1 hour and 30 minutes. The reaction solution was allowed to cool and then taken up in water (30 mL) and washed with ether (3 x 10 mL). Rotary evaporation removed the water, and the resulting solid was dissolved in methanol (60 mL). Then propylene oxide was added until precipitation started. The white precipitate was collected by filtration, washed with ethanol and ether, and then dried under high vacuum. Yield: 1.17 g (61%). ^{1}H NMR (250 MHz, D_2O) 1.35 (m, 11H, c-C_6H_{11}), 2.98 (m, 1H, CH), 7.15 (d, J_{PH} = 525 Hz, 1H, PH) ; ^{31}P NMR(101 MHz, D_2O) 18 ppm. FABMS (glycerol) m/e 178.2 $(M + H)^+$; C, 47.46; H, 9.01; N, 7.90; found C, 47.65; H, 8.81; N, 7.91.

2.4.4 Synthesis and Characterization of Protected 1-Amino-1-Cyclohexylmethanephosphonous acids

1-[*N*-(benzyloxycarbonyl)amino]-1 cyclohexylmethanephosphonous acid (30)

The phosphonous acid **29** (0.567 g, 3.20 mmol) was taken up in H_2O (8 mL). The acid dissolved after the pH was adjusted to about 9.5 with 4N NaOH. Then a solution of *N*-(benzyloxycarbonyloxy)succimide (0.867 g, 3.52 mmol) in dioxane (4 mL) was added over a period of 15 minutes. The pH was periodically checked and adjusted to 9.5. After stirring at room temperature for six hours, the reaction mixture was extracted with ether (2 x 6 mL). 6 N HCl (12 mL) was added to the aqueous phase. The white precipitate was collected by filtration and was dried under high vaccum. Yield: 0.769 g (77%). ^{1}H

NMR (250 MHz, CD_3OD) 1.35 (m, 11H, c-C_6H_{11}), 3.45 (m, 1H, CH), 5.05 (s, 2H, $PhCH_2$), 5.38 (br s, 1H, NH), 7.12 (d, J_{PH} = 575 Hz, 1H, PH)) 7.33 (m, 5H, Ph); ^{31}P NMR (101 MHz, CD_3OD) 30 ppm. FABMS (glycerol) m/e 311.7 $(M + H)^+$; C, 58.01; H, 6.70; N, 4.50; found C, 57.81; H, 6.61; N, 4.55.

1-[*N*-(2-nitrobenzenesulfonyl)amino]-1 cyclohexylmethanephosphonous acid (31)

The phosphonous acid **29** (0.682 g, 3.85 mmol) was taken up in H_2O (10 mL). The acid dissolved after the pH was adjusted to about 9.5 with 4N NaOH. This solution was brought to 4 °C , and then a solution of 2-nitrobenzenesulfonyl chloride (0.939 g, 4.24 mmol) in dioxane (4 mL) was added over a period of 15 minutes. The pH was periodically checked and adjusted to 9.5. After stirring at 4 °C for six hours, the reaction mixture was allowed to warm to room temperature. It was extracted with ether (2 x 6 mL). 6 N HCl (14 mL) was added to the aqueous phase. The white precipitate was collected by filtration and was dried under high vaccum. Yield: 1.07 g (94%). ^1H NMR (250 MHz, DMSO) 1.53 (m, 11H, c-C_6H_{11}), 3.25 (m, 1H, CH), 4.85 (d, J_{PH} = 525 Hz, 1H, PH), 8.12 (m, 4H, Ph), 8.56 (d, 1H, NH), ^{31}P NMR (101 MHz, DMSO) 30 ppm. FABMS (3-NBA) m/e 363.0 $(M + H)^+$; C, 43.11; H, 5.25; N, 7.73; found C, 42.90; H, 5.50; N, 7.69.

1-[*N*-(4,4-dimethyl-2,6-dioxocyclohexylidene ethyl) amino]-1-cyclohexylmethanephosphonous acid (32)

The phosphonous acid **29** (0.823 g, 4.65 mmol) was placed in a flask equipped with a condenser, heating mantle, and an argon inlet. Dry CH_2Cl_2 (12 mL) was added to the reaction vessel and stirred vigorously. TMS-Cl (1.18 mL, 9.31 mmol) was added in one portion. The mixture was refluxed for 2 hours and then cooled in an ice bath. DIEA (1.45 mL, 8.37 mL) and 2-acetyldimedone (0.564 g, 3.10 mmol) were added in

succession. The reaction mixture was stirred with cooling for 20 minutes and then warmed to room temperature for 2 hours. The reaction mixture was concentrated and then distributed between Et_2O (25 mL) and 2.5% $NaHCO_3$ (50 mL). The aqueous layer was extracted with 2 x 20 mL of Et_2O. The aqueous layer was then acidified to pH 2 with 1 N HCl and extracted with 3 x 15 mL of EtOAc. The combined aqueous layers were then dried over Na_2SO_4, filtered, concentrated, and dried *in vacuo*. Appropriate solvents were used to recrystallized the final product. Yield after recrystallization: 0.40 g (37%). ^{1}H NMR (250 MHz, DMSO) 0.98 (s, 6H, $(CH_3)_2$) 1.53 (m, 11H, c-C_6H_{11}), 2.25 (s, 3H, CH_3), 2.50 (s, 4H, $2CH_2$) 4.15 (m, 1H, CH), 7.00 (d, J_{PH} = 500 Hz, 1H, PH), 13.5 (d, 1H, NH), ^{31}P NMR (101 MHz, DMSO) 24 ppm. FABMS (3-NBA) m/e 342.1 $(M + H)^+$; C, 59.80; H, 8.21; N, 4.10; found C, 59.73; H, 8.37; N, 3.99.

2.4.5 Synthesis and Characterization of Protected 1-Amino-1-Cyclohexylmethane-H-Phosphinate Esters

1-[*N*-(benzyloxycarbonyl)amino]-1-cyclohexylmethanephosphonous acid, *p*-nitrobenzyl ester [Cbz-CyhGly ψ [POH(O*p*Nb)] (4)

According to the procedure described by Sampson and Bartlett, EDC (0.698 g, 3.64 mmol) was added to a solution of the Cbz-protected phosphonous acid **30** (0.566 g, 1.82 mmol) and para-nitrobenzyl alcohol (0.279 g, 1.82 mmol) in anhydrous CH_2Cl_2 (10 mL). After stirring at room temperature for 10 hours, the solution was diluted with EtOAc (100 mL), washed with saturated KH_2PO_4 (2 x 50 mL) , saturated $NaHCO_3$ (50 mL), and brine (50 mL), dried over Na_2SO_4, filtered, and evaporated to dryness. A white powder was obtained. Yield: 0.67 g (82%). ^{1}H NMR (250 MHz, $CDCl_3$) 1.38 (m, 11H, c-C_6H_{11}), 3.92 (m, 1H, CH-P), 5.10 (s, 2H, CH_2OOC), 5.42 (d, 2H, CH_2OP), 5.44 (br s, 1H, NH), 7.12 (d, JPH = 560 Hz, 1H, P-H), 7.33 (m, 5H, Ph), 7.89 (d, 2H, Ph-NO2), 8.18

(d, 2H, Ph-NO_2); ^{31}P NMR (101 MHz, $CDCl_3$) 36.1 and 37.1 ppm (1:1.1); FABMS (NBA) m/e 447.8 $(M + H)^+$; C, 59.22; H, 5.83; N, 6.27; found C, 59.36; H, 5.89; N, 6.15.

1-[*N*-(2-nitrobenzenesulfonyl)amino]-1 cyclohexylmethanephosphonous acid, *p*-nitrobenzyl ester (21)

To a solution of the NBS-protected phosphonous acid **31** (0.615 g, 1.70 mmol) and para-nitrobenzyl alcohol (0.260 g, 1.70 mmol) was added EDC (0.487 g, 2.54 mmol) in anhydrous CH_2Cl_2 (10 mL). After stirring at room temperature for 10 hours, the solution was diluted with EtOAc (100 mL), washed with saturated KH_2PO_4 (2 x 50 mL), saturated $NaHCO_3$ (50 mL), and brine (50 mL), dried over Na_2SO_4, filtered, and evaporated to dryness. A white powder was obtained. Yield: 0.67 g (94%). ^1H NMR (250 MHz, $CDCl_3$) 1.55 (m, 11H, c-C_6H_{11}), 3.85 (m, 1H, CH-P), 5.20 (m, 2H, CH_2OP), 5.35 (d, J_{PH} = 510 Hz, 1H, P-H), 7.85 (d, 2H, Ph-NO2), 8.20 (m, 4H, $PhSO_2$) 8.35 (d, 2H, Ph-NO_2) 8.62 (s, 1H, NH); ^{31}P NMR (101 MHz, $CDCl_3$) 35.5 and 36.5 ppm; FABMS (3-NBA) m/e 498.1 $(M + H)^+$; C, 48.30; H, 4.83; N, 8.50; found C, 48.44; H, 5.00; N, 8.57.

1-[*N*-(4,4-dimethyl-2,6-dioxocyclohexylidene ethyl) amino]-1-cyclohexylmethanephosphonous acid, para-nitrobenzyl ester (22)

To a solution of the Dde-protected phosphonous acid **32** (0.133 g, 0.389 mmol) and para-nitrobenzyl alcohol (0.0596 g, 0.389 mmol) was added EDC (0.170 g, 0.887 mmol) in anhydrous CH_2Cl_2 (5 mL). After stirring at room temperature for 10 hours, the solution was diluted with ethyl acetate (50 mL), washed with saturated KH_2PO_4 (2 x 25 mL), saturated sodium bicarbonate (25mL), and brine (25 mL), dried over Na_2SO_4, filtered, and evaporated to dryness. A white powder was obtained. Yield: 0.11 g (57%). ^1H NMR (250 MHz, DMSO) 1.1 (s, 6H, $(CH_3)_2$) 1.50 (m, 11H, c-C_6H_{11}), 2.35 (s, 3H, CH_3), 2.62 (s, 4H, $2CH_2$) 4.15 (m, 1H, CH), 5.25 (m, 2H, CH_2Ph), 7.15 (d, J_{PH} = 530 Hz,

1H, PH), 7.8 (d, 2H, PhNO2), 8.44 (d, 2H, PhNO2), 14.1 (br s, 1H, NH), ^{31}P NMR (101 MHz, DMSO) 32.9, 34.4 ppm. FABMS (3-NBA) m/e 477.1 $(M + H)^+$; C, 60.51; H, 6.93; N, 5.88; found C, 60.69; H, 7.05; N, 5.86.

2.4.6 Preparation of Oxazaphospholine 7 using PS-DIEA Resin

In a glovebox, the phosphonochloridite **3** (0.05 g, 0.11 mmol) in CH_2Cl_2 (0.5 mL) was added to a suspension of PS-DIEA resin (3.68 mmol/g (loading), 0.06 g, 0.21 mmol) in dichloromethane. The reaction mixture stirred at room temperature for 30 minutes. Then the resin was filtered and washed with anhydrous CH_2Cl_2 (3 x 0.2 mL). Major ^{31}P NMR (101 MHz, CH_2Cl_2) peaks of filtrate: 180 ppm (proposed oxazaphospholine **7**), 27 ppm (triphenylphosphine oxide). No signal was detected on the solid support by gel ^{31}P NMR.

2.4.7 Synthesis and Characterization of Complex Phosphonamide and Thiophosphonamide Dipeptides

Cbz-CyhGly ψ [P (O) (OPNB) NH] Trp-NH_2 (1a)

It was prepared according to the general procedure. Yield: (18%). ^{1}H NMR (250 MHz, CD_3CN) 1.5 (m, 11H, c-C_6H_{11}), 3.2 (m, 2H, CH_2-indole), 4.0 (m, 1H, CH-P), 4.5 (m, 1H, $CHCONH_2$), 5.1 (m, 4H, $CH_2OOC + CH_2OP$), 5.7 (m, 3H, $NHP + NH_2$), 6.5 (br d, 1H, NHCO), 7.2 (m, 4H, indole), 7.4 (d, 1H, vinylic), 7.6 (m, 5H, C_6H_5), 7.7 (d, 2H, Ph), 8.2 (d, 2H, Ph) 9.2 (br s, 1H, NH-indole); ^{31}P NMR (101 MHz, CD_3CN) 28 and 29 ppm. FABMS (3-NBA) m/e 648.2 $(M + H)^+$.

Cbz-CyhGly ψ [P (S) (OPNB) NH] Trp-NH_2 (1b)

It was prepared according to the general procedure. Yield: (14%) ^{1}H NMR (250 MHz, CD_3CN) 1.5 (m, 11H, c-C_6H_{11}), 3.2 (m, 2H, CH_2-indole), 4.0 (m, 1H, CH-P), 4.5 (m, 1H, $CHCONH_2$), 5.1 (m, 4H, $CH_2OOC + CH_2OP$), 6.0 (m, 3H, $NHP + NH_2$), 6.5 (br

d, 1H, NHCO), 7.1 (m, 4H, indole), 7.3 (d, 1H, vinylic), 7.5 (m, 5H, C_6H_5), 7.7 (d, 2H, Ph), 8.1 (d, 2H, Ph) 9.2 (br s, 1H, NH-indole); ^{31}P NMR (101 MHz, CD_3CN) 28 and 29 ppm. FABMS (3-NBA) m/e 664.1 $(M + H)^+$.

Cbz-CyhGly ψ [P (O) (OPNB) NH] Trp-OMe (1c)

It was prepared according to the general procedure. Yield: (15%) ^1H NMR (250 MHz, CD_3CN) 1.5 (m, 11H, c-C_6H_{11}), 3.3 (m, 2H, CH_2-indole), 3.5 (s, 3H, OCH_3), 3.7 (m, 1H, CH-P), 4.3 (m, 2H, $CHCOOCH_3$ + PNH), 4.9 (m, 4H, CH_2OOC + CH_2OP), 5.8 (dd, 1H, NHOC), 7.0 (m, 4H, indole), 7.2 (d, 1H, vinylic), 7.5 (m, 5H, C_6H_5), 7.7 (d, 2H, Ph), 8.1 (d, 2H, Ph) 9.3 (br s, 1H, NH-indole); ^{31}P NMR (101 MHz, CD_3CN) 28 and 29 ppm. FABMS (3-NBA) m/e 663.2 $(M + H)^+$.

Cbz-CyhGly ψ [P (S) (OPNB) NH] Trp-OMe (1d)

It was prepared according to the general procedure. Yield: (30%) ^1H NMR (250 MHz, CD_3CN) 1.5 (m, 11H, c-C_6H_{11}), 3.2 (m, 2H, CH_2-indole), 3.6 (s, 3H, OCH_3), 4.1 (m, 1H, CH-P), 4.4 (m, 2H, $CHCOOCH_3$ + PNH), 4.9 (m, 4H, CH_2OOC + CH_2OP), 5.7 (dd, 1H, NHCO), 7.2 (m, 4H, indole), 7.4 (d, 1H, vinylic), 7.6 (m, 5H, C_6H_5), 7.7 (d, 2H, Ph), 8.2 (d, 2H, Ph) 9.2 (br s, 1H, NH-indole); ^{31}P NMR (101 MHz, CD_3CN) 28 and 29 ppm. FABMS (3-NBA) m/e 678.2 $(M + H)^+$.

Synthesis of Cbz-CyhGly ψ [P (S) (OPNB) NH] Trp-OMe (1d) using PS-Ph_3PCl_2

In a glovebox, the H-phosphinate ester 4 (0.05 g, 0.11 mmol) in CH_2Cl_2 (1mL) and pyridine (4 μL, 0.06 mmol) was added to the PS-Ph_3PCl_2 resin (1.24 mmol/g, 0.2 g, 0.176 mmol, Argonaut Technologies), which was suspended in CH_2Cl_2 (~ 1 mL). The reaction mixture was periodically stirred for 1.5 hours, and then the activated species was filtered from the resin. ^{31}P NMR (101 MHz, CH_2Cl_2) of activated species: 195 ppm.

Under argon, a solution of D-tryptophan methyl ester (0.04 g, 0.16 mmol) in CH_2Cl_2 (0.5 mL) was added dropwise over 15 minutes to the activated species. After 30 minutes, a ^{31}P NMR spectrum was taken. The coupling peaks resonated around 135 and 137 ppm. To the resulting phosphonamidites was added elemental sulfur (3 mg, 0.11 mmol). The sulfurized species resonated around 81 ppm. FABMS (NBA) m/e 541.2 (Desired mass-*p*Nb).

2.4.8 Synthesis and Characterization of Thiophosphonamides, Phosphonamides, and Thiophosphonates

Cbz-CyhGly ψ [P (S) (OPNB) NH] Leu-OMe (12)

It was prepared according to the general procedure (0.23 mmol scale) and purified by pressure alumina chromatography using EtOAc-Hexane (1:1) as the eluent. Yield: 39 mg (28%). ^{1}HNMR (250 MHz, CD_3CN) 0.88 (d, 6H, $(CH_3)_2$), 1.20 (m, 1H, $CH(CH_3)_2$), 1.73 (m, 11H, c-C_6H_{11}), 3.18 (m, 2H, CH_2), 3.62 (s, 3H, OCH_3), 4.14 (m, 1H, CH-P), 4.4 (m, 1H, $CHCOOCH_3$ + PNH), 5.02 (m, 4H, CH_2OOC + CH_2OP), 5.87 (d, 1H, NHCO), 7.36 (m, 5H, C_6H_5), 7.57 (d, 2H, Ph), 8.22 (d, 2H, Ph); ^{31}P NMR (101 MHz, CD_3CN) 86.9 and 88.3 ppm. FABMS (3-NBA) m/e 606.3 $(M + H)^+$.

Cbz-CyhGly ψ [P (S) (OPNB) NH] Gly-OEt (13)

It was prepared according to the general procedure (0.14 mmol scale). Yield: 20 mg (26%). ^{1}H NMR (250 MHz, CD_3CN) 0.95 (d, 3H, CH_3), 1.65 (m, 11H, c-C_6H_{11}), 2.75 (m, 2H, CH_2), 3.98 (m, 1H, CH-P), 4.23 (q, 2H, OCH_2CH_3), 5.02 (m, 3H, CH_2OOC + PNH), 5.52 (s, 2H, OCH_2Ph), 5.89 (d, 1H, NHCO), 7.36 (m, 5H, C_6H_5), 7.50 (d, 2H, Ph), 8.15 (d, 2H, Ph); ^{31}P NMR (101 MHz, CD_3CN) 89.7 ppm. FABMS (3-NBA + Li) m/e 570.2 $(M + Li)^+$.

Cbz-CyhGly ψ [P (O) (OPNB) NH] Gly-OEt (14)

It was prepared according to the general procedure (0.14 mmol scale). Yield: 16 mg (21%). ^{1}H NMR (250 MHz, CD_3CN) 0.95 (d, 3H, CH_3), 1.66 (m, 11H, c-C_6H_{11}), 2.75 (m, 2H, CH_2), 3.95 (m, 1H, CH-P), 4.20 (q, 2H, OCH_2CH_3), 5.00 (m, 3H, CH_2OOC + PNH), 5.52 (s, 2H, OCH_2Ph), 5.87 (d, 1H, NHCO), 7.36 (m, 5H, C_6H_5), 7.50 (d, 2H, Ph), 8.15 (d, 2H, Ph); ^{31}P NMR (101 MHz, CD_3CN) 39.2 ppm. FABMS (3-NBA + Li) m/e 554.2 $(M + Li)^+$.

Cbz-CyhGly ψ [P (S) (O*p*Nb) (OBn)] (19)

It was prepared according to the general procedure (0.22 mmol scale) and purified by flash chromatography (silica) using EtOAc-Hexane (1:5) as the eluent. Yield: 19 mg (15%). ^{1}H NMR (250 MHz, $CDCl_3$) 1.55 (m, 11H, c-C_6H_{11}), 4.25 (m, 1H, CH-P), 5.12 (m, 7H, $3CH_2$ + NH), 7.35 (m, 10H, $2C_6H_5$), 7.50 (d, 2H, Ph), 8.18 (d, 2H, Ph); ^{31}P NMR (101 MHz, $CDCl_3$) 95.1 ppm. HRMS (ESI/FTMS (CH_2Cl_2)) m/e 569.1862 $(M + H)^+$.

Cbz-CyhGly ψ [P (S) (OPNB) O] Ala-OMe (20)

It was prepared according to the general procedure (0.11 mmol scale). Yield: 19 mg (30%). ^{1}H NMR (250 MHz, CD_3CN) 1.53 (m, 11H, c-C_6H_{11}), 2.85 (m, 3H, CH_3), 4.26 (m, 1H, CH-P), 5.28 (m, 5H, $2CH_2$ + PNH), 5.89 (dd, 1H, NHCO), 7.36 (m, 5H, C_6H_5), 7.45 (d, 2H, Ph), 8.15 (d, 2H, Ph); ^{31}P NMR (101 MHz, CD_3CN) 96.4, 97.3 ppm. FABMS (3-NBA) m/e 565.2 $(M + H)^+$.

2.5 References

2.1 Kaplan, A. P.; Bartlett, P. A. *Biochemistry* **1991**, 30, 8165.

2.2 Bertenshaw, S. R.; Rogers, R. S.; Stern, M. K.; Norman, B. H. *J. Med. Chem.* **1993**, 36, 173.

2.3 Bartlett, P. A.; Hanson, J. E.; Giannousis, P. P. *J. Org. Chem.* **1990**, 55, 6268.

2.4 Ikeda, S.; Ashley, J. A.; Wirsching, P.; Janda, K. D. *J. Am. Chem. Soc.* **1992**, 114, 76.

2.5 Giannousis, P. P.; Bartlett, P. A. *J. Med. Chem.* **1987**, 26, 1603.

2.6 Barelli, H.; Dive, V.; Yiotakis, A.; Vincent, J. P.; Checler, F. *Biochem. J.* **1992**, 287, 621.

2.7 Allen, J. G.; Atherton, F. R.; Hall, M. J.; Hassall, C. H.; Holmes, S. W.; Lambert, R. W.; Nisbet, L. J.; Ringrose, P. S. *Nature* **1978**, 272, 56.

2.8 Lejczak, B.; Kafarski, P.; Sztajer, H.; Mastalerz, P.; *J. Med. Chem.* **1986**, 29, 2212.

2.9 Hirschmann, R.; Smith, A. B., III; Taylor, C. M.; Benkovic, P. A.; Taylor, S. D.; Yager, K. M.; Sprengeler, P. A.; Benkovic, S. J. *Science* **1994**, 265, 234.

2.10 Fernandez, M. d. F.; Vlaar, C. P.; Fan, H.; Liu, Y.-H.; Fronczek, F. R.; Hammer, R. P. *J. Org. Chem.* **1995**, 60, 7390.

2.11 Smith, A. B., III; Taylor, C. M.; Benkovic, P. A.; Taylor, S. D.; Hirschmann, R. *Tetrahedron Lett.* **1994**, 35, 6853.

2.12 Hirschmann, R.; Yager, K. M.; Taylor, C. M.; Witherington, J.; Sprengeler, P. A.; Phillips, B. W.; Moore, W.; Smith, A. B., III. *J. Am. Chem. Soc.* **1997**, 119, 8177.

2.13 Rahil, J.; Haake, P. *J. Am. Chem. Soc.* **1981**, 103, 1723.

2.14 Yamauchi, K.; Ohtsuki, S.; Kinoshia, M. *J. Org. Chem.* **1984**, 49, 1158.

2.15 Elliot, R. L.; Marks, N.; Berg, M. J.; Portoghese, P. S. *J. Med. Chem.* **1985**, 28, 1208.

2.16 Mucha, A. ; Kafarski, P. *Tetrahedron* **1994**, 50, 12743.

2.17 Relles, H. M.; Schluenz, R. W. *J. Am. Chem. Soc.* **1974**, 96, 6469.

2.18 Musiol, Hans J.; Grams, F.; Rudolph-Bohner, S.; Moroder, L. *J. Org. Chem.* **1994**, 59, 6144.

2.19 Malachowski, W. P.; Coward, J. K. *J. Org. Chem.* **1994**, 59, 7616.

2.20 Maffre-Lafon, D.; Escale, R.; Girard, J. P. *Tetrahedron Lett.* **1994**, 35, 4097.

2.21 Jacobsen, N. E.; Bartlett, P. A. *J. Am. Chem. Soc.* **1981**, 103, 654.

2.22 Thorsett, E. D.; Harris, E. E.; Peterson, E. R.; Greenlee, W. J.; Patchett, A. A.; Ulm, E. H.; Vassil, T. C. *Proc. Natl. Acad. Sci. U. S. A.* **1982**, 79, 2176.

2.23 Benoiton, N. L. In *The Peptides*; Undenfriend, S., Meienhofer, J., Eds.; Academic Press: San Diego, CA **1983**; Vol. 5, Chapter 4.

2.24 Miller, S. C.; Scanlan, T. S. *J. Am. Chem. Soc.* **1998**, 120, 2690.

2.25 Bycroft, B. W.; Chan, W. C.; Chhabra, S. R.; Teesdale-Spittle, P. H.; Hardy, P. M. *J. Chem. Soc., Chem. Commun.* **1993**, 776.

2.26 Bycroft, B. W.; Chan, W. C.; Chhabra, S. R.; Hone, N. D. *J. Chem. Soc., Chem. Commun.* **1993**, 778.

2.27 Vedejs, E.; Kongkittingam, C. *J. Org. Chem.* **2000**, 65, 2309.

2.28 Wells, A. *Synthetic Commun.* **1994**, 24, 1715.

2.29 Baylis, E. K.; Campbell, C. D.; Dingwall, J. G. *J. Chem. Soc. Perkin Trans. 1* **1984**, 2845.

2.30 Dumy, P.; Escale, R.; Girard, J. P.; Parello, J.; Vidal, J. P. *Synthesis* **1992**, 1226.

2.31 Bolin, D. R.; Sytwu, I. -I.; Humiec, F.; Meienhofer, J. *Int. J. Peptide Protein Res.* **1989**, 33, 353.

2.32 Sampson, N. S.; Bartlett, P. A. *Biochemistry* **1991**, 30, 2255.

Chapter 3

Synthesis of α,α-Dialkylated Amino Acid-Rich Peptides with Antimicrobial Activity

3.1 Introduction

The classical α-helix and the 3_{10}-helix are the two most prevalent helices found in proteins.[3.1-3.2] Whereas the α-helix is characterized by 3.6 residues per turn and a (*i*, *i* + 4), thirteen-membered, hydrogen-bonding pattern, the 3_{10}-helix is distinguished by 3 residues per turn and a (*i*, *i* + 3), ten-membered, hydrogen-bonding configuration. The conformational parameters of the two helices are not widely different; however, the 3_{10}-helix is slightly tighter and more elongated than the α-helix.[3.1-3.2] The 3_{10}-helix is less common than the α-helix; it accounts for approximately 10 % of all helical structures found in proteins.[3.2-3.3] Nevertheless, structural work conducted on the 3_{10}-helix suggests that it plays a very important biochemical role.[3.3] It is considered to be a protein folding intermediate to the α-helical conformation.[3.4-3.6] Furthermore, it is believed that protein recognition steps could possibly involve facile transitions between α- and 3_{10}-helices.[3.4,3.7] Therefore, there has been an enormous interest in trying to understand the preferences for α- or 3_{10}-helical conformations and the transitions between these two states.[3.2-3.3,3.8-3.10]

It is well-established that α-aminoisobutyric acid (Aib), as well as several other α, α-dialkylated amino acids, are strong promoters of the 3_{10}-/α-helical conformation.[3.8-3.11] The backbone torsional angles (ϕ, ψ) (Figure 3.1) of an Aib residue are severely restricted, resulting in the pronounced propensity of this residue to favor helical structures, even in short peptides.[3.8-3.12] Some proteinogenic amino acids, like leucine

and alanine, also promote helicity but not to the extent required for preparation of short 3_{10}- or α-helical peptides.[3.10]

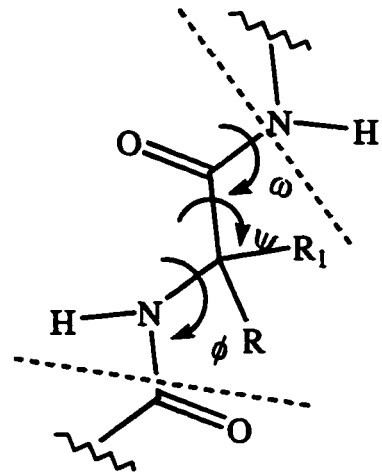

Allowable phi, psi angle pair for Aib (R, $R_1 = CH_3$)
-57 °C, -47 °C (right-handed α- or 3_{10}-helix)
57, °C, 47 °C (left-handed α- or 3_{10}-helix)

Figure 3.1 Backbone torsional angles of an Aib residue

The type of helix that an Aib-rich peptide preferentially forms is governed by several factors such as main-chain length, Aib content, sequence, and environmental conditions. Karle et. al reported that Aib-rich peptides with 5 residues or less give rise to 3_{10}-helices, but peptides with ten or more residues form α-helices.[3.12] For medium length peptides (6-10), either an α- or 3_{10}- helix can form, depending mainly on the percentage of Aib's or α,α-amino acids (ααAAs) contained in a peptide. Six residue or longer peptides with 50 % or more ααAAs are reported to form a 3_{10}-helix while those containing less than 50% generally favor an α-helix.[3.9,3.12] Basu *et al.* reported that the location of monosubstituted amino acids in Aib-rich peptides also affected the 3_{10}/α-helix equilibrium: the α-helix is favored when two monosubstituted amino acids are next to each other, but the 3_{10}-helix, when no two monosubstituted amino acids are next to each other.[3.9] As far as solvent

effects, several studies (theoretical and empirical) revealed that Aib-rich peptides favor the α-helix in polar media but the 3_{10}-helix in nonpolar media.[3.3,3.6,3.13-3.14]

Until recently, most studies conducted on the solvent effects on the 3_{10}-/α-helix equilibrium were limited to spectroscopic measurements of hydrophobic peptides (e.g., oligomers of Aib) in organic solvents or X-ray structure determinations of peptides crystallized from organic solvents.[3.3,3.8,3.10,3.13-3.15] Toniolo *et al.* reported the first short (7-mer) Aib-rich peptide that exhibited its 3_{10}-helical structure in pure water (Figure 3.2). The peptide comprised the extremely water-solubilizing, azacrown-functionalized α-amino acid, L-2-amino-3[1-(1,4,7-triazacyclo-nonane)]propanoic acid (ATANP).[3.1,3.16] In addition, the design and synthesis of short, amphipathic α- and 3_{10}-helices, incorporating 60% Aib content and the water-solubilizing α,α-disubstituted amino acid, Api (4-aminopiperidine-4-carboxylic acid), that exhibited their designed structures (Figure 3.2) in aqueous media (25 mM SDS) were reported by Yokum *et al.*[3.17] They also reported that amphipathic design was foremost in controlling secondary structure (helical preference), overriding traditional key factors such as the number of ααAAs and the order of the α-amino acids and ααAAs in a sequence. Furthermore, the peptides exihibited substantial antibacterial activity.[3.18]

An amphipathic helix is a protein helix that has opposing polar and non-polar faces oriented along its axis.[3.19] Scores of naturally occurring antimicrobial peptides contain an amphipathic α-helix as the primary structural motif.[3.20-3.21] They kill bacteria by primarily disrupting the cell membrane. Many studies directed toward understanding the structure-activity relationships (SAR) of natural antimicrobial peptides indicate that their amphipathic character plays a vital role in their biological activities (peptide

membrane interactions).[3.20-3.21] Also, a reported, general trend exists between the helicity of an amphipathic peptide and bioactivity. Generally, the higher a peptide's helicity is, the higher its bioactivity. However, amphipathic, α-helical peptides with 18 or more residues tend to have high cytotoxicity. Short peptides (10-16 residues of varying sequences) containing the amphiphathic α-helix as a consistent structural feature were

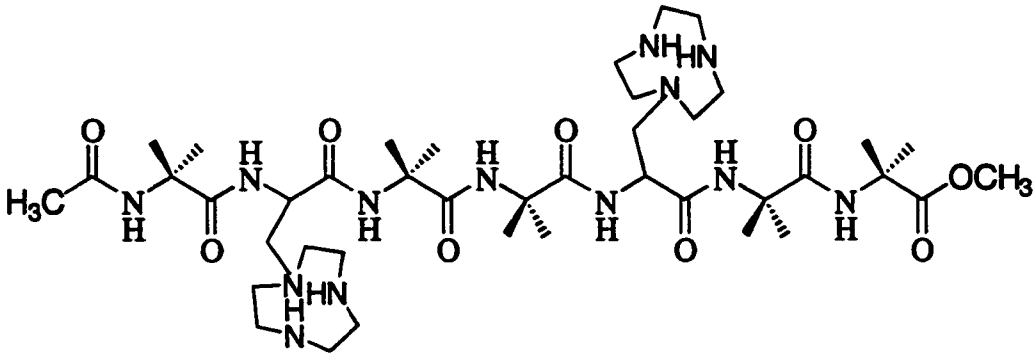

Ac-Aib-ATANP-Aib-Aib-ATANP-Aib-Aib-OCH_3

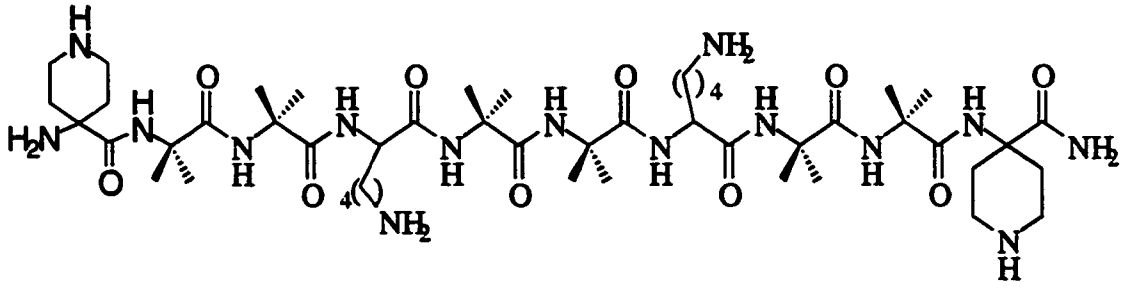

H-Api-Aib-Aib-Lys-Aib-Aib-Lys-Aib-Aib-Api-NH_2

Figure 3.2 Short, water-soluble 3_{10}-helical peptides. The top peptide has 3_{10}-helicity in pure water and the bottom peptide (Ipi-10), in aqueous 25 mM SDS.

shown to have comparable antimicrobial activities as longer or native peptides. They have also exhibited a higher degree of selectivity of bacterial killing over lysis of red blood cells.[3.20-3.22] Conversely, many natural peptide antibiotics, especially those containing Aib residues, are thought to form 3_{10}-helices.[3.23-3.25] In addition to reports of

short, amphipathic α-helical peptides with significant antimicrobial activity, there has also been a report of short, amphipathic, 3_{10}-helical peptides exhibiting antibacterial activity.[3.25] Since 3_{10}-helical peptides are about 20% longer than α-helical peptides with the same number of residues, amphipathic 3_{10}-helical peptides could possibly retain biological activity at shorter peptide lengths than analogous α-helical peptides.

In our work we were interested in the design and efficient synthesis of short, amphipathic 3_{10}-helical peptides (Aib-rich) that are capable of exhibiting good antimicrobial activity and low cytotoxicity. The general strategy was to shorten the amphipathic 10-mer (Ipi-10) in Figure 3.2 to a 9-mer by removing the *N*-terminal Api residue. We proposed that removal of this residue would increase the 3_{10}-helicity-and therefore bioactivity-of the resulting 9-mer in an aqueous medium due to the removal of electrostatic repulsive interactions that may exist between the N-terminus amine and charged Api-residue. We observed that the 7-mer peptide (Figure 3.2), which folded into a 3_{10}-helix in pure water,[3.1,3.16] had shorter α-amino acid side-chains than the 10-mer peptide. Therefore, we decided to expand the scope of our research by investigating the effects of further shortening of the length (methylene groups) of the lysine residues in our 9-mer peptide. We also envisioned an increased 3_{10}-helicity trend with decreased side-chain length in our designed peptides. Furthermore, we were interested in the solvent (aqueous-organic) effects on the 3_{10}-/α-helix equilibrium on our designed, amphipathic 3_{10}-helical peptides.

Electronic circular dichroism (CD) is the most widely employed spectroscopic technique for monitoring the secondary structure of peptides and proteins as a function of solvent.[3.27] Both 3_{10}-and α-helical peptides give rise to negative CD bands around 222

nm ($n \rightarrow \pi^*$) and 207 nm ($\pi \rightarrow \pi^*$).[3.23] A positive band around 191 nm ($\pi \rightarrow \pi^*$) is also characteristic of both types of helical peptides, although it is usually much weaker in 3_{10} helical peptides. The ratio R of the intensity of the negative bands, where R = $[\theta]_{n \rightarrow \pi^*}/[\theta]_{\pi \rightarrow \pi^*}$, is a generally accepted parameter used to distinguish a 3_{10}-helix from an α-helix. For an α-helix R ≈ 1, but for a 3_{10} helix R ≈ ≤ 0.4.[3.22]

3.2 Results and Discussion

3.2.1 Peptide Design and Synthesis

The four homologous series of short peptides (9-mers) **3.1-3.4** and their acetylated versions **3.5-3.8** listed in Table 3.1 are *de novo* designed peptides composed of 78% α,α-disubstituted amino acids (ααAAs). The sequences of **3.1-3.8** were based on one of the peptides (**3.9**) first described by Yokum *et al.*[3.17] Peptide **3.1** is actually **3.9** minus the N-terminal Api (4-aminopiperidine-4-carboxylic acid) residue. Like **3.9**, peptides **3.1-3.8** were designed to form amphipathic, 3_{10}-helical peptides. The 9-mers **3.1-3.8** contain either two lysines or two lysine analogs-ornithine, 2, 4 diaminobutanoic acid (Dab), or 2, 3 diaminopropanoic acid (Dap)-and 7 achiral ααAAs-six Aib residues and one Api residue. The distinction between each peptide, besides acetylation, is the length (# of methylene groups) of the side-chains of its α-amino acids (Figure 3.3). In this study we primarily investigated, starting with **3.1**, how further shortening (main-chain and side-chain) of **3.9** would affect the resulting peptide's secondary structure in various solvent media, antimicrobial activity, and cytotoxicity. Furthermore, we hypothesized that removal of the positive charge (- Api) at the N-terminus of **3.9** would increase the designed amphipathic, 3_{10}-helicity of the resulting peptide in aqueous media, thereby, possibly improving bioactivity due to an overall better peptide-membrane interaction.

Table 3.1 Sequences of peptides **3.1-3.10**

Peptide #,	Name	Sequence
3.1	Ipi-9	H-Aib-Aib-Lys-Aib-Aib-Lys-Aib-Aib-Api-NH_2
3.2	Ipiorn-9	H-Aib-Aib-Orn-Aib-Aib-Orn-Aib-Aib-Api-NH_2
3.3	Ipidab-9	H-Aib-Aib-Dab-Aib-Aib-Dab-Aib-Aib-Api-NH_2
3.4	Ipidap-9	H-Aib-Aib-Dap-Aib-Aib-Dap-Aib-Aib-Api-NH_2
3.5	AcIpi-9	Ac-Aib-Aib-Lys-Aib-Aib-Lys-Aib-Aib-Api-NH_2
3.6	AcIpiorn-9	Ac-Aib-Aib-Orn-Aib-Aib-Orn-Aib-Aib-Api-NH_2
3.7	AcIpidab-9	Ac-Aib-Aib-Dab-Aib-Aib-Dab-Aib-Aib-Api-NH_2
3.8	AcIpidap-9	Ac-Aib-Aib-Dap-Aib-Aib-Dap-Aib-Aib-Api-NH_2
3.9	Ipi-10	H-Api-Aib-Aib-Lys-Aib-Aib-Lys-Aib-Aib-Api-NH_2
3.10	AcIpi-10	Ac-Api-Aib-Aib-Lys-Aib-Aib-Lys-Aib-Aib-Api-NH_2

The ααAAs were incorporated into **3.1-3.8** to induce a stable, helical, secondary structure in the short peptides. The L-lysine or L-lysine-like residues were included to induce a right-handed helix (detectable by CD) and were separated well in the middle of the sequences (in 4th and 7th position) to have the greatest effect.[3.9] As mentioned above the peptides were designed to be amphipathic with the charged Api and lysine or lysine-like residues forming the hydrophilic face and the nonpolar Aib residues forming the hydrophobic face. As seen in Figure 3.4 the designed peptides are more amphipathic in the 3_{10}-helical representation.

The % 3_{10}-helix was estimated using the following equation: % 3_{10}-helix = (100) $[[\theta]_{\pi\rightarrow\pi^*} / -21{,}500]$, where the minimum for $[\theta]_{\pi\rightarrow\pi^*}$ is observed from 205-209 nm.[3.17,3.28]

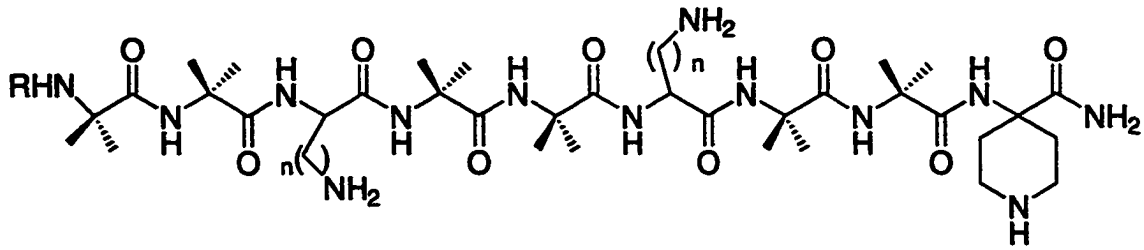

R-Aib-Aib-Xxx-Aib-Aib-Xxx-Aib-Aib-Api-NH_2

Xxx = Lys (n = 4), Orn (n = 3), Dab (n = 2), or Dap (n = 1) R = H, Ac, Api, Ac-Api

Figure 3.3 General chemical structure of peptides **3.1-3.10**

The CD spectra of H-(Leu-Arg-Leu)$_8$-OH in diphosphatidylcholine liposomes served as the model 3_{10}-helix, where $[\theta]_{\pi\rightarrow\pi^*}$ = -21,500 deg cm^2 dmol^{-1} is defined as 100% 3_{10}-helix.[3.28] No formal methods have been suggested in literature for the estimation of % 3_{10}-helicity. For estimation of the % α-helix the following equation was employed: % α-helix = -100 ($[\theta]_{n\rightarrow\pi^*}$ + 3000) / 33,000, where the minimum for the $[\theta]_{n\rightarrow\pi^*}$ is observed from 222-225 nm.[3.29]

Solid-phase synthetic techniques were employed, using a Milligen 9050 peptide synthesizer, in the prepartion of our designed peptides **3.1-3.8** and peptides **3.10-3.12.** The ααAAs employed in our synthesis were Fmoc-Api(Boc)-OH, Fmoc-Aib-OH, and the dimer, Fmoc-Aib-Aib-OH (Figure 3.5). The synthesis of peptides containing multiple ααAAs is inherently complicated due to severe steric hindrance caused by tetrasubstitution at the α-carbon. Previously, the use of ααAA residues has been limited because of the difficulty of coupling or harsh conditions used for their incorporation.[3.11] Carpino's development of acid fluorides for ααAA couplings provided the first method for an efficient, mild synthesis (solution- and solid-phase) of peptides rich in ααAAs.[3.30-3.31] This method was initially employed in the preparation of **3.9** and **3.10**,[3.17] upon which the design of our targets are partially based, with unsatisfactory yields. We therefore

attempted the preparation of our first peptide **3.1** by using a reported improved *in situ* coupling protocol described by Albericio et al.[3-32] In this method the phosphonium-based

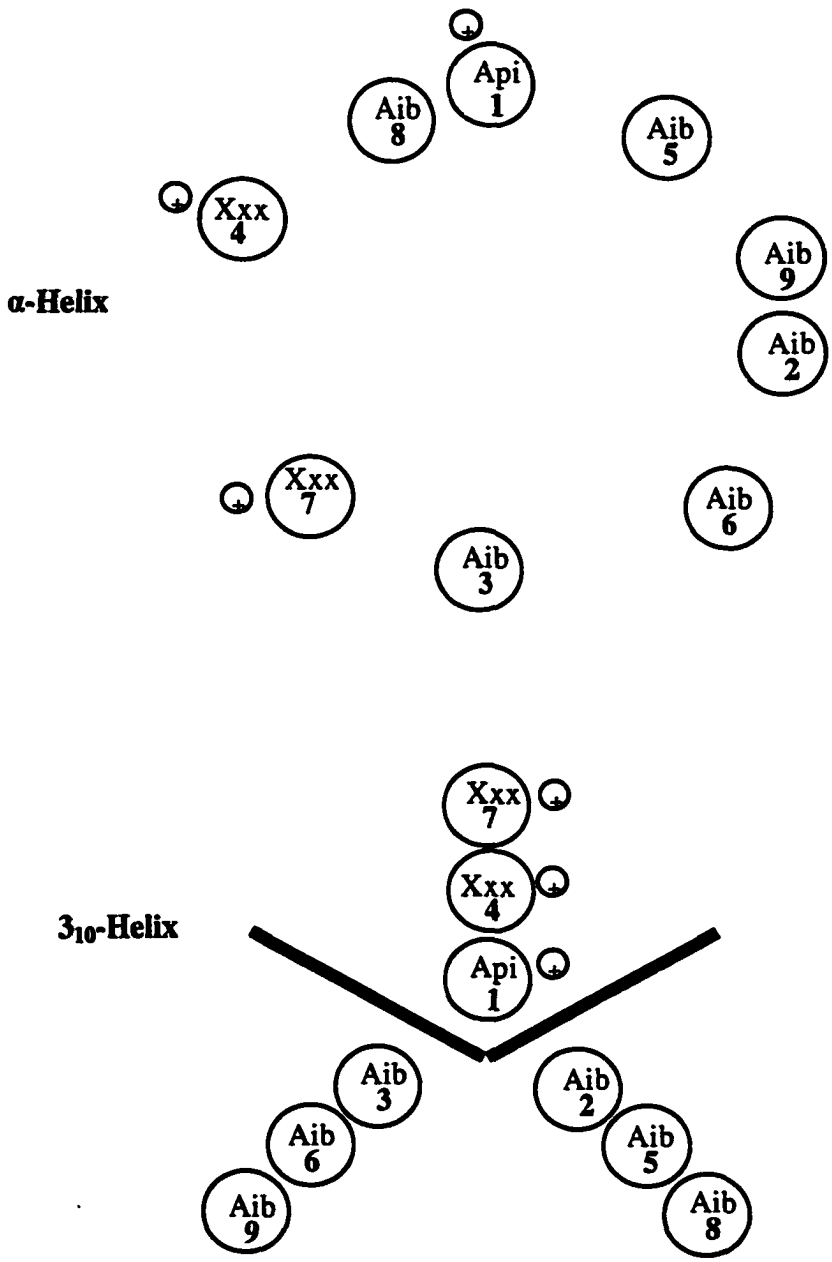

R-Aib-Aib-Xxx-Aib-Aib-Xxx-Aib-Aib-Api-NH_2

Xxx = Lys, Orn, Dab, or Dap R = H, Ac

Figure 3.4 The α- and 3_{10}-helical wheel diagrams and sequence of peptides **3.1- 3.8**

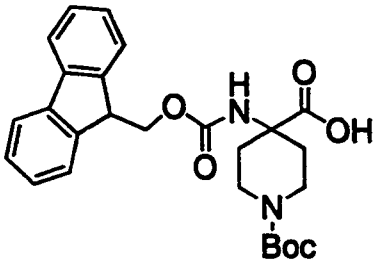

Fmoc-Api (Boc)-OH

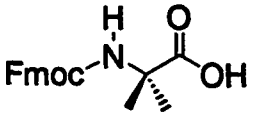

Fmoc-Aib-OH

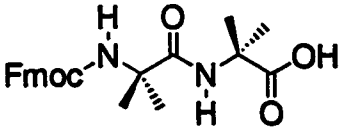

Fmoc-Aib-Aib-OH

Figure 3.5 The residues employed in synthesis of peptides **3.1-3.10**

amino acid (Api, Aib, and Lys), 8 equivalents of DIEA, and a Fmoc-PAL-PEG-PS resin were employed. However, unsatisfactory yields (2-5%) were also obtained initially with this method. From analysis of the Fmoc UV traces, which were used to monitor or gauge the efficiency of each coupling step, it was determined that every second Aib was not coupling efficiently. Therefore, in an effort to improve the yield of **3.1**, every second Aib in the sequence was double coupled. Again, no significant improvement in yields was observed, even with refluxing at 50 °C.

Our next strategy was to employ the Aib residue as a dimer (Fmoc-Aib-Aib-OH). We reasoned that the use of the dimer could at least eliminate or lessen the formation of deletion sequences (seen in MALDI of collected HPLC fractions), thus, potentially improving the yields of **3.1**. Conversely, we recognized that the use of an Aib dimer could possibly impose even more steric hindrance. Nevertheless, we prepared (solution-phase) Fmoc-Aib-Aib-OH for use in preparation of **3.1** and, eventually, the other peptides listed in Table 3.1.

The dimer, Fmoc-Aib-Aib-OH, was prepared (Scheme 3.1) by using a combination of Carpino's acid fluoride method[3.30-3.31] and Bolin's procedure.[3.33] The monomer, Fmoc-Aib-OH, was first treated with cyanuric fluoride to form the amino acid fluoride **3**. Compound **3** was then reacted with the silylated amino acid **5**, which was prepared from the reaction of H-Aib-OH **4** and trimethylsilylchloride (TMS-Cl), to form the dimer **6**, after recrystallization from chloroform/hexane, in 70% yield.

In the first attempted synthesis of **3.1** employing the Aib dimer and application of heat (50 °C), we observed, from the Fmoc UV traces, that the first dimer of the sequence coupled very poorly but the rest of the Aib dimers coupled very well. However, the overall yield (~ 2%) of **3.1** was still low because of the very inefficient coupling of the first dimer. We therefore decided to use the Aib monomers, followed by double coupling after each one, for the first two Aib's in the sequence but to continue to use the Aib dimer in the rest of the sequence along with refluxing (50 °C). This modification resulted in a significant yield increase for **3.1** (20% yield). The dramatic improvement in efficiency of preparation of **3.1** can be readily observed in the semi-preparatory HPLC chromatograms presented in Figure 3.6 and Figure 3.7. Also, this method was used to prepare the rest of the peptides listed in Table 3.1 in yields up to 25%. Analytical HPLC was used to check the purity of the peptides (e.g., see Figure 3.8, Figure 3.9, Figure 3.10, Figure 3.11, Figure 3.12, and Figure 3.13,).

The good synthetic results of our target 9-mers and 10-mers (Table 3.1) were attributed mainly to the incorporation of our Aib dimer. The use of Fmoc-Aib-Aib-OH lessened the formation of deletion sequences while increasing the yields of the desired sequences. However, as alluded to above, the Aib dimer wasn't effective, in terms of

peptide yield, when used for the first two Aibs in the synthesis of the peptides. This was attributed to steric factors arising potentially from the coupling of three sequential ααAAs (Api + Aib dimer) as well as steric bulkiness from the resin. The sequential coupling of Aibs is generally difficult due to inherent strain caused by the additional substituent on the α-carbon. Our dimer lessens that complexity significantly because instead of being involved in sequential Aib couplings, the dimer is actually coupled to an α-amino acid in each peptide's sequence.

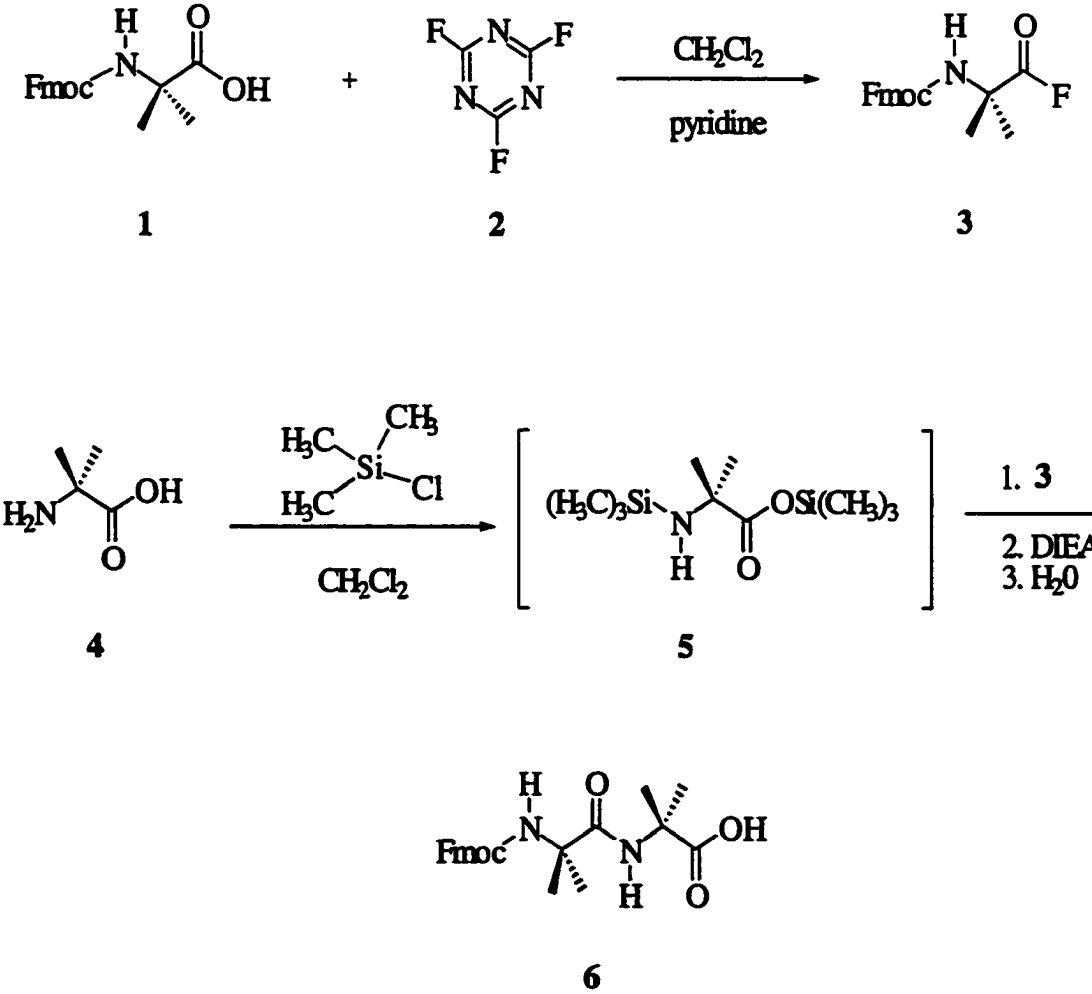

Scheme 3.1 Synthesis of Fmoc-Aib-Aib-OH **6**

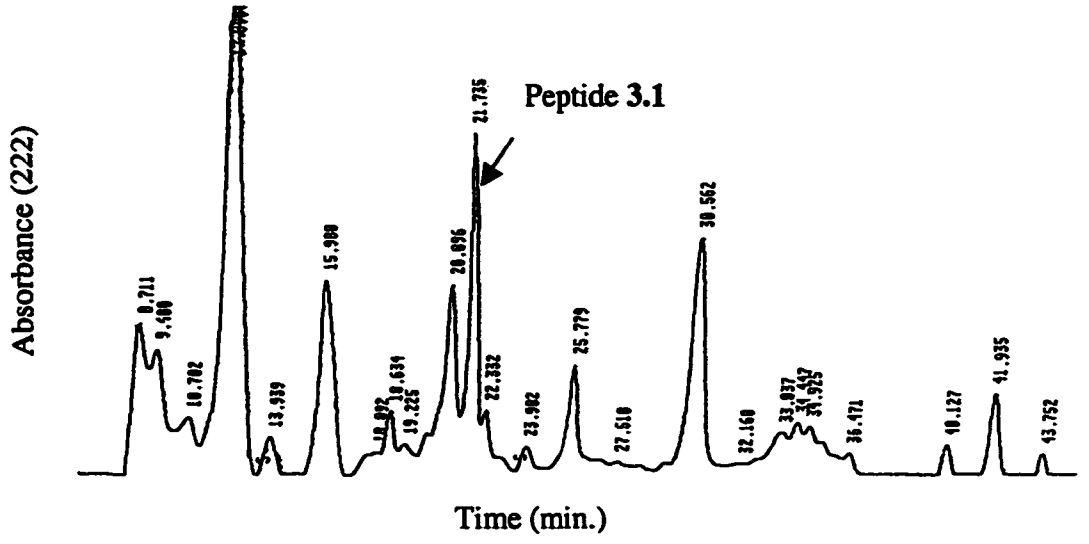

Figure 3.6 Semi-preparatory HPLC profile of crude containing peptide **3.1** before improved coupling protocol. HPLC was carried out on a Waters 5 μm C_4 reversed-phase column (8 x 100 mm) using a mobile phase of water (0.05 %, v/v, TFA) and acetonitrile (0.05 %, v/v, TFA), a gradient of 10-50 % of organic phase over 50 minutes and flow rate of 1 mL/min. The absorption (UV) was monitored at 222 nm.

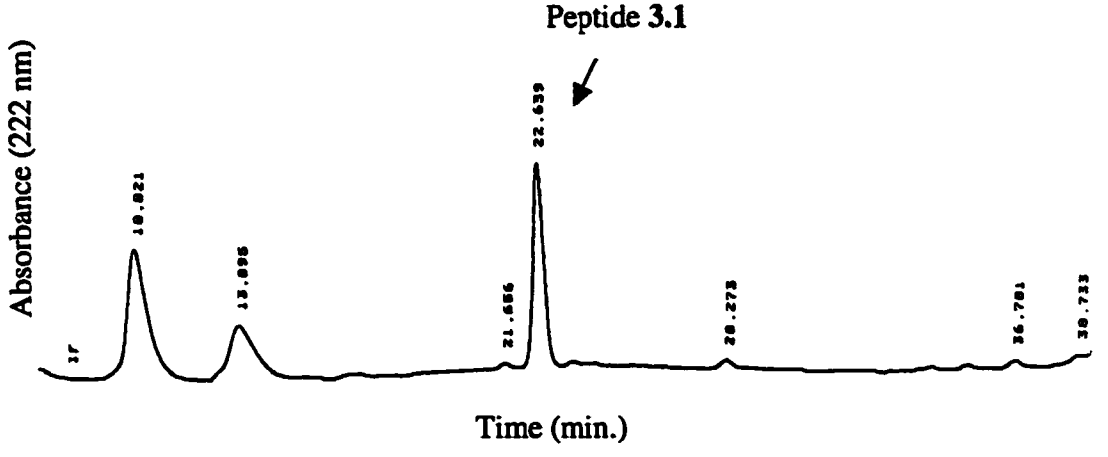

Figure 3.7 Semi-preparatory HPLC profile of crude containing peptide **3.1** after employing improved coupling protocol. HPLC was carried out on a Waters 5 μm C_4 reversed-phase column (8 x 100 mm), a gradient of 10-50 % of organic phase over 50 minutes and flow rate of 1 mL/min. The absorption (UV) was monitored at 222 nm.

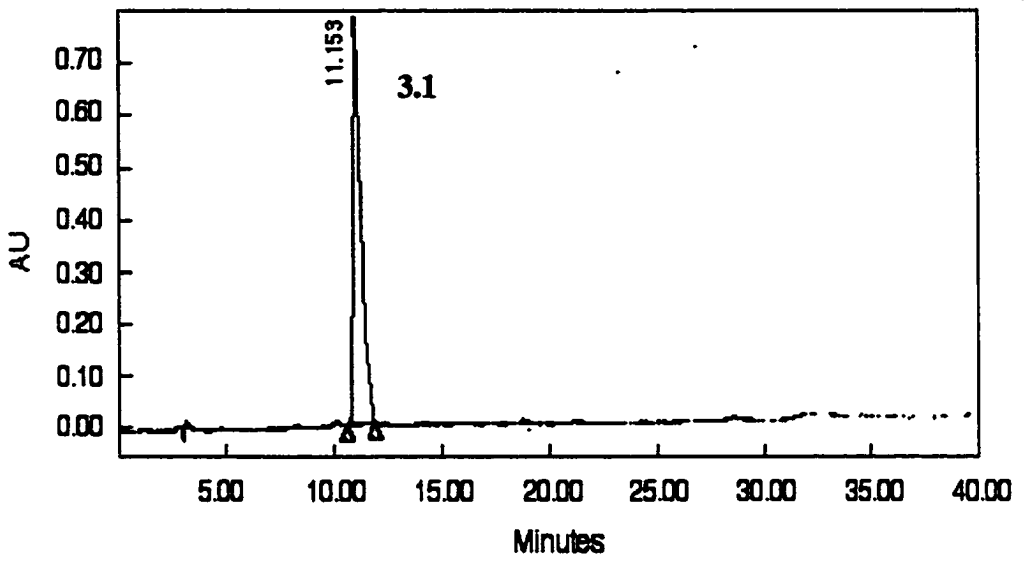

Figure 3.8 Analytical HPLC purity check of isolated **3.1**. HPLC was carried out on a Vydac 5-μM C-18 column (250 x 4 mm) using a mobile phase of H_2O (0.05%, v/v, TFA) and CH_3CN (0.05%, v/v, TFA) with a gradient of 50-100% of the organic phase over 40 min. and a flow rate of 1 mL/min.

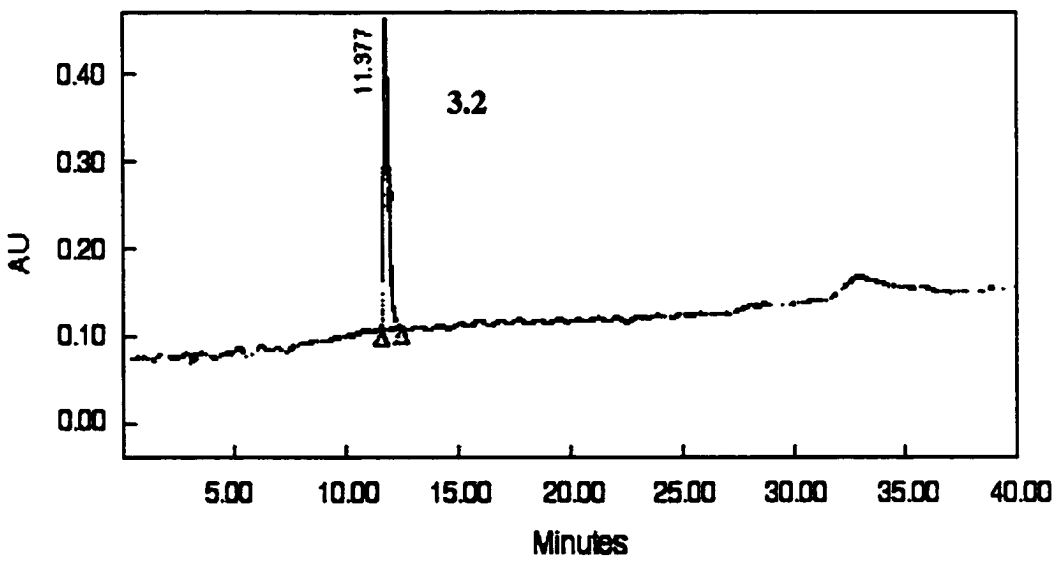

Figure 3.9 Analytical HPLC purity check of isolated **3.2**. HPLC was carried out on a Vydac 5-μM C-18 column (250 x 4 mm) using a mobile phase of H_2O (0.05%, v/v, TFA) and CH_3CN (0.05%, v/v, TFA) with a gradient of 50-100% of the organic phase over 40 min. and a flow rate of 1 mL/min.

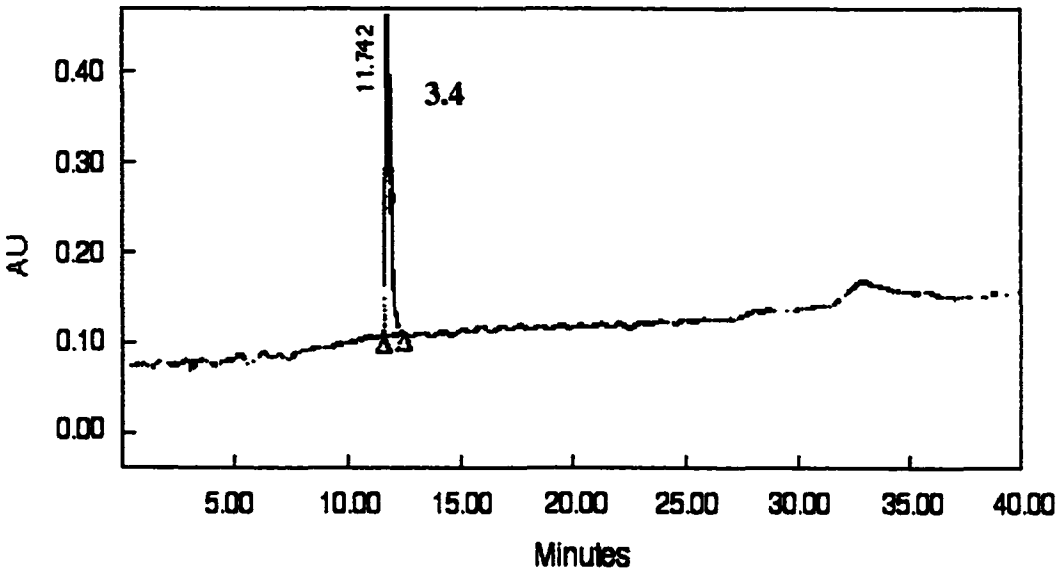

Figure 3.10 Analytical HPLC purity check of isolated **3.4**. HPLC was carried out on a Vydac 5-μM C-18 column (250 x 4 mm) using a mobile phase of H_2O (0.05%, v/v, TFA) and CH_3CN (0.05%, v/v, TFA) with a gradient of 50-100% of the organic phase over 40 min. and a flow rate of 1 mL/min.

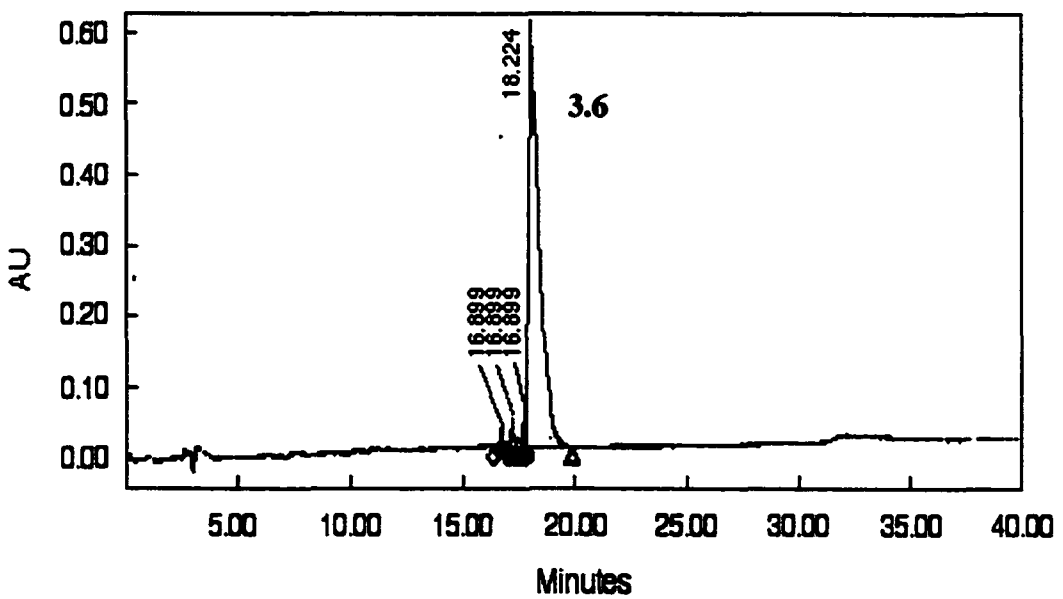

Figure 3.11 Analytical HPLC purity check of isolated **3.6**. HPLC was carried out on a Vydac 5-μM C-18 column (250 x 4 mm) using a mobile phase of H_2O (0.05%, v/v, TFA) and CH_3CN (0.05%, v/v, TFA) with a gradient of 50-100% of the organic phase over 40 min. and a flow rate of 1 mL/min.

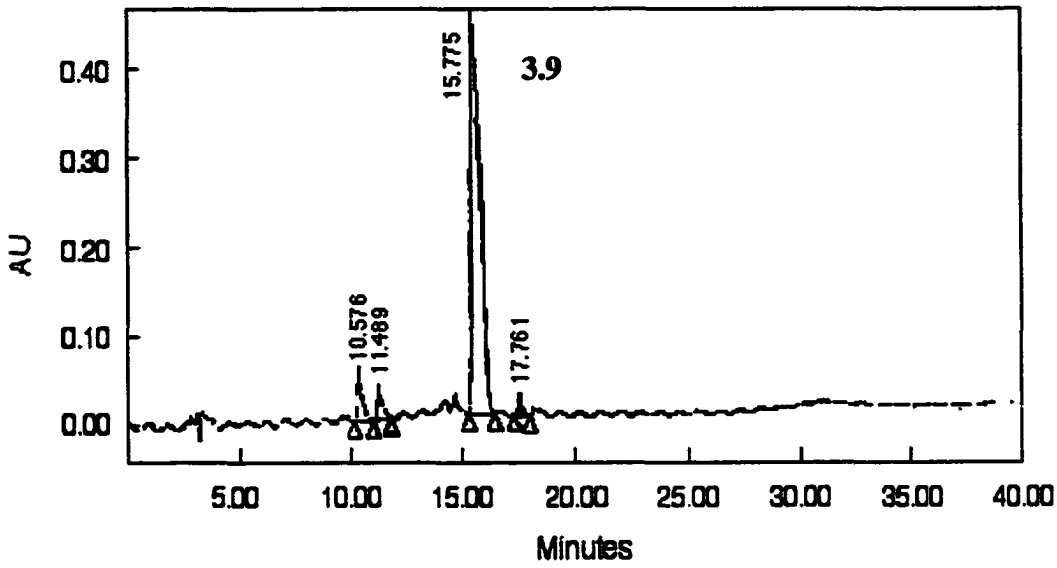

Figure 3.12 Analytical HPLC purity check of isolated **3.9**. HPLC was carried out on a Vydac 5-μM C-18 column (250 x 4 mm) using a mobile phase of H_2O (0.05%, v/v, TFA) and CH_3CN (0.05%, v/v, TFA) with a gradient of 50-100% of the organic phase over 40 min. and a flow rate of 1 mL/min.

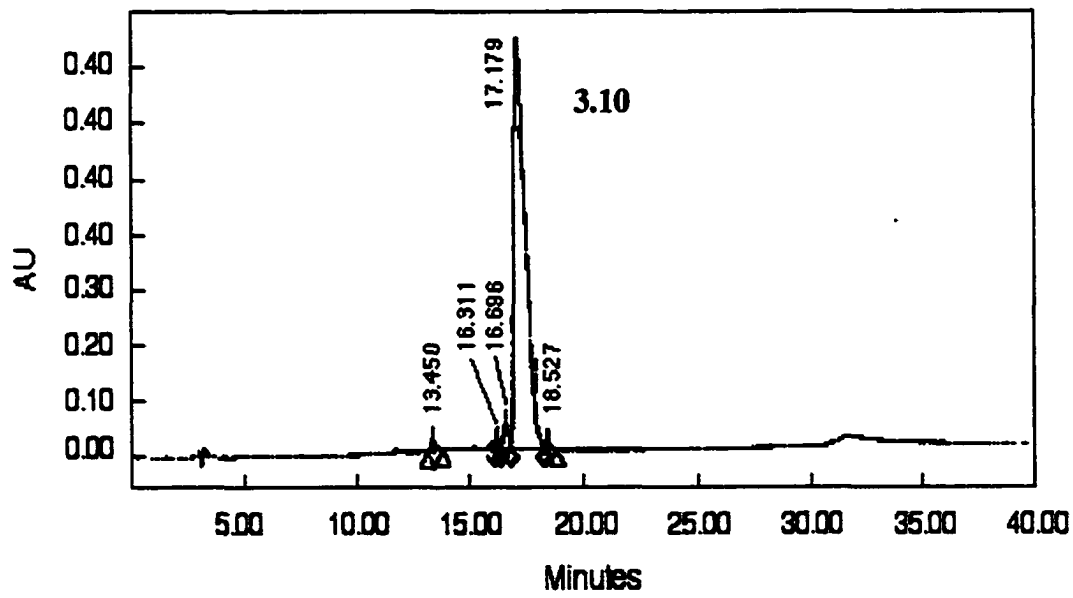

Figure 3.13 Analytical HPLC purity check of isolated **3.10**. HPLC was carried out on a Vydac 5-μM C-18 column (250 x 4 mm) using a mobile phase of H_2O (0.05%, v/v, TFA) and CH_3CN (0.05%, v/v, TFA) with a gradient of 50-100% of the organic phase over 40 min. and a flow rate of 1 mL/min.

3.2.2 Solvent Effects on 3_{10}-/α-Helix Equilibrium

Peptides **3.1-3.8** were studied in six different solvent systems: 25 mM SDS, sodium phosphate buffer (pH = 7), CH_3CN-TFE (trifluoroethanol) (9:1), and CH_3CN-H_2O [(9:1), (3:1), and (1:1)]. The designed 3_{10}-helical structure of **3.1** (Ipi-9) was most evident in 25 mM SDS (Table 3.2). However, since its R value, 0.51, is higher than the theoretically accepted value, Ipi-9 is most likely a mixture of both 3_{10} helices (estimated 23%) and α-helices (estimated 17%). In buffer, Ipi-9 exhibits a more α-helical (R = 0.62, 16%) structure, although weak, than 3_{10} helical. Also, for Ipi-9, as the percentage (50-100%)of organic composition increases in the aqueous/organic mixtures, the percent α-helicity increases, with the high being 49% in CH_3CN-TFE (9:1). This same trend of increased α-helicity in the 50-100% aqueous/organic mixtures is also observed with **3.2** (Ipiorn-9) (Table 3.3). However, in SDS micelles, the CD spectrum (R = 0.86) of Ipiorn-9 is indicative of an α-helical (13%) structure. The designed 3_{10}-helical structure of Ipiorn-9 is observed most or best in buffer, where its R value is 0.48 and estimated 3_{10}-helicity is 24%. The R values and the estimated percent helicity of both Ipiorn-9 and Ipidab-9 in buffer and 50-75% aqueous/organic mixtures reflect, in general, a significant population of both 3_{10}- and α-helical conformations (Table 3.4). Based on the characteristic minima ($n\rightarrow\pi^*$ and $\pi\rightarrow\pi^*$) of helices, Ipidap-9 appears to be helical only in CH_3CN-H_2O (9:1). In this latter solvent system, Ipidap-9 is α-helical with a R value of 0.72 and 28% helicity. In CH_3CN-TFE (9:1), Ipidap-9 appears to be a random coil with a minimum centered around 197 nm and a maximum around 215 nm.

As stated in the "Peptide Design" section, the construction of Ipi-9 was based on the 3_{10}-helical design of Ipi-10. Indeed, at low temperatures (0-5 °C) in 25 mM SDS, Ipi-10 is folded into its designed structure (R = 0.32, 25% 3_{10}-helicity) as opposed to Ipi-

9, which favors an α-helical structure (R = 0.65, 15% α-helicity) at low temperatures in SDS micelles. Solutions of SDS micelles, which possess a negatively charged head group and aliphatic tail, are known for induction of ordered structures in peptides and proteins. The induction of secondary structure is initiated by the binding of the anionic surfactant to the cationic side-chain groups of the peptide; this enhances the binding affinity of the peptides to the hydrophobic interior.[3.34] Therefore, the observance of the designed 3_{10}-helix preferably in Ipi-10 than Ipi-9 may be due to the smaller hydrophilic face of Ipi-9; the hydrophilic faces of Ipi-9 and Ipi-10 (R = 0.32) are composed of 3 residues and 4 residues, respectively. The larger positively charged face of Ipi-10 (+ 5 overall charge) probably allows for more efficient micelle binding, resulting in better 3_{10}-helical stabilization than Ipi-9 (+ 4 overall charge) at low temperatures in 25 mM SDS. Conversely, at 25 °C in 25 mM SDS, Ipi-10 appears to be α-helical (R = 0.67, 11%) while the secondary structure of Ipi-9 appears to be leaning more toward 3_{10}-helical (R = 0.51, 23% 3_{10} helicity). Furthermore, for Ipi-10, the same trend, 3_{10} to α-helical transition as the temperature is increased to 25 °C in SDS, is also seen in the 50-100% aqueous/organic mixtures (compare Table 3.5 to Table 3.6).

Of the four 3_{10}-helical designed peptides **3.1-3.4**, **3.1** (Ipi-9) possesses the most estimated 3_{10}-helical character in SDS (Figure 3.14). Peptides **3.2-3.3** are more α-helical in SDS, which is probably due to incomplete micelle binding. This incomplete binding may have caused the solvent environment of **3.2-3.3** to have greater aqueous solvent characteristics. An α-helix is generally more energetically favored than a 3_{10}-helix in an aqueous environment. This is due to the more favorable interactions of the additional exposed carbonyls and amides of an α-helix with water.[3.3] In contrast, 3_{10}-helical

peptides are generally more stable in a non-polar environment, which arises from the additional hydrogen bond formed as compared to the α-helix.[3.3]

Table 3.2 CD data and derived structural parameters for Ipi-9 at 25 °C.

Solvent	$[\theta]_{\pi\rightarrow\pi^*}$ [a,b]	$[\theta]_{n\rightarrow\pi^*}$ [a,c]	R	% Helicity
25 mM SDS	-5025	-2582	0.51	*d*
9:1 CH_3CN-TFE	-19394	-13410	0.69	49 (α)
9:1 CH_3CN-H_2O	-17720	-11936	0.67	45 (α)
3:1 CH_3CN-H_2O	-7528	-4879	0.64	24 (α)
1:1 CH_3CN-H_2O	-888	-729	0.82	11 (α)
Buffer (pH = 7)	-3491	-2170	0.62	16 (α)

[a]Units for [θ] are deg cm^2 $dmol^{-1}$.
[b]The minimum for the $[\theta]_{\pi\rightarrow\pi^*}$ band is observed in the range from ~ 205-209 nm.
[c]The minimum for the $[\theta]_{\pi\rightarrow\pi^*}$ band is observed in the range from ~ 222-225 nm.
[d]The % α-helix is estimated at 17%, and the % 3_{10}-helix is estimated at 23%.

Table 3.3 CD data and derived structural parameters for Ipiom-9 at 25 °C.

Solvent	$[\theta]_{\pi\rightarrow\pi^*}$ [a,b]	$[\theta]_{n\rightarrow\pi^*}$ [a,c]	R	% Helicity
25 mM SDS	-1336	-973	0.72	13 (α)
9:1 CH_3CN-TFE	-12866	-8555	0.66	35 (α)
9:1 CH_3CN-H_2O	-4873	-7696	1.5	32 (α)
3:1 CH_3CN-H_2O	-3407	-1911	0.56	15 (α)
1:1 CH_3CN-H_2O	-2975	-1614	0.54	14 (α)
Buffer (pH = 7)	-5111	-2474	0.48	*d*

[a]Units for [θ] are deg cm^2 $dmol^{-1}$.
[b]The minimum for the $[\theta]_{\pi\rightarrow\pi^*}$ band is observed in the range from ~ 205-209 nm.
[c]The minimum for the $[\theta]_{\pi\rightarrow\pi^*}$ band is observed in the range from ~ 222-225 nm.
[d]The % α-helix is estimated at 16%, and the % 3_{10}-helix is estimated at 24%.

Table 3.4 CD data and derived structural parameters for Ipidab-9 at 25 °C.

Solvent	$[\theta]_{\pi\rightarrow\pi^*}$[a,b]	$[\theta]_{n\rightarrow\pi^*}$[a,c]	R	% Helicity
25 mM SDS	-955	-583	0.61	11 (α)
9:1 CH_3CN-TFE	-3173	-1990	0.62	15 (α)
9:1 CH_3CN-H_2O	-2000	-2500	1.2	16 (α)
3:1 CH_3CN-H_2O	-3363	-2179	0.64	16 (α)
1:1 CH_3CN-H_2O	-4166	-2637	0.63	17 (α)
Buffer (pH = 7)	-4115	-2364	0.57	*d*

[a]Units for [θ] are deg cm^2 $dmol^{-1}$.
[b]The minimum for the $[\theta]_{\pi\rightarrow\pi^*}$ band is observed in the range from ~ 205-209 nm.
[c]The minimum for the $[\theta]_{\pi\rightarrow\pi^*}$ band is observed in the range from ~ 222-225 nm.
[d]The % α-helix is estimated at 16%, and the % 3_{10}-helix is estimated at 19%.

Table 3.5 CD data and derived structural parameters for Ipi-10 at 5 °C.

Solvent	$[\theta]_{\pi\rightarrow\pi^*}$[a,b,c]	$[\theta]_{n\rightarrow\pi^*}$[a,c,d]	R[c]	% Helicity[c]
25 mM SDS	-5316	-1750	0.32	25 (310)
9:1 CH_3CN-TFE	-9916	-3145	0.33	45 (310)
9:1 CH_3CN-H_2O	-6740	-3605	0.54	e
1:1 CH_3CN-H_2O	-4204	-3118	0.74	10 % (α)

[a]Units for [θ] are deg cm^2 $dmol^{-1}$.
[b]The minimum for the $[\theta]_{\pi\rightarrow\pi^*}$ band is observed in the range from ~ 205-209 nm.
[c] Data from reference
[d]The minimum for the $[\theta]_{\pi\rightarrow\pi^*}$ band is observed in the range from ~ 222-225 nm.
[e]The % α-helix is estimated at 12%, and the % 3_{10}-helix is estimated at 31%.

Table 3.6 CD data and derived structural parameters for Ipi-10 at 25 °C.

Solvent	$[\theta]_{\pi\rightarrow\pi^*}$[a,b]	$[\theta]_{n\rightarrow\pi^*}$[a,c]	R	% Helicity
25 mM SDS	-941	-627	0.67	11 (α)
9:1 CH_3CN-TFE	-14603	-10189	0.70	40 (α)
9:1 CH_3CN-H_2O	-7347	-7163	0.97	30 (α)
3:1 CH_3CN-H_2O	-4770	-3831	0.80	25 (α)
1:1 CH_3CN-H_2O	-1020	-1576	1.5	14 (α)
Buffer (pH = 7)	-7382	-7190	0.97	31 (α)

[a]Units for [θ] are deg cm^2 $dmol^{-1}$.
[b]The minimum for the $[\theta]_{\pi\rightarrow\pi^*}$ band is observed in the range from ~ 205-209 nm.
[c]The minimum for the $[\theta]_{\pi\rightarrow\pi^*}$ band is observed in the range from ~ 222-225 nm.

However, Ipiorn-9, of the four peptides, exhibited the highest estimated 3_{10}-helicity (24%) in aqueous buffer (Figure 3.15). Therefore, shortening the side-chain of Ipi-9 to form Ipiorn-9 resulted in better 3_{10}-helical stabilization in an aqueous buffer medium, although this 3_{10} helical stabilization wasn't afforded to Ipiorn-9 in 25 mM SDS, which may have been due to a host of factors such as ion pairing of the charged polar groups with SDS sulfonates or even incomplete micelle binding. Maybe the shorter side-chains of Ipiorn-9 interacted less favorably than the side-chains of Ipi-9 with the hydrophobic region of the SDS micelles. Further shortening of Ipiorn-9 to Ipidab-9 resulted, based on R values, in primarily an α-helix in the 90% organic but a significant population of both helical forms in the other solvent systems tested; however, the helices were generally much weaker, based on the absolute ellipticity values, than the helices of Ipi-9 and Ipiorn-9 (Table 3.4 and Figure 3.16). A decrease in absolute ellipticity is often observed with a decrease in a peptide's main-chain.[3.23] In this study, a shortening of a peptide's side-chain also seems to correlate with a decrease in absolute ellipticity.

Furthermore, this observed weakening of helicity may be caused by the charged amines of the shorter side-chains of Ipidab-9 hydrogen-bonding to nearby carbonyls, thereby, decreasing the stability of the folded structures by weakening the strength of the intramolecular hydrogen-bonds. Similar kinds of bifurcated hydrogen bonds in proteins between a helix and water or a side-chain have been reported and analyzed.[3.12]

Further shortening of Ipidab-9 to form Ipidap-9 results in further helical destabilization in all of the solvent systems except CH_3CN-H_2O (9:1), in which an α-helical (R = 0.72, 28%) structure is observed. Ipidap-9 seems to form a random coil in CH_3CN-TFE (9:1) (Figure 3.17). Ipidap-9 lacks a well-defined structure in the other solvent systems but is not completely random; a blue shift is observed for the $\pi \rightarrow \pi^*$ transition. The observed wavelengths of Ipidap-9's $\pi \rightarrow \pi^*$ transitions in buffer, CH_3CN-H_2O (1:1), CH_3CN-H_2O (3:1), and 25 mM SDS were 199 nm, 190 nm, 198 nm, and 195 nm, respectively. However, the $n \rightarrow \pi^*$ transitions in those solvent systems were observed around the wavelength (222 nm) expected in a helical peptide.

The terminally-blocked, 3_{10}-helical peptide (7-mer), described by Toniolo *et al.*, had a reported R value of 0.36 in buffer (pH = 7, 25 °C). In buffer (pH = 7, 25 °C), Ipi-10 has a R value of 0.97, and Ipiorn-9, a R value of 0.48. Therefore, our designed 9-mer, Ipiorn-9, is more 3_{10}-helical in neutral buffer than Ipi-10 but less 3_{10}-helical than the 7-mer peptide. The 7-mer is composed of 71% ααAAs, and Ipiorn-9, 78% ααAAs. Further shortening of the main-chain of Ipiorn-9 would still result in a significant percentage, 75%, of ααAAs. Therefore, the further shortening of the main-chain of Ipiorn-9, along with the amphipathic design tool, could possibly lead to a 3_{10}-helical structure that is even more comparable to the terminally-blocked 7-mer peptide.

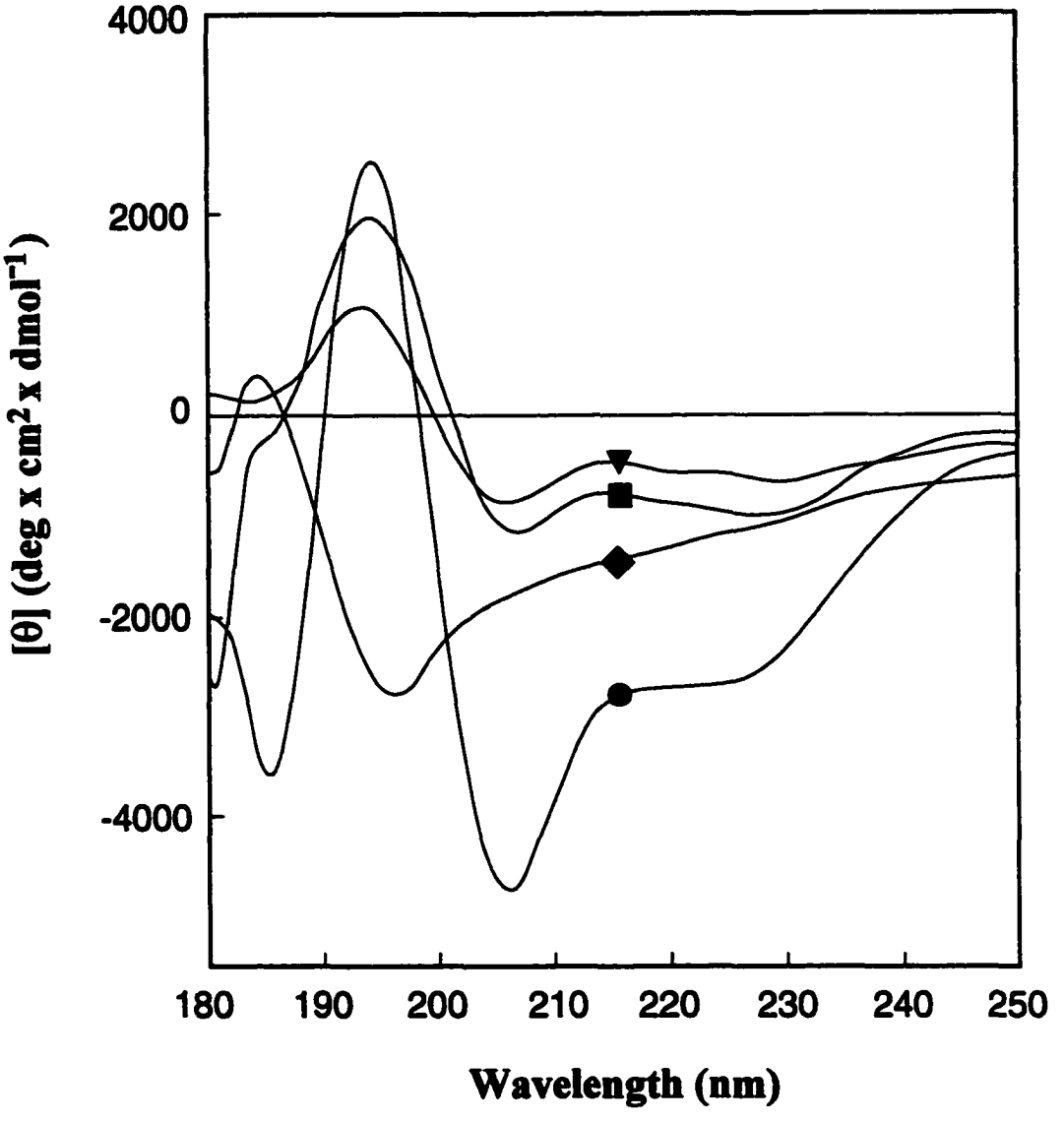

Figure 3.14 CD spectra of Ipi-9 (●), Ipiorn-9 (■), Ipidab-9 (▼) and Ipidap-9 (◆) in 25 mM SDS.

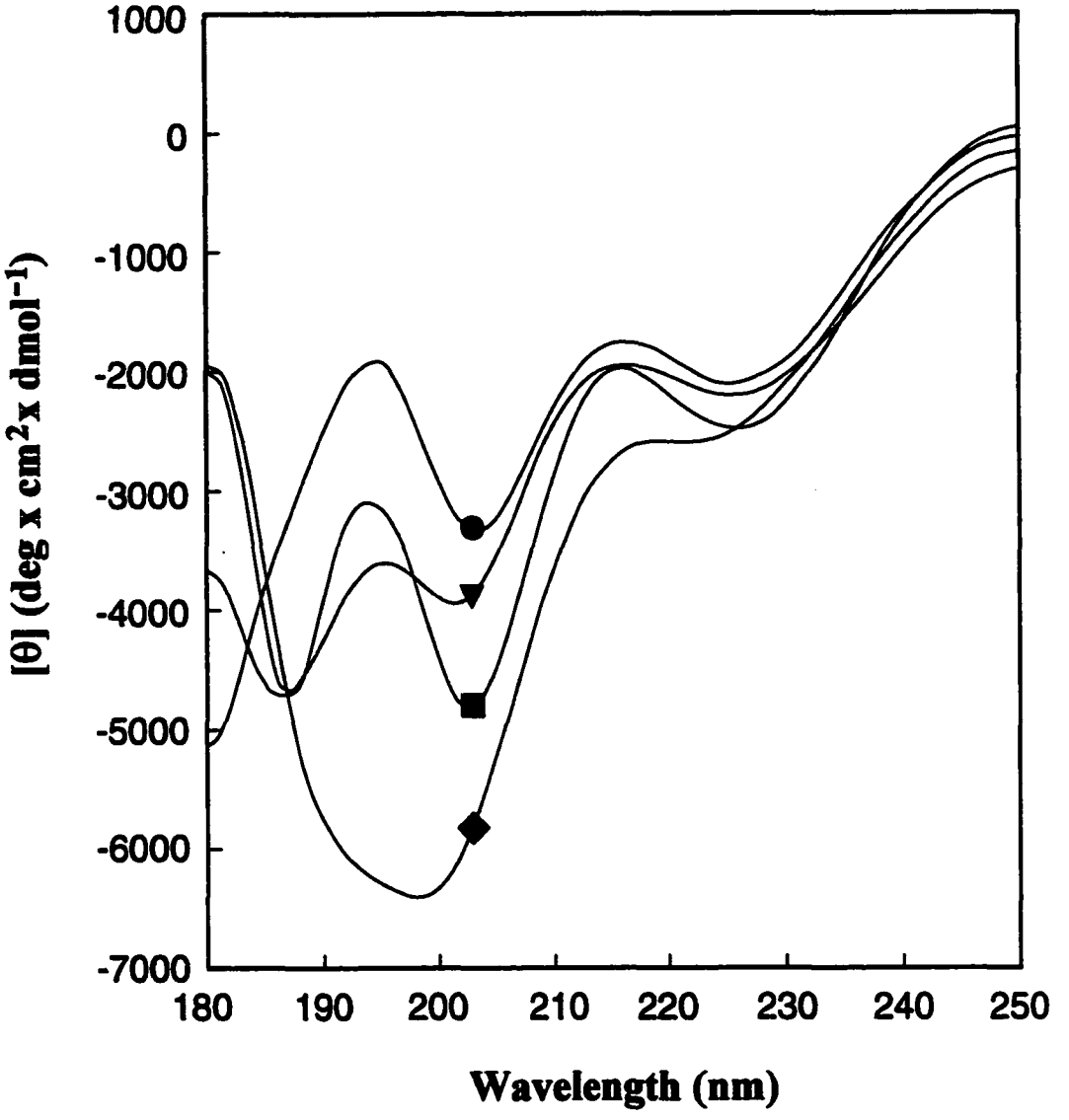

Figure 3.15 CD spectra of Ipi-9 (●), Ipiorn-9 (■), Ipidab-9 (▼) and Ipidap-9 (◆) in neutral, aqueous buffer at 25 °C.

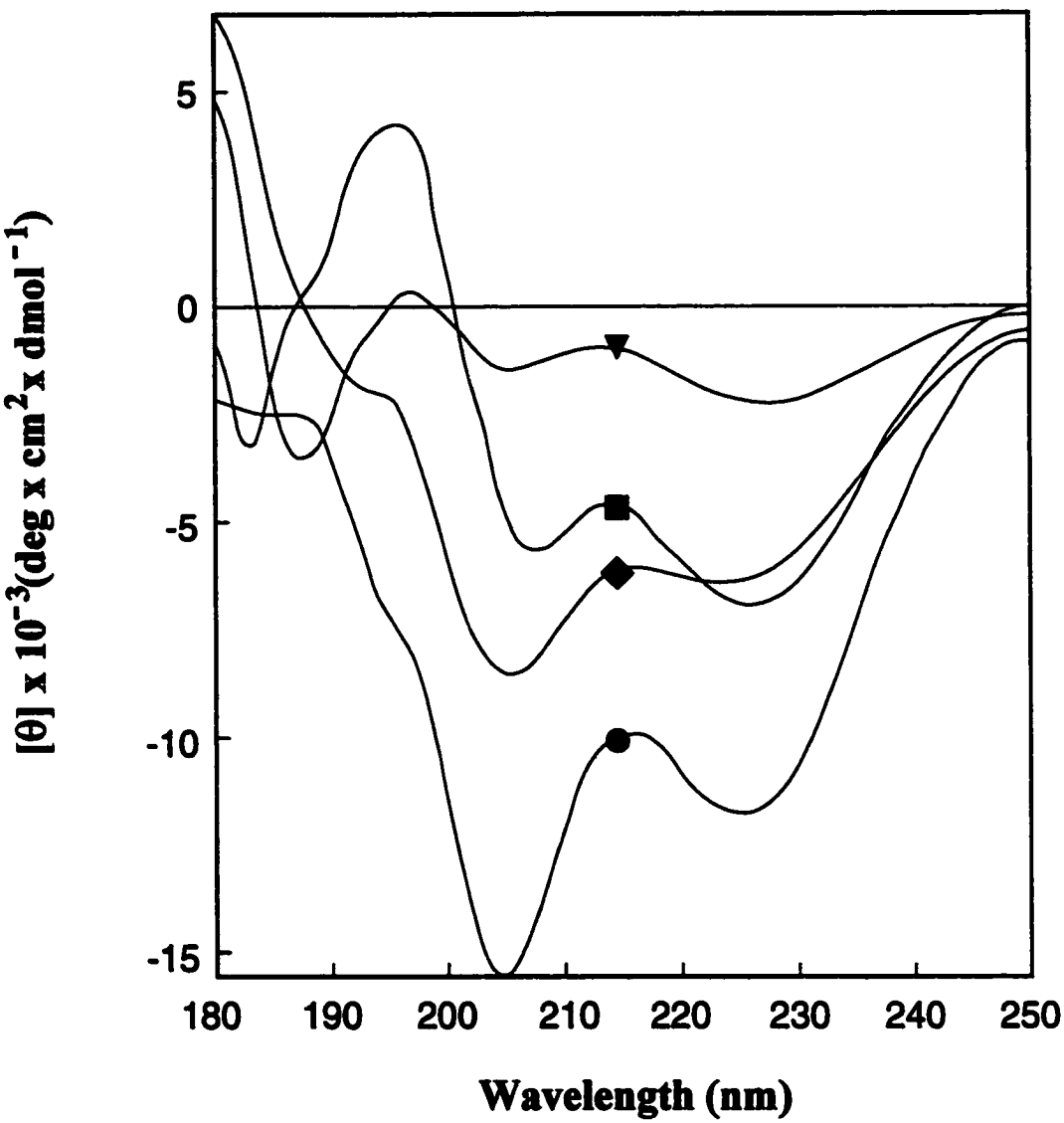

Figure 3.16 CD spectra of Ipi-9 (●), Ipiorn-9 (■), Ipidab-9 (▼) and Ipidap-9 (◆) in CH_3CN-H_2O (9:1) at 25 °C.

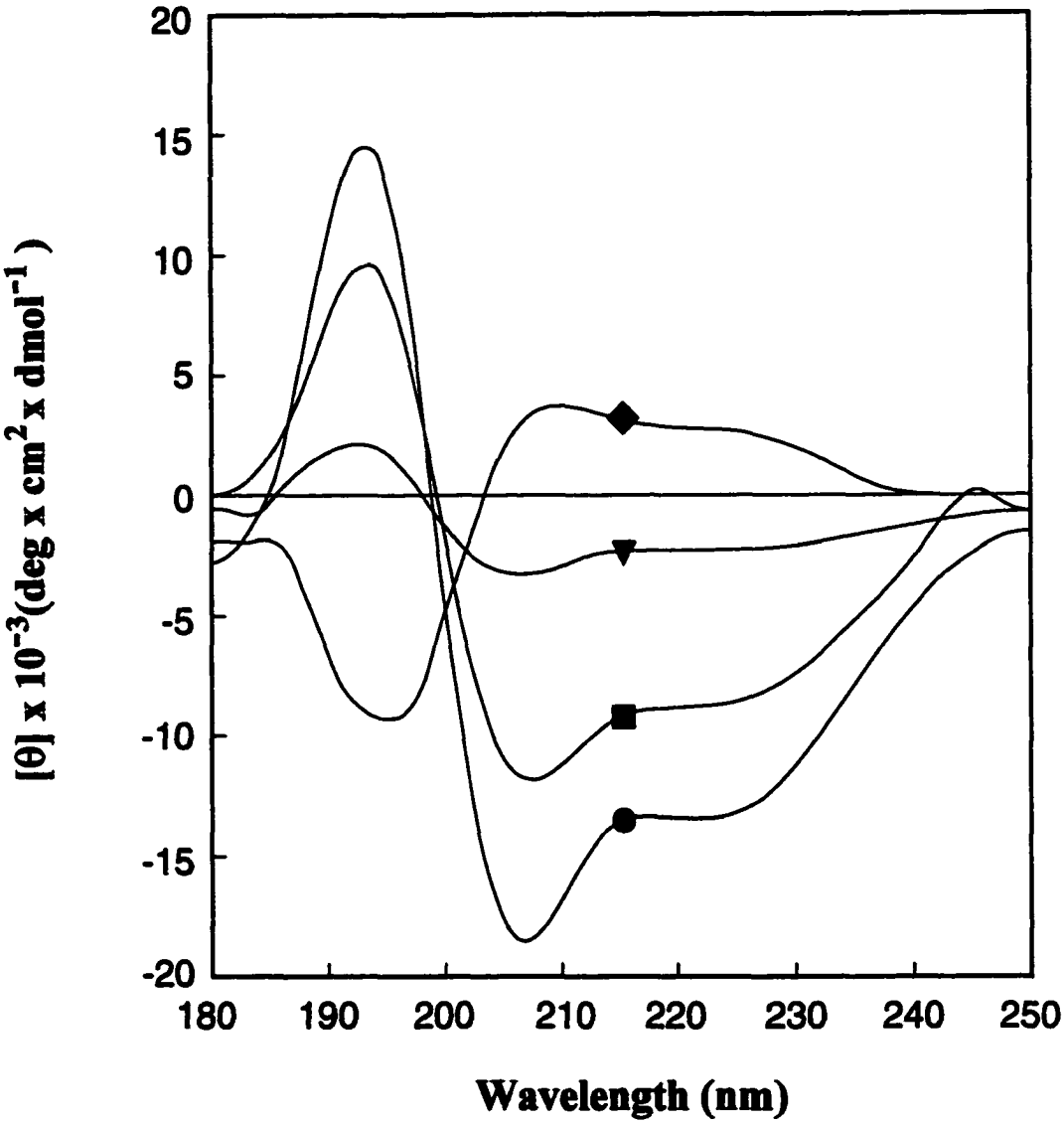

Figure 3.17 CD spectra of Ipi-9 (●), Ipiorn-9 (■), Ipidab-9 (▼) and Ipidap-9 (◆) in CH_3CN-TFE (9:1) at 25 °C.

Temperature dependence of the CD spectra of **3.1-3.4** in buffer and of **3.1-3.2** in 25 mM SDS were obtained. CD spectra of each peptide were recorded at temperatures in 10° increments from 30 to 70 °C. In buffer all of the peptides were more α-helical than 3_{10}-helical at all temperatures tested (Table 3.7, Table 3.8, Table 3.9, and Table 3.10).

Table 3.7 CD data and derived structural parameters for Ipi-9 in buffer (pH = 7) at 30 to 70 °C.

Temperature	$[\theta]_{\pi\rightarrow\pi^*}$[a,b]	$[\theta]_{n\rightarrow\pi^*}$[a,c]	R	% Helicity
30	-3584	-2775	0.77	18 (α)
40	-1475	-1006	0.68	12 (α)
50	-2170	-1544	0.71	14 (α)
60	-2047	-1149	0.56	13 (α)
70	-1923	-1293	0.67	13 (α)

[a]Units for [θ] are deg cm^2 $dmol^{-1}$.
[b]The minimum for the $[\theta]_{\pi\rightarrow\pi^*}$ band is observed in the range from 205-209 nm.
[c]The minimum for the $[\theta]_{\pi\rightarrow\pi^*}$ band is observed in the range from 222-225 nm.

Table 3.8 CD data and derived structural parameters for Ipiorn-9 in buffer (pH = 7) at 30 to 70 °C.

Temperature	$[\theta]_{\pi\rightarrow\pi^*}$[a,b]	$[\theta]_{n\rightarrow\pi^*}$[a,c]	R	% Helicity
30	-6269	3694	0.59	20 (α)
40	-5082	-3119	0.61	19 (α)
50	-2354	-1668	0.71	14 (α)
60	-3147	-1902	0.60	15 (α)
70	-2871	-1814	0.63	15 (α)

[a]Units for [θ] are deg cm^2 $dmol^{-1}$.
[b]The minimum for the $[\theta]_{\pi\rightarrow\pi^*}$ band is observed in the range from ~ 205-209 nm.
[c]The minimum for the $[\theta]_{\pi\rightarrow\pi^*}$ band is observed in the range from ~ 222-225 nm.

Table 3.9 CD data and derived structural parameters for Ipidab-9 in buffer (pH = 7) at 30 to 70 °C.

Temperature	$[\theta]_{\pi\rightarrow\pi^*}$[a,b]	$[\theta]_{n\rightarrow\pi^*}$[a,c]	R	% Helicity
30	-1143	-868	0.76	12 (α)
40	-156	-189	1.2	10 (α)
50	-626	-608	0.97	11 (α)
60	-549	-500	0.91	11 (α)
70	-664	-487	0.73	11 (α)

[a]Units for [θ] are deg cm^2 $dmol^{-1}$.
[b]The minimum for the $[\theta]_{\pi\rightarrow\pi^*}$ band is observed in the range from ~ 205-209 nm.
[c]The minimum for the $[\theta]_{\pi\rightarrow\pi^*}$ band is observed in the range from ~ 222-225 nm.

The greatest percentage of α-helicity for each peptide was shown at 30 °C. As the temperature increased to 70 °C, the general trend observed was weakening of the helicity of the peptides, which was indicated graphically by the decreasing intensity of the molar ellipticities of the characteristic minima and numerically by the calculated, decreasing percent helicity (Figure 3.18, Figure 3.19, Figure 3.20, Figure 3.21). Interestingly, Ipidap-9, which didn't have a well-defined structure in buffer at 25 °C, possessed the two minima transition bands characterized by helical peptides at 30-70 °C. In this study, no helix-coil transition nor α-helix to 3_{10}-helix transition was observed. Furthermore, data obtained by heating and cooling experiments for each peptide were not significantly different, which demonstrate the reversibility of the thermal transition from 30 to 70 °C in buffer.[3.35]

There appeared to have been a small α- to 3_{10}-helical transition in 25 mM SDS for Ipi-9 in the temperature range of 30 to 70 °C (Table 3.11 and Figure 3.22). This is based

Table 3.10 CD data and derived structural parameters for Ipidap-9 in buffer (pH = 7) at 30 to 70 °C.

Temperature	$[\theta]_{\pi\rightarrow\pi^*}$[a,b]	$[\theta]_{n\rightarrow\pi^*}$[a,c]	R	% Helicity
30	-6100	-3793	0.62	20 (α)
40	-6375	-3585	0.56	20 (α)
50	-3258	-2193	0.67	16 (α)
60	-3736	-2106	0.56	15 (α)
70	-4348	-2525	0.58	17 (α)

[a]Units for [θ] are deg cm^2 $dmol^{-1}$.
[b]The minimum for the $[\theta]_{\pi\rightarrow\pi^*}$ band is observed in the range from ~ 205-209 nm.
[c]The minimum for the $[\theta]_{\pi\rightarrow\pi^*}$ band is observed in the range from ~ 222-225 nm.

on the percent 3_{10}-helicity and R values of Ipi-9. At 30 °C and 70 °C the R values and percent 3_{10}-helicity of Ipi-9 are 0.5, 13% and 0.38, 18%, respectively. For Ipiorn-9, the percent 3_{10}-helicity (~9%) remains fairly constant over the range of temperatures in 25 mM SDS; however, there was a noticeable decrease in the R values (Table 3.11 and Figure 3.23). At 30 °C and 70 °C the R values of Ipiorn-9 were 0.42 and 0.26, respectively. Overall, it appears that both Ipi-9 and Ipiorn-9 possess their designed 3_{10}-helical structures in 25 mM SDS at higher temperatures (30 to 70 °C).

Increasing the temperature of a SDS micelle solution generally increases its critical micelle concentration (CMC).[3.36] Our studies were performed in 25 mM SDS, which is high above its CMC; therefore, the concentration of micelles versus monomer surfactants may not have changed significantly with the increase in temperature.

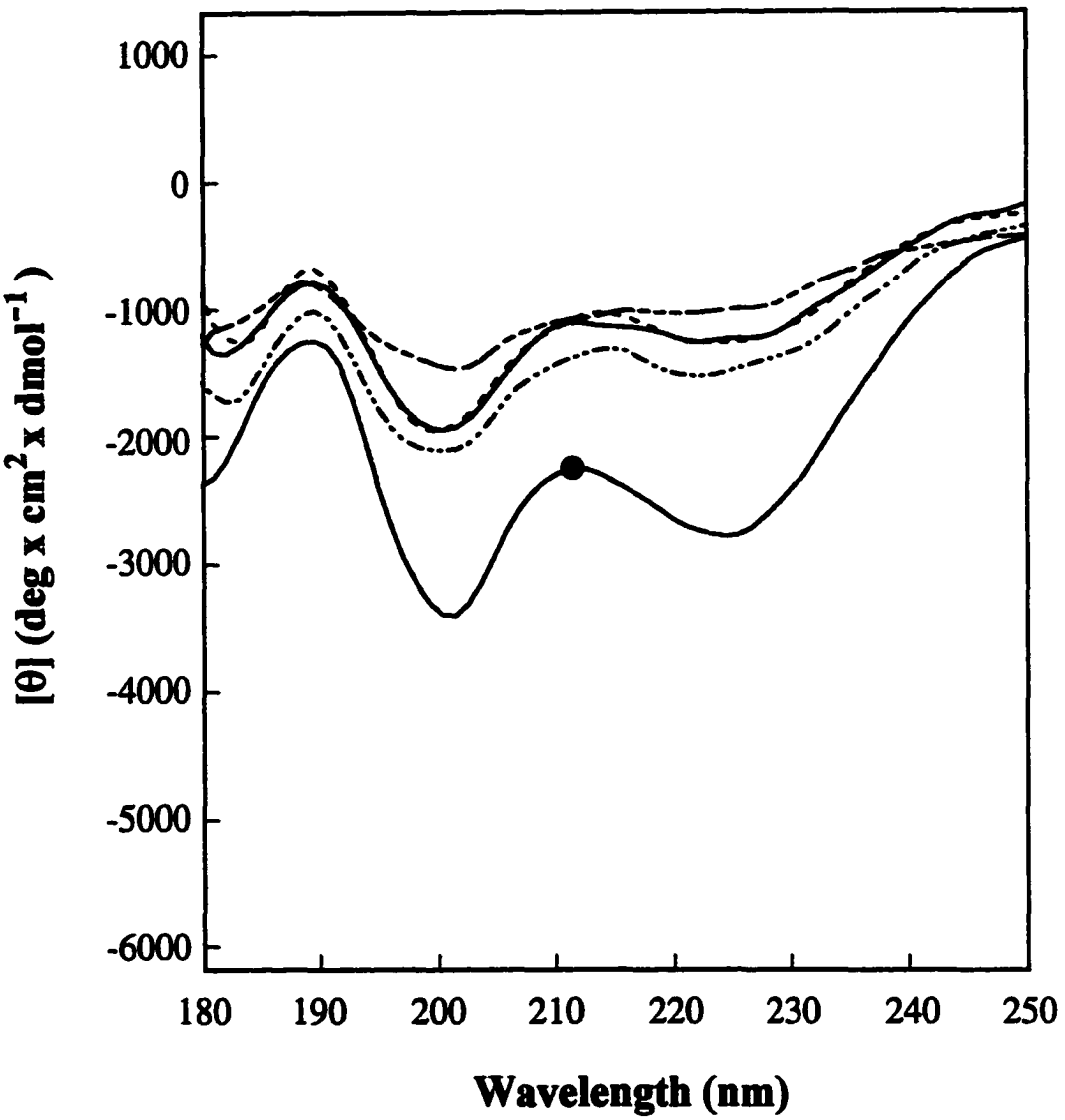

Figure 3.18 CD spectra of Ipi-9 at 30°C (●),40°C (– – –), 50°C (——), 60°C (- - - -), 70°C (———) in neutral, aqueous buffer.

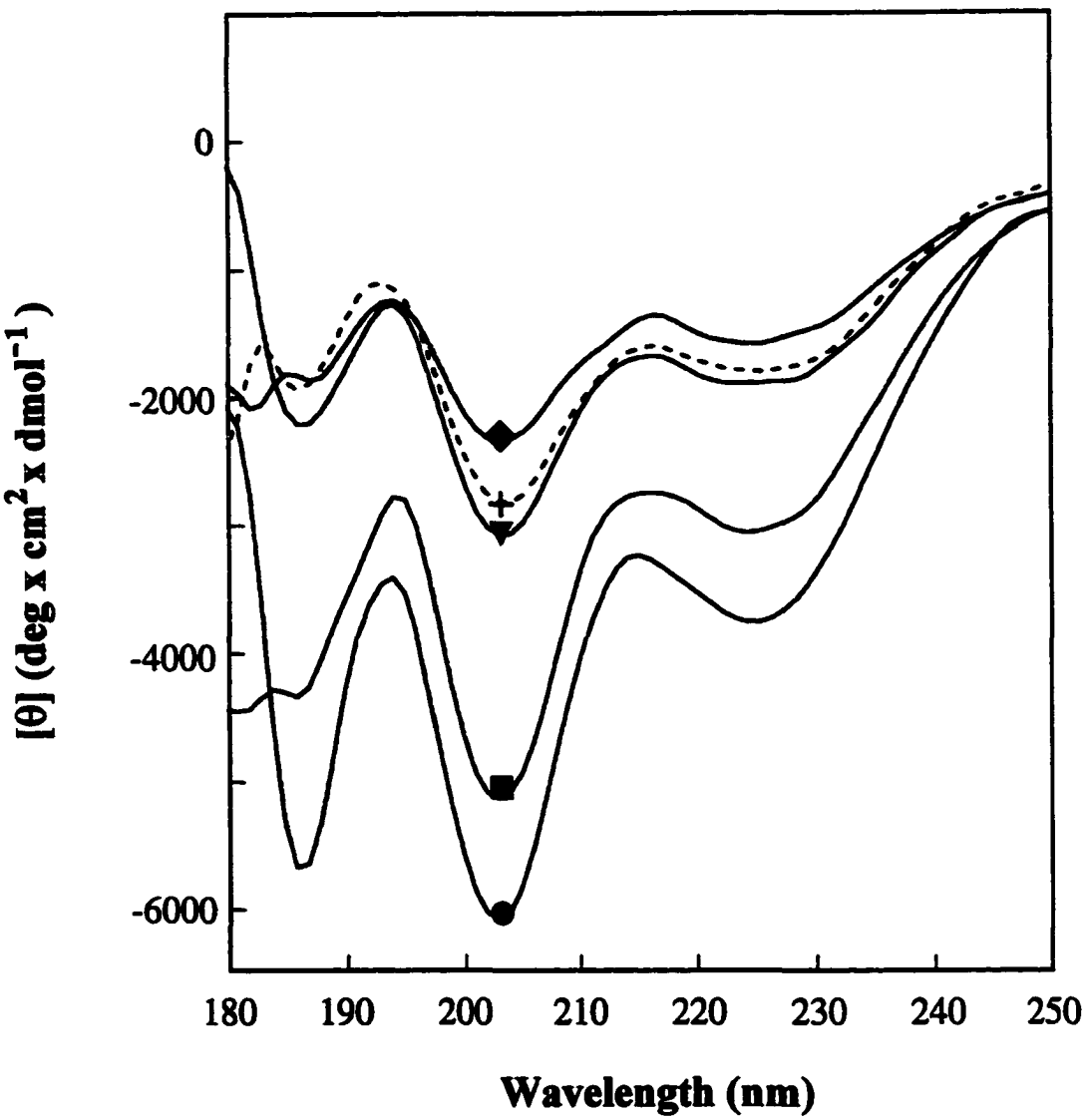

Figure 3.19 CD spectra of Ipiorn-9 at 30°C (●),40°C (■), 50°C (◆), 60°C (▼), and 70°C (+) in neutral, aqueous buffer.

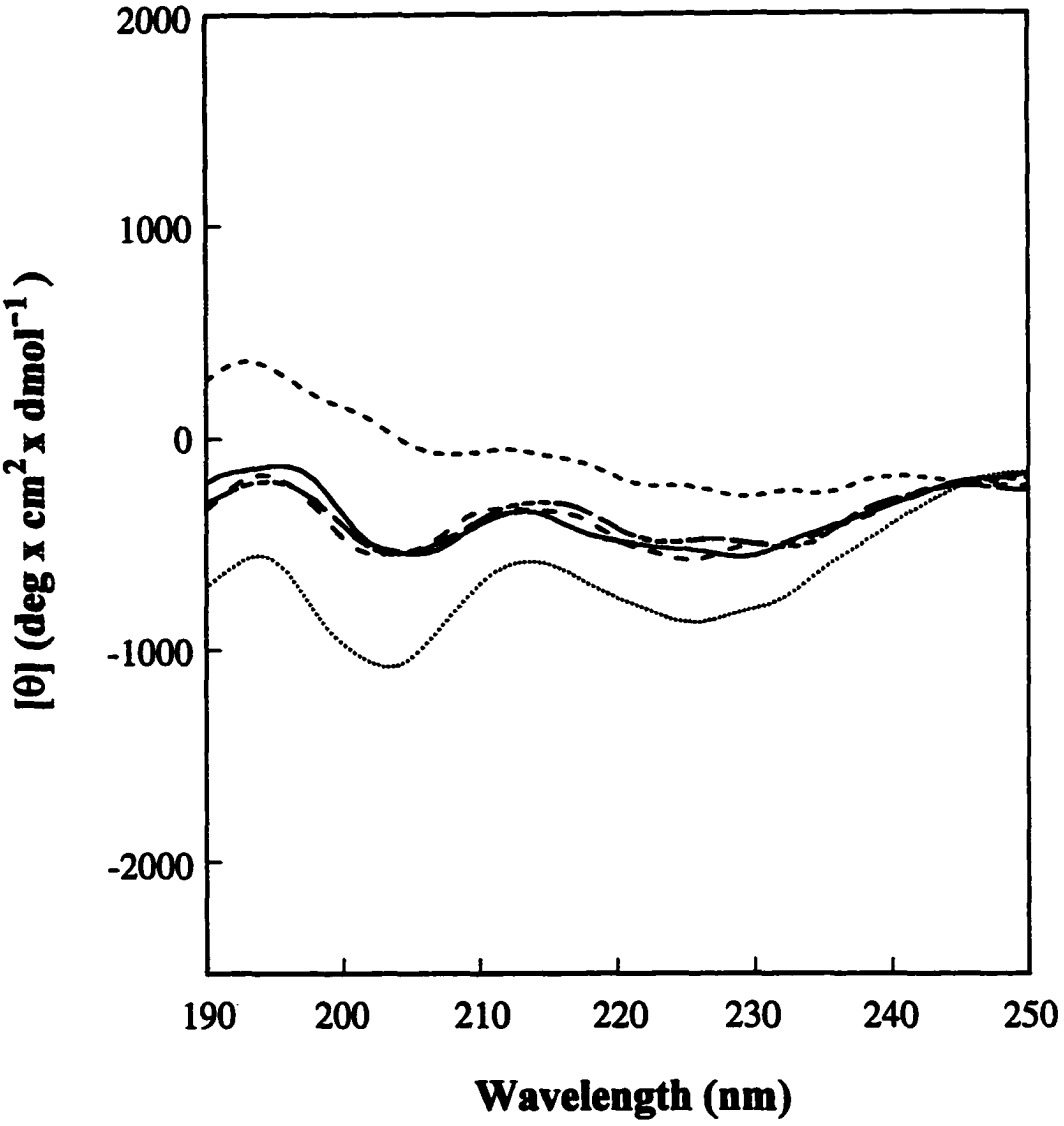

Figure 3.20 CD spectra of Ipidab-9 at 30°C (———),40°C (- - - -), 50°C (– – –), 60°C (—·—·—), 70°C (——) in neutral, aqueous buffer.

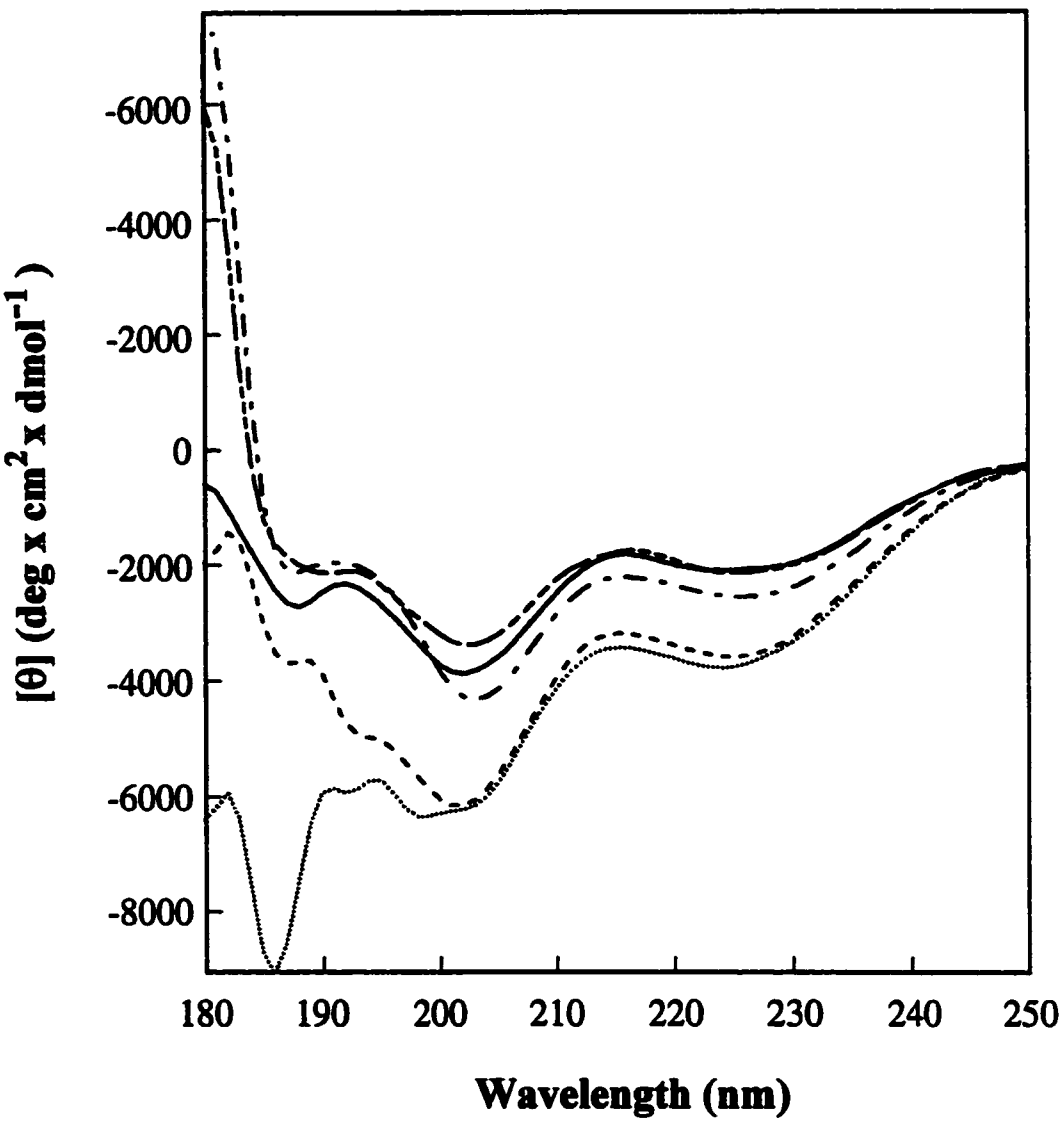

Figure 3.21 CD spectra of Ipidap-9 at 30°C (———),40°C (- - - -), 50°C (—·—·—), 60°C (———), 70°C (——) in neutral, aqueous buffer.

However, the size and shape of the micelles could have possibly changed during the rise in temperature. Ramesh and Labes[3.37] suggest a spherical to cylindrical to a bilayer structure as the temperature increases. It has been suggested that the differences in helical content are possibly due to the relative binding affinity of peptides with SDS micelles.[3.19] Increasing the temperature of our SDS solution may have modified the shape or size of the micelles resulting in a more favorable interaction with the peptides.

Table 3.11 CD data and derived structural parameters for Ipi-9 in 25 mM SDS at 30 to 70 °C.

Temperature	$[\theta]_{\pi\rightarrow\pi^*}$[a,b]	$[\theta]_{n\rightarrow\pi^*}$[a,c]	R	% Helicity
30	-2727	-1380	0.50	13 (3_{10})
40	-3277	-1548	0.47	15 (3_{10})
50	-3258	-1349	0.41	15 (3_{10})
60	-3731	-1385	0.37	17 (3_{10})
70	-3813	-1467	0.38	18 (3_{10})

[a]Units for [θ] are deg cm^2 $dmol^{-1}$.
[b]The minimum for the $[\theta]_{\pi\rightarrow\pi^*}$ band is observed in the range from ~ 205-209 nm.
[c]The minimum for the $[\theta]_{\pi\rightarrow\pi^*}$ band is observed in the range from ~ 222-225 nm.

A study was also conducted on the effect of the different solvent systems described above on the designed 3_{10}-helical acetylated peptides **3.5-3.9**. Blocking of the N-terminus, as well as the C-terminus, of a designed helical peptide generally adds to its stability; it eliminates the fixed-end charges that could cause either destabilization of helices or inhibition of formation of helices.[3.38] Stability is also afforded helical peptides that are N-acetylated at the N-terminus due to the additional hydrogen bond; the carbonyl of the blocking group acts an extra hydrogen bond acceptor.[3.16] The first reported

Table 3.12 CD data and derived structural parameters for Ipiorn-9 in 25 mM SDS at 30 to 70 °C.

Temperature	$[\theta]_{\pi\rightarrow\pi^*}$[a,b]	$[\theta]_{n\rightarrow\pi^*}$[a,c]	R	% Helicity
30	-1941	-812	0.42	9 (3_{10})
40	-1860	-695	0.37	9 (3_{10}))
50	-1893	-735	0.38	9 (3_{10})
60	-1958	-435	0.22	9 (3_{10})
70	-1944	-515	0.26	9 (3_{10})

[a]Units for [θ] are deg cm^2 $dmol^{-1}$.
[b]The minimum for the $[\theta]_{\pi\rightarrow\pi^*}$ band is observed in the range from ~ 205-209 nm.
[c]The minimum for the $[\theta]_{\pi\rightarrow\pi^*}$ band is observed in the range from ~ 222-225 nm.

experimental CD spectrum for a right-handed 3_{10}-helical peptide in TFE was a short, hydrophobic, acetylated peptide (Ac-[L-(α-Me)Val]$_8$-OtBu).[3.1] Also, the acetylated peptide, Ac-Aib-ATANP-(Aib)$_2$-ATANP-(Aib)$_2$-OMe, was the first reported example of a short peptide assuming 3_{10}-helical conformation in pure water.[3.16] Peptide **3.6** (AcIpiorn-9) assumed its designed 3_{10}-helical structure appreciably in 25 mM SDS and CH_3CN-TFE (9:1). Its R values and percent 3_{10}-helicity was, in SDS, 0.42 and 11%, respectively, and 0.24 and 20%, respectively, in CH_3CN-TFE (9:1) (Table 3.13; Figure 3.24; Figure 3.25). Peptide **3.7** (AcIpidab-9) assumed a 3_{10} helical structure in CH_3CN-TFE (9:1) with a R value of 0.49 and 22% estimated 3_{10}-helicity (Table 3.14), and peptide **3.10** assumed a 3_{10}-helical structure in 25 mM SDS with a R value of 0.38 and 41 % 3_{10}-helicity (Table 3.15). For the other acetylated peptides, **3.5** (Table 3.16) and **3.8** (Table 3.17), mainly α-helices formed in the six solvent systems, particularly in neutral buffer (Figure 3.26) and CH_3CN-H_2O (9:1) (Figure 3.27), employed except for **3.8** in 25 mM SDS, in which no clear helical or secondary structure was evident.

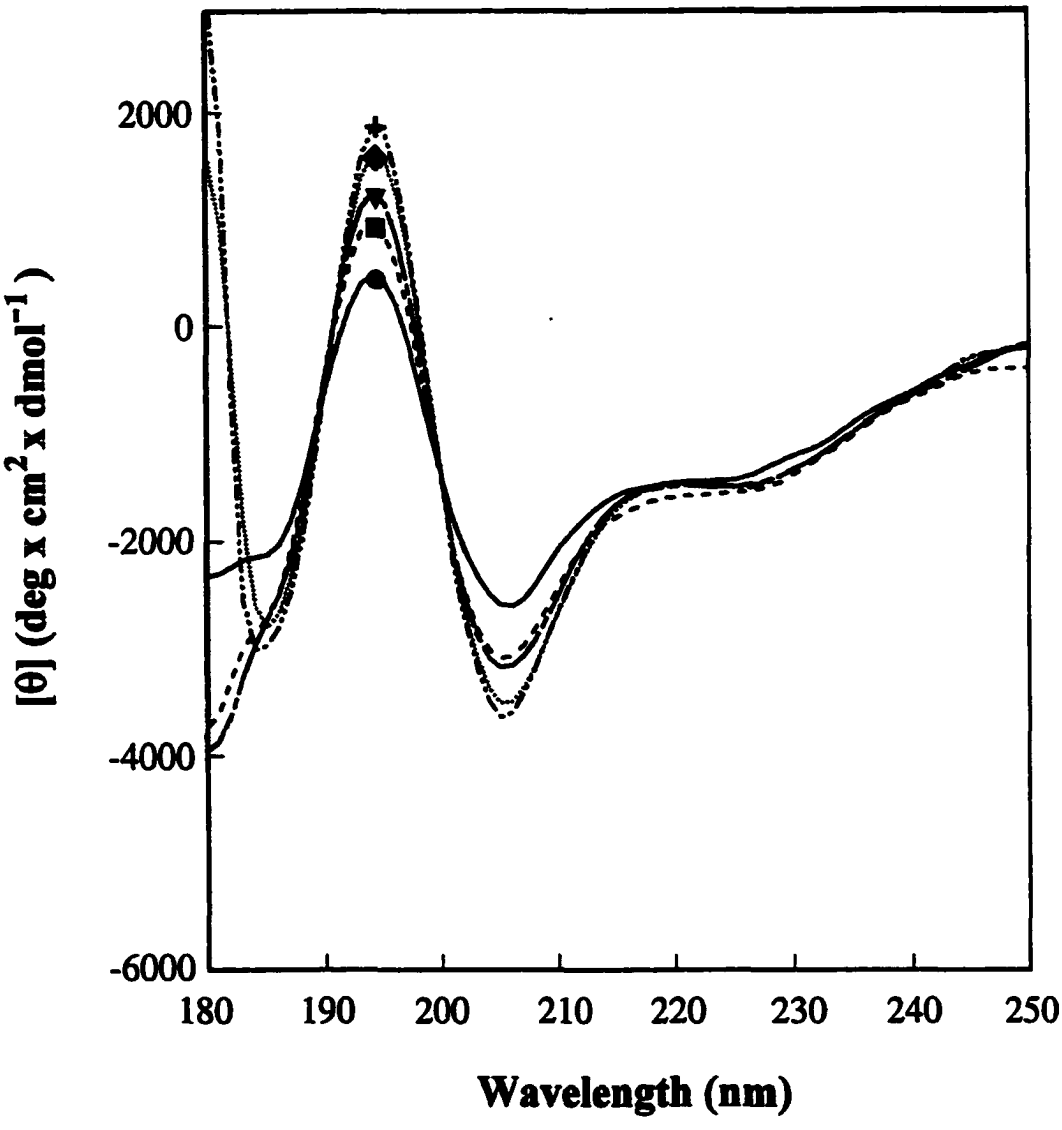

Figure 3.22 CD spectra of Ipi-9 at 30°C (▼), 40°C (◆), 50°C (■),60°C (●) and 70°C (+) in 25mM SDS

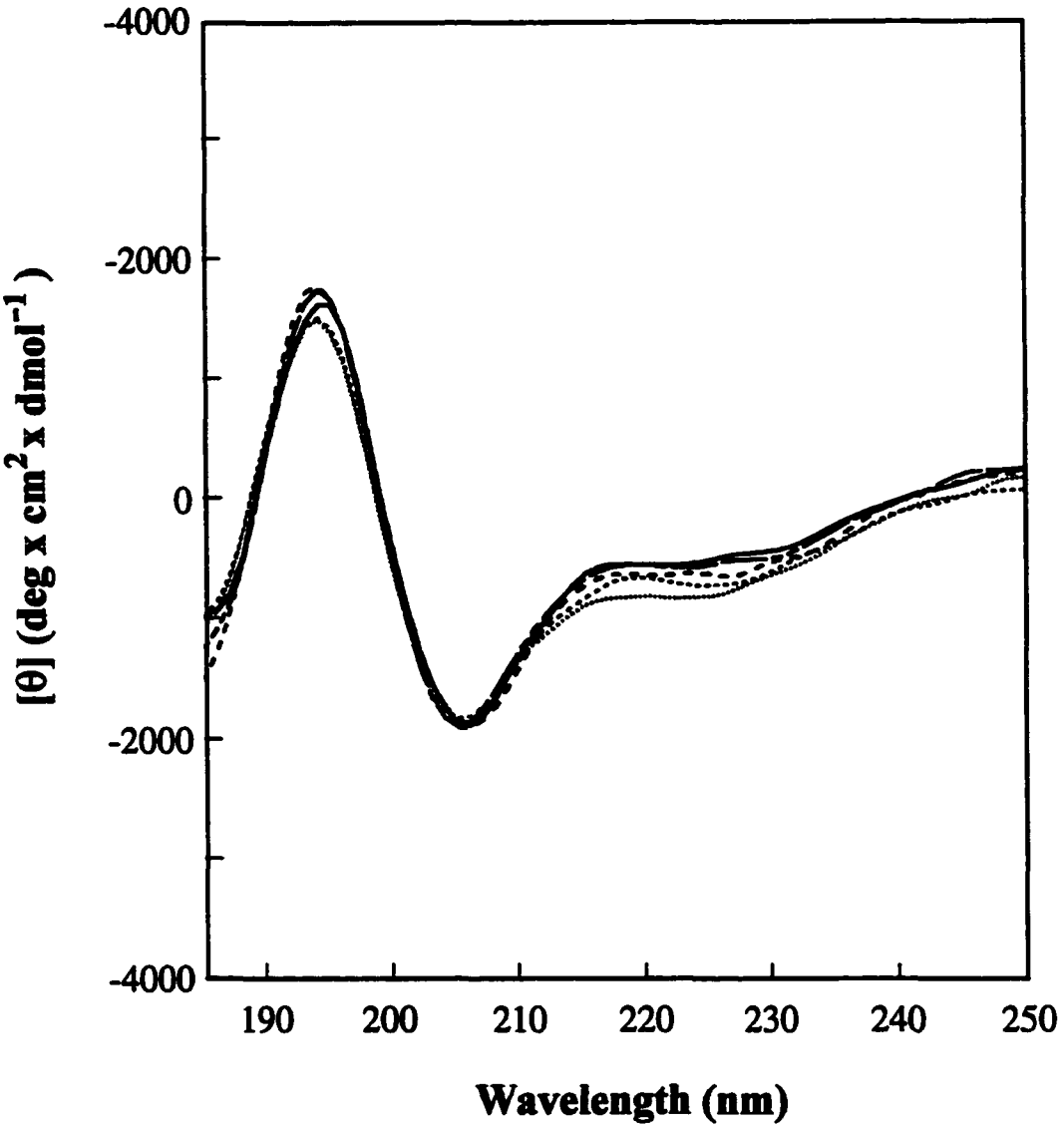

Figure 3.23 CD spectra of Ipiorn-9 at 30°C (·····),40°C (-----), 50°C (- - - -), 60°C (— — —), 70°C (——) in 25 mM SDS.

Table 3.13 CD data and derived structural parameters for AcIpiorn-9 at 25 °C.

Solvent	$[\theta]_{\pi\rightarrow\pi^*}$[a,b]	$[\theta]_{n\rightarrow\pi^*}$[a,c]	R	% Helicity
25 mM SDS	-2432	-1037	0.42	11 (3_{10})
9:1 CH_3CN-TFE	-4287	-1023	0.24	20 (3_{10})
9:1 CH_3CN-H_2O	-11606	-11811	1	45 (α)
3:1 CH_3CN-H_2O	-3510	-3044	0.85	18 (α)
1:1 CH_3CN-H_2O	-2489	-2003	0.80	15 (α)
Buffer (pH = 7)	-7330	-8145	1.1	34 (α)

[a]Units for [θ] are deg cm^2 $dmol^{-1}$.
[b]The minimum for the $[\theta]_{\pi\rightarrow\pi^*}$ band is observed in the range from ~ 205-209 nm.
[c]The minimum for the $[\theta]_{\pi\rightarrow\pi^*}$ band is observed in the range from ~ 222-225 nm.

Table 3.14 CD data and derived structural parameters for AcIpidab-9 at 25 °C.

Solvent	$[\theta]_{\pi\rightarrow\pi^*}$[a,b]	$[\theta]_{n\rightarrow\pi^*}$[a,c]	R	% Helicity
25 mM SDS	-1706	-983	0.57	12 (α)
9:1 CH_3CN-TFE	-4700	-2329	0.49	22 (3_{10})
9:1 CH_3CN-H_2O	-1513	-2660	1.7	17 (α)
3:1 CH_3CN-H_2O	-1600	-1433	0.89	13 (α)
1:1 CH_3CN-H_2O	-1303	-1654	1.2	14 (α)
Buffer (pH = 7)	-2228	-2451	1.1	16 (α)

[a]Units for [θ] are deg cm^2 $dmol^{-1}$.
[b]The minimum for the $[\theta]_{\pi\rightarrow\pi^*}$ band is observed in the range from ~ 205-209 nm.
[c]The minimum for the $[\theta]_{\pi\rightarrow\pi^*}$ band is observed in the range from ~ 222-225 nm

Table 3.15 CD data and derived structural parameters for AcIpi-10 at 25 °C.

Solvent	$[\theta]_{\pi\rightarrow\pi^*}$[a,b]	$[\theta]_{n\rightarrow\pi^*}$[a,c]	R	% Helicity
25 mM SDS	-8814	-3362	0.38	41 (3_{10})
9:1 CH_3CN-TFE	-25375	-19938	0.78	70 (α)
9:1 CH_3CN-H_2O	-12701	-13864	1.1	51 (α)
3:1 CH_3CN-H_2O	-12240	-12714	1	47 (α)
1:1 CH_3CN-H_2O	-9857	-10075	1	40 (α)
Buffer (pH = 7)	-9794	-9294	0.94	37 (α)

[a]Units for [θ] are deg cm^2 $dmol^{-1}$.
[b]The minimum for the $[\theta]_{\pi\rightarrow\pi^*}$ band is observed in the range from ~ 205-209 nm.
[c]The minimum for the $[\theta]_{\pi\rightarrow\pi^*}$ band is observed in the range from ~ 222-225 nm.

Table 3.16 CD data and derived structural parameters for AcIpi-9 at 25 °C.

Solvent	$[\theta]_{\pi\rightarrow\pi^*}$[a,b]	$[\theta]_{n\rightarrow\pi^*}$[a,c]	R	% Helicity
25 mM SDS	-4877	-3151	0.64	*d*
9:1 CH_3CN-TFE	-19472	-13295	0.68	49 (α)
9:1 CH_3CN-H_2O	-18611	-17432	0.93	62 (α)
3:1 CH_3CN-H_2O	-9548	-8136	0.85	34 (α)
1:1 CH_3CN-H_2O	-8025	-7748	0.96	32 (α)
Buffer (pH = 7)	-3998	-4277	1.1	22 (α)

[a]Units for [θ] are deg cm^2 $dmol^{-1}$.
[b]The minimum for the $[\theta]_{\pi\rightarrow\pi^*}$ band is observed in the range from ~ 205-209 nm.
[c]The minimum for the $[\theta]_{\pi\rightarrow\pi^*}$ band is observed in the range from ~ 222-225 nm.
[d]The % α-helix is estimated at 19%, and the % 3_{10}-helix is estimated at 23%.

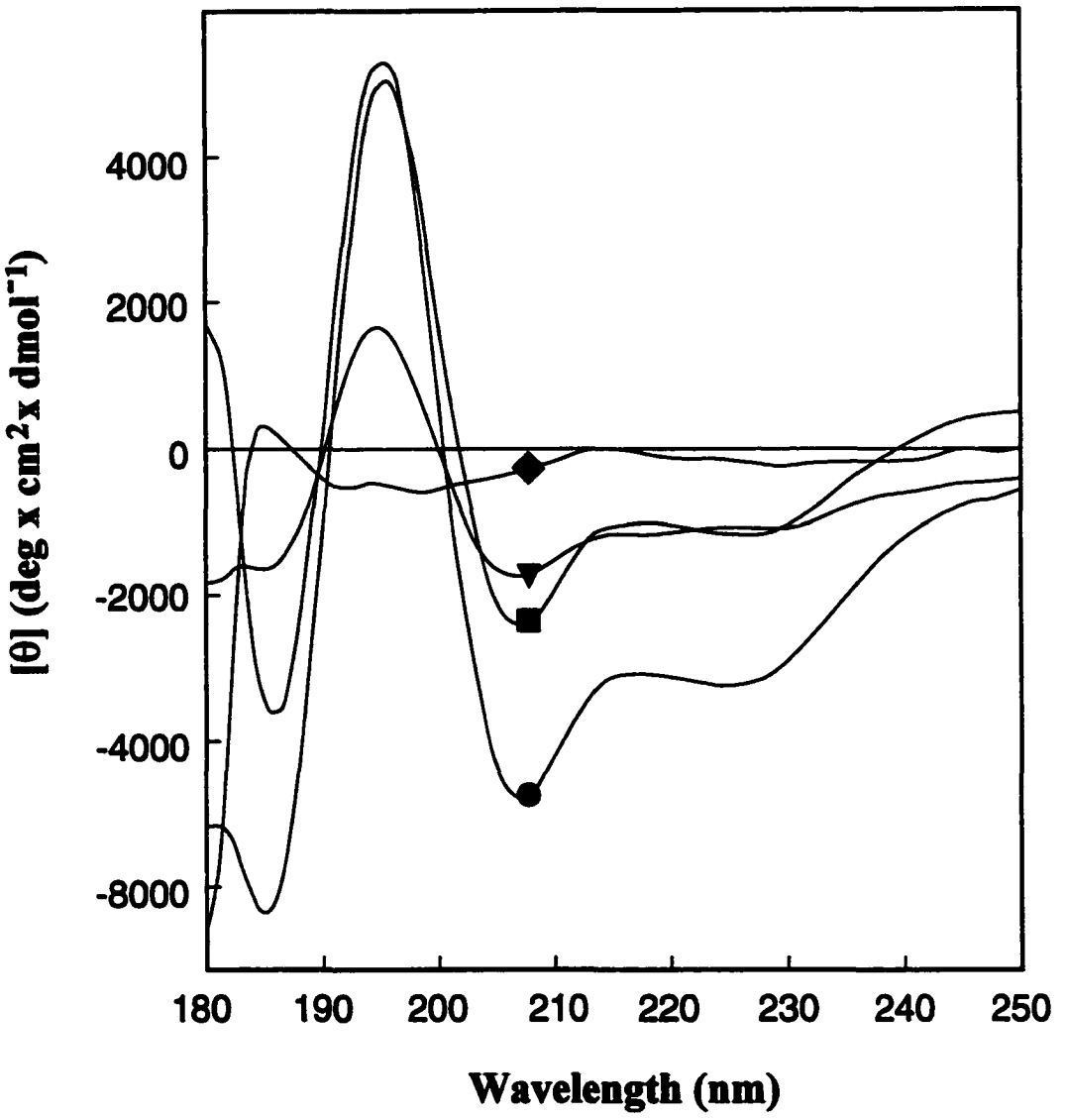

Figure 3.24 CD spectra of AcIpi-9 (●), AcIpiorn-9 (■), AcIpidab-9 (▼) and AcIpidap-9 (◆) in 25 mM SDS.

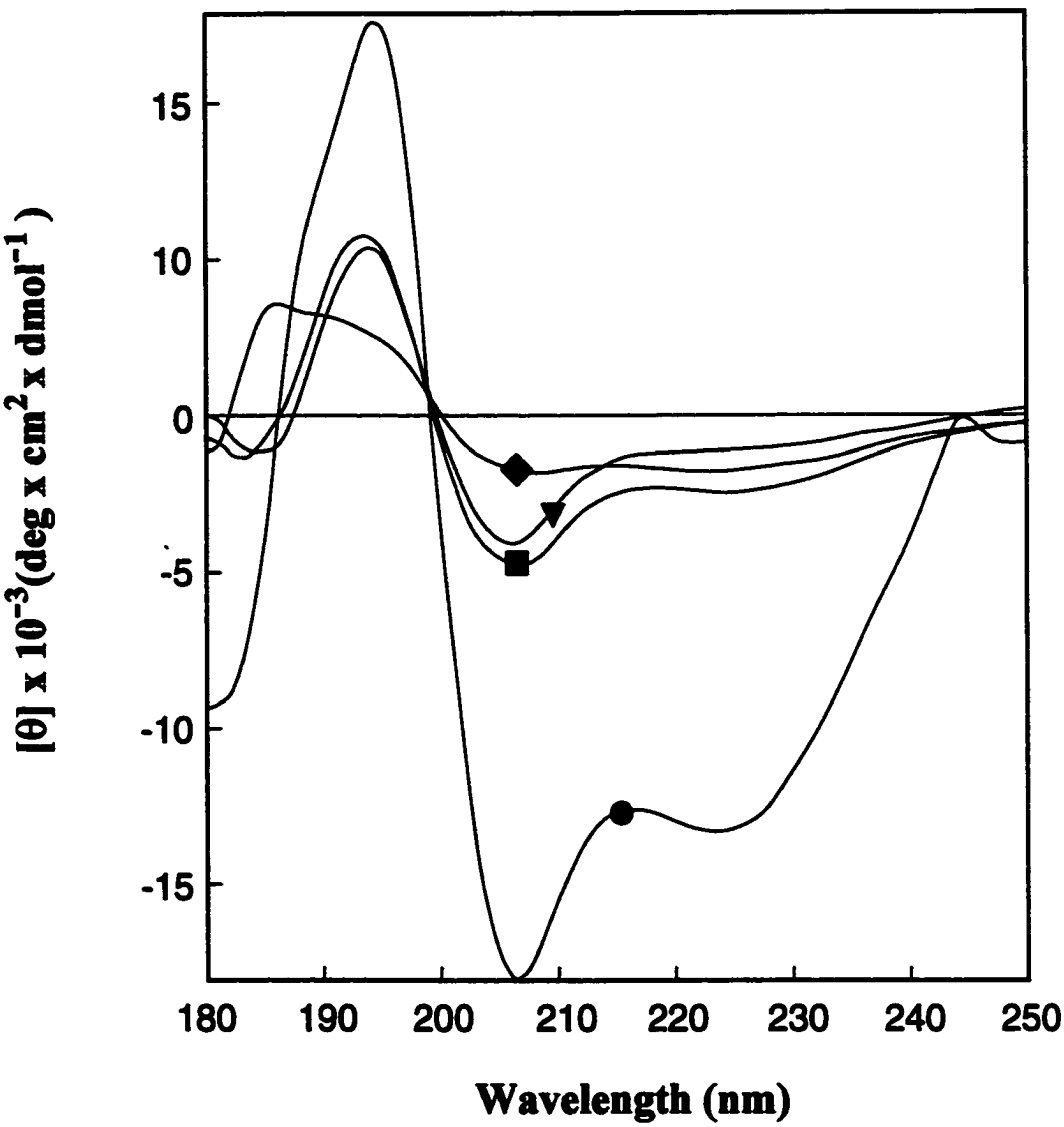

Figure 3.25 CD spectra of AcIpi-9 (●), AcIpiorn-9 (■), AcIpidab-9 (▼) and AcIpidap-9 (◆) in CH_3CN-TFE (9:1) at 25°C.

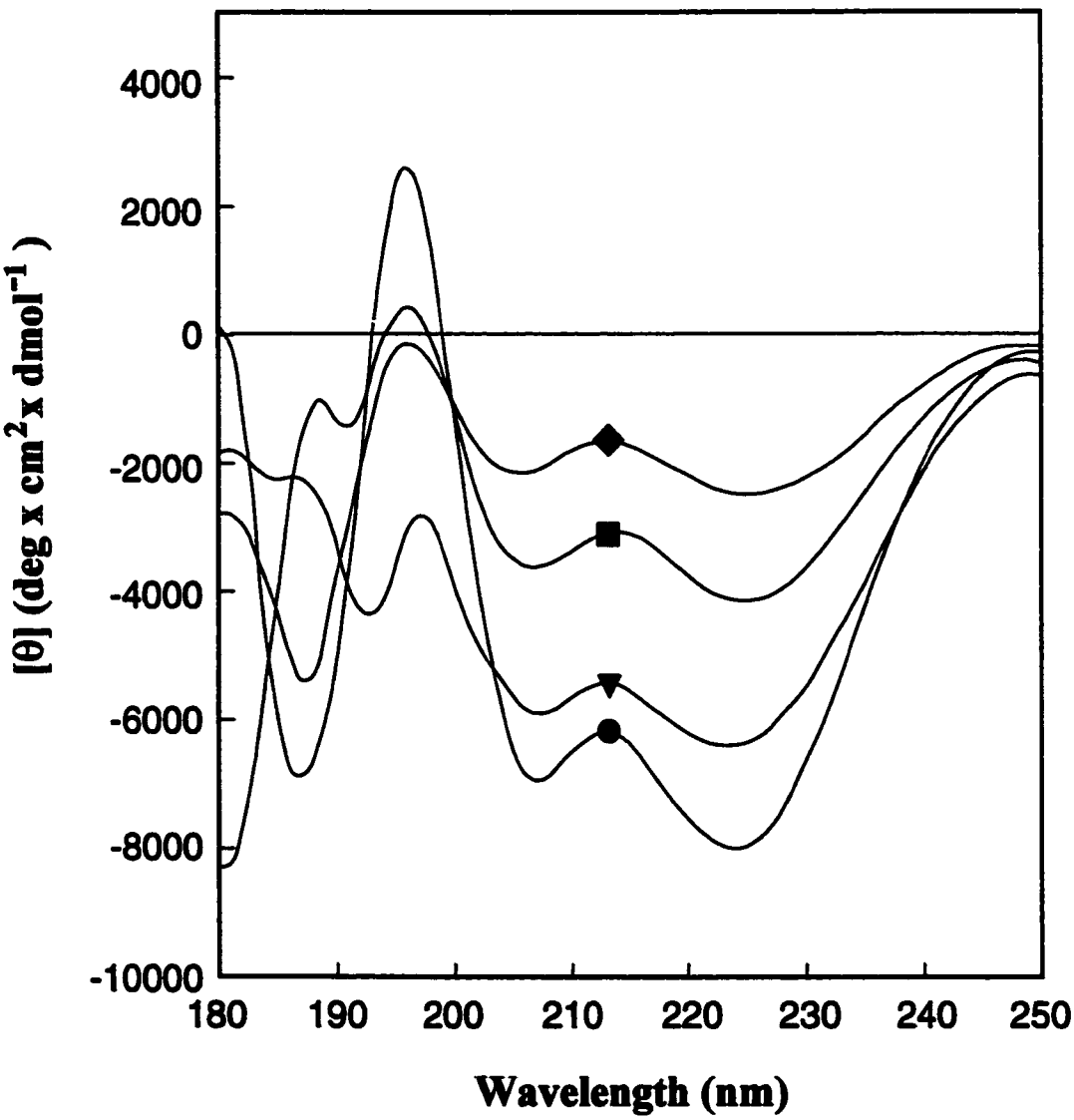

Figure 3.26 CD spectra of AcIpi-9 (■), AcIpiorn-9 (●), AcIpidab-9 (◆) and AcIpidap-9 (▼) in buffer.

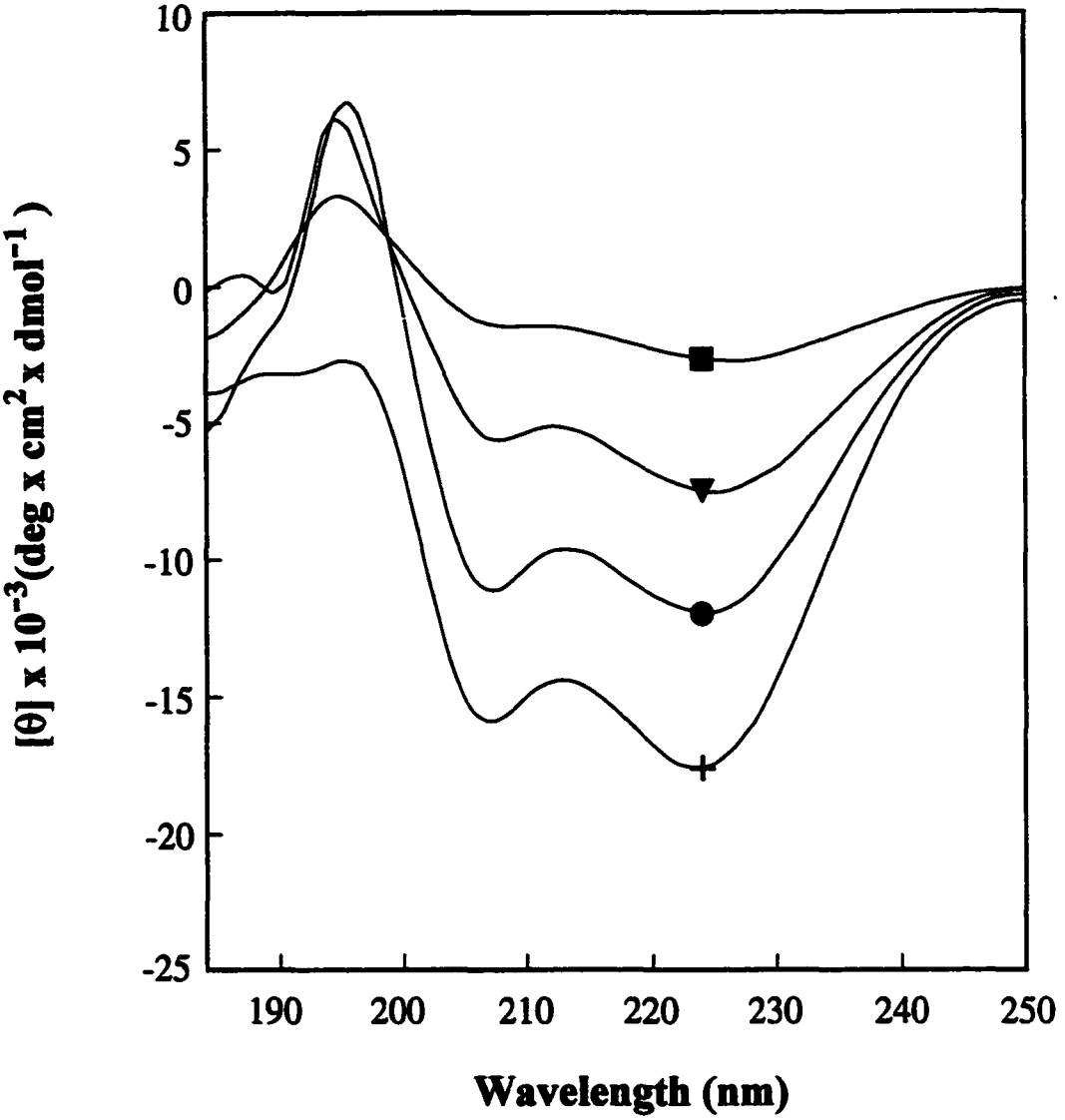

Figure 3.27 CD spectra of AcIpi-9 (+), AcIpiorn-9 (●), AcIpidab-9 (■), AcIpidap-9 (▼) in CH_3CN-H_2O (9:1) at 25°C.

Table 3.17 CD data and derived structural parameters for AcIpidap-9 at 25 °C.

Solvent	$[\theta]_{\pi\rightarrow\pi^*}$[a,b]	$[\theta]_{n\rightarrow\pi^*}$[a,c]	R	% Helicity
9:1 CH_3CN-TFE	-1898	-1618	0.85	14 (α)
9:1 CH_3CN-H_2O	-5963	-7554	1.2	32 (α)
3:1 CH_3CN-H_2O	-4017	-3188	0.79	19 (α)
1:1 CH_3CN-H_2O	-6008	-4980	0.82	24 (α)
Buffer (pH = 7)	-5895	-6515	0.9	29 (α)

[a]Units for [θ] are deg cm^2 $dmol^{-1}$.
[b]The minimum for the $[\theta]_{\pi\rightarrow\pi^*}$ band is observed in the range from ~ 205-209 nm.
[c]The minimum for the $[\theta]_{\pi\rightarrow\pi^*}$ band is observed in the range from ~ 222-225 nm.

The helicity of AcIpi-9 and AcIpiorn-9 was measured in buffer at three different pH's, 2, 4, and 7 (Table 3.18 and Table 3.19). Based on the R values (0.87-1.1) of both peptides, α-helicity is predominantly observed at all tested pH's. The most stable α-helical structure was observed for AcIpiorn-9 at pH 4. For both acetylated peptides the weakest α-helical structure was observed at pH 2 (Figure 3.28 and Figure 3.29). The more acidic medium may have interfered with the helices' intramolecular hydrogen bonding pattern.

In our study, we observed an average increase in stability (based on general increase in ellipticity) with the acetylated peptides vs. the non-acetylated peptides. Also, our actual design (3_{10}-helical) of the peptides were observed best with the acetylated peptides, specifically, AcIpiorn-9, AcIpidab-9, and AcIpi-10 in either or both 25 mM SDS and CH_3CN-TFE (9:1) (Figure 3.12 and Figure 3.13). Particularly noteworthy are the differences in CD data obtained for Ipiorn-9 and its acetylated version, AcIpiorn-9.

The designed, 3_{10}-helical structure of Ipiorn-9 was observed best in buffer, where its R value is 0.48. However, AcIpiorn-9 was better stabilized (based on molar ellipticity) as an α-helix in buffer, where its R value is 1.1. The R values of Ipiorn-9 in 25 mM SDS (R = 0.72) and in CH_3CN-TFE (9:1, R = 0.66) indicate that Ipiorn-9 exhibits more α-helical than 3_{10}-helical structures in these solvent systems. In contrast, the R values of AcIpiorn-9 in 25 mM SDS (R = 0.42) and in CH_3CN-TFE (9:1, R = 0.24) indicate that AcIpiorn-9 folded appreciably into its designed, 3_{10}-helical structure under these solvent conditions.

Table 3.18 CD data and derived structural parameters for AcIpi-9 at 25 °C.

pH	$[\theta]_{\pi\rightarrow\pi^*}$[a,b]	$[\theta]_{n\rightarrow\pi^*}$[a,c]	R	% Helicity
2	-1873	-1722	0.92	14 (α)
4	-2619	-2474	1	17 (α)
7	-3998	-4277	1.1	22 (α)

[a]Units for [θ] are deg cm^2 $dmol^{-1}$.
[b]The minimum for the $[\theta]_{\pi\rightarrow\pi^*}$ band is observed in the range from 205-209 nm.
[c]The minimum for the $[\theta]_{\pi\rightarrow\pi^*}$ band is observed in the range from 222-225 nm.

Table 3.19 CD data and derived structural parameters for AcIpiorn-9 at 25 °C.

pH	$[\theta]_{\pi\rightarrow\pi^*}$[a,b]	$[\theta]_{n\rightarrow\pi^*}$[a,c]	R	% Helicity
2	-4268	-3714	0.87	20 (α)
4	-12431	-11282	0.91	43 (α)
7	-7330	-8145	1.1	34 (α)

[a]Units for [θ] are deg cm^2 $dmol^{-1}$.
[b]The minimum for the $[\theta]_{\pi\rightarrow\pi^*}$ band is observed in the range from ~ 205-209 nm.
[c]The minimum for the $[\theta]_{\pi\rightarrow\pi^*}$ band is observed in the range from ~ 222-225 nm.

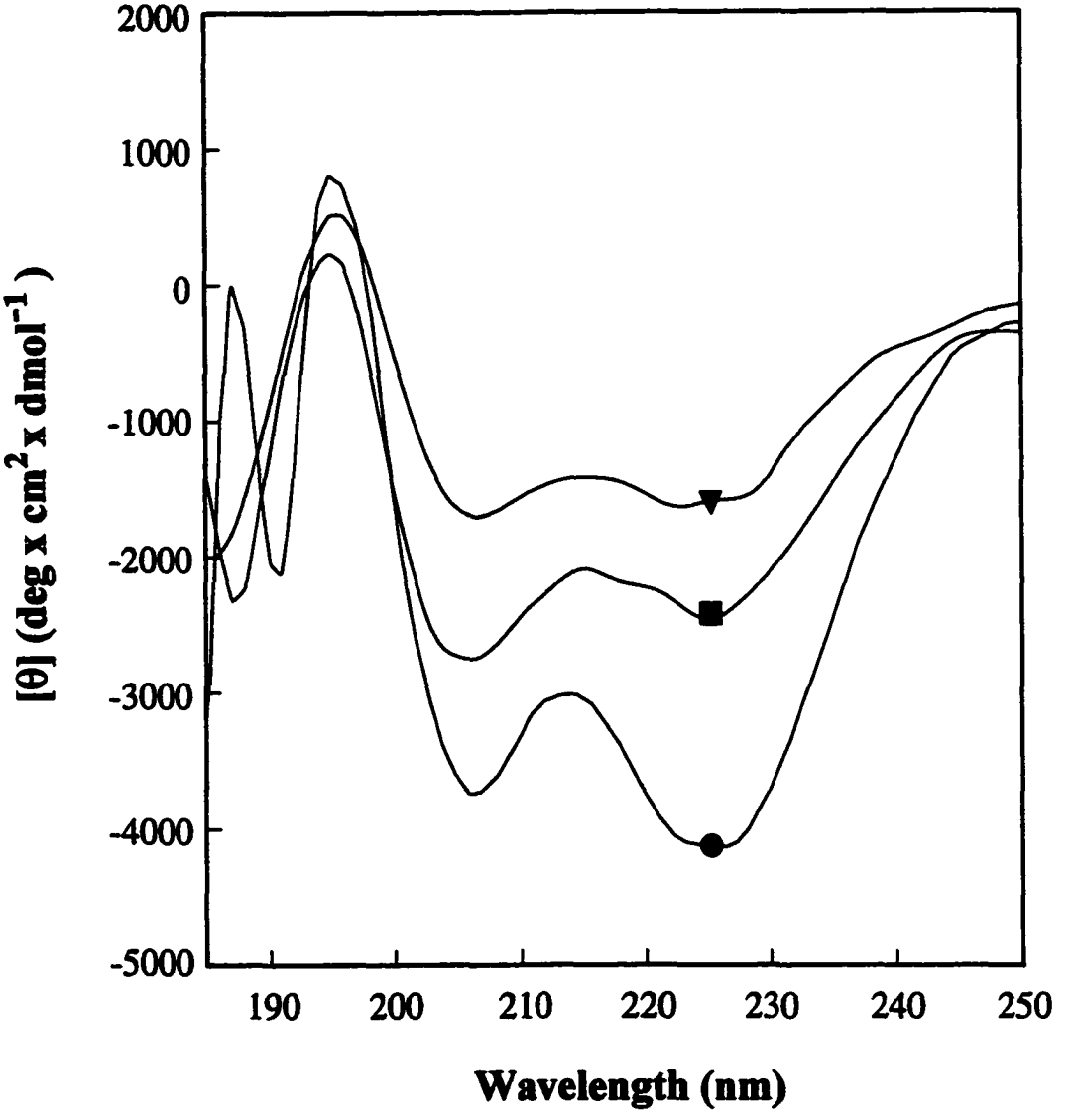

Figure 3.28 CD spectra of AcIpi-9 in buffer at pH 7 (●), pH 4 (■) and pH 2(▼)

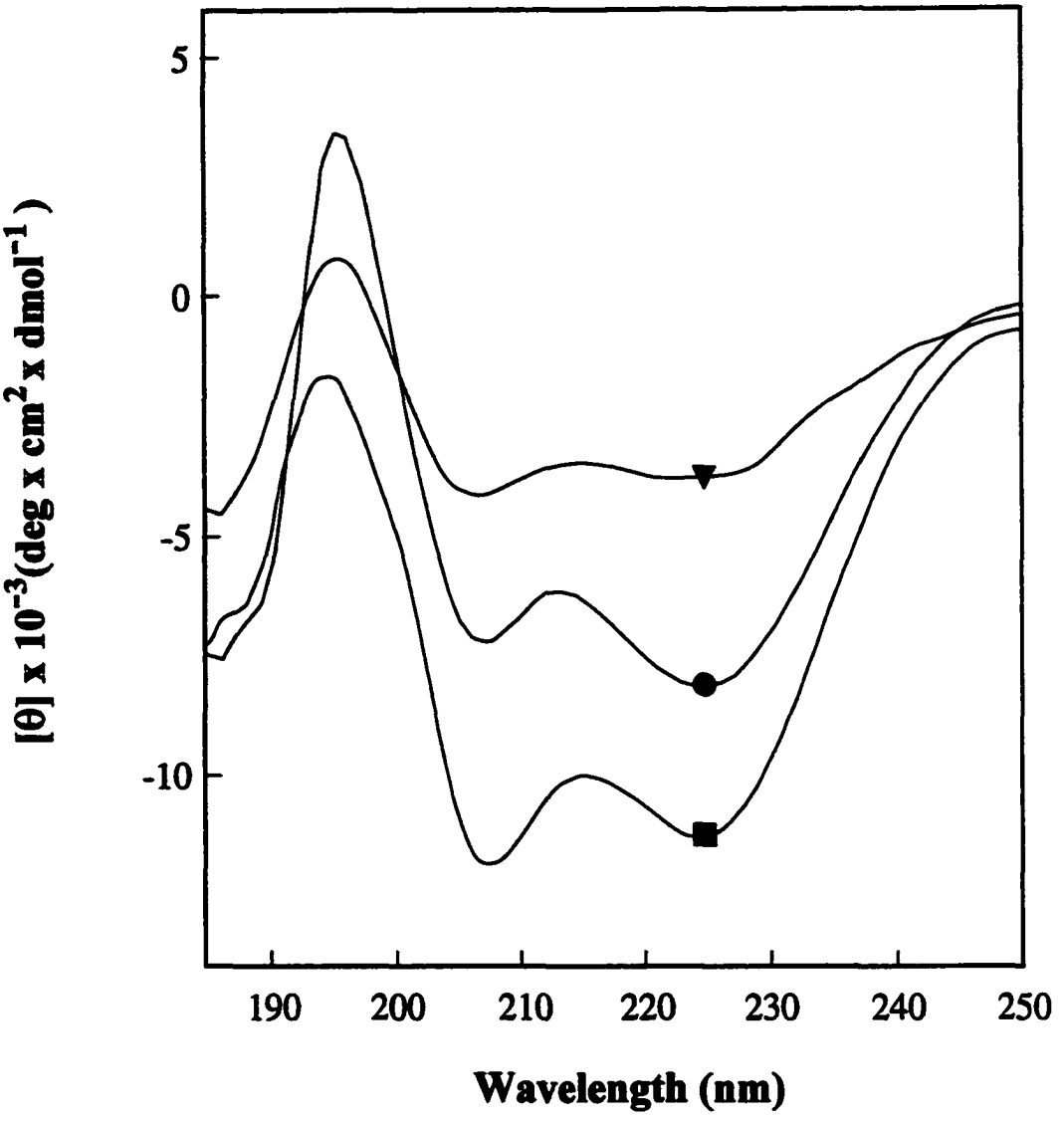

Figure 3.29 CD spectra of AcIpiom-9 in buffer at pH 7 (●), pH 4 (■) and pH 2(▼)

The 3_{10}-helical design of our peptides were in accord with the general factors (e.g., helix length, number of Aib's, position of α-amino acids) that favor 3_{10}-helix formation, although α-helices were observed for most of the peptides under the six solvent conditions. The amphipathic design tool, undoubtedly, played a major role in the 3_{10}-helices considerably forming in the above, acetylated peptides, especially in the SDS micelle media. The length of the side-chains may have also been a factor, particularly for AcIpiorn-9. The shortening of AcIpi-9 to AcIpiorn-9 led to R values, in 25 mM SDS and CH_3CN-TFE (9:1), that were more indicated of a 3_{10}-helix. However, further shortening of the side-chains of AcIpiorn-9 to AcIpidab-9 and AcIpidap-9 led to R values that were increasingly above the accepted value ($R \approx \leq 0.4$). Furthermore, the extra hydrogen bond and slight increase in hydrophobicity in the acetylated peptides may have resulted in the increased propensity of **3.6-3.7** to fold into a 3_{10}-helix in 100 % organic media.

3.2.3 Bioactivity of Designed Peptides

Many natural antimicrobial peptides of greatly differing sequences have been isolated with amphipathic, helical domains as a consistent structural feature.[3.20-3.21] Also, scores of de novo peptides that comprise only a putative amphipathic helix have activity comparable to or greater than that of natural peptide antibiotics.[3.20,3.22] As discussed in the previous section, our peptides were designed to be amphipathic, like natural antimicrobial peptide, as well as 3_{10}-helical. Amphipathic peptides with 18 or more residues could possess high cytotoxicity.[3.39] It's been reported that by simply reducing the length of peptides to 14 residues decrease cytotoxicity while retaining much of the antimicrobial activity.[3.20,3.22] Peptides **3.1-3.8** were prepared to test the hypothesis that retention of biological activity and lowering of cytotoxicity could be achieved by further

shortening (main and side-chains) of the 10-mer peptide, Ipi-10. The secondary structure of the peptides in the model membrane, SDS, was correlated with their biological activity.

The MIC's (minimum inhibitory concentration) for the peptides tested against *Escherichia coli* and *Staphylococcus aureus* are summarized in Table 3.20. *E. coli* is a Gram-negative bacterium, and *S. aureus* is a Gram-positive bacterium. The distinction between Gram-negative and Gram-positive bacteria is based on the differential staining procedure, Gram Stain. Gram-negative bacteria stains red, but Gram-positive, purple. This difference in reaction to the Gram Stain is due primarily to the differences in the cell wall structure of Gram-negative and Gram-positive bacteria.[3.40] The cell wall of a Gram-negative bacteria is multilayered; it is comprised of thin layer of peptidoglycan (layer composed of *N*-acetylglucosamine, *N*-acetylmuramic acid, and a few amino acids) and an outer membrane composed of lipopolysaccharaide, lipoprotein, and other complex macromolecules. The cell wall of Gram-positive bacteria, on the other hand, consists chiefly of a thick layer of peptidoglycan; it lacks the outer membrane present in Gram-negative cells.[3.40]

Peptide **3.1** (Ipi-9) inhibits the growth of *E. coli* at a minimum concentration of 140 μM; it is about 3 times less active than **3.2** (Ipiorn-9). Ipidab-9 (**3.3**) inhibits *E. Coli* at approximately 149 μM, which is comparable to **3.1**. Ipidap-9 (**3.4**), with a MIC greater than 300 μM, was the least active toward *E. coli*. Of the acetylated peptides **3.5-3.8**, AcIpi-9 (**3.5**), with a MIC of 134 μM, exhibited the best activity against *E. coli*. None of the peptides had particularly good inhibitory activity against *S. aureus*.

Antimicrobial peptides kill bacteria by disrupting the cell membrane.[3.19-3.20] It's been reported that the CD spectra of peptides in micelles suggest a structure/function relationship for the bioactive peptides.[3.20] SDS has an aliphatic tail and a negatively charged head group (sulfate). The micelles that SDS forms partially emulate the amphipathic environment of membranes. The anionic head groups provide the initial electrostatic interactions (with cationic side groups of peptides) needed and enhances the binding affinity of peptides to the non-polar interior, thereby, inducing an intrinsic, ordered structure. Because Ipi-9, of the four, non-acetylated designed peptides, possesses the most amphipathic, 3_{10}-helical structure in SDS, it was expected to be the most active against the bacteria; however, Ipiorn-9 was the most active. Ipiorn-9 did, however, have the highest, of the four peptides in all the tested six solvent systems, percentage of amphipathic, 3_{10}-helicity in buffer. The order of activity of Ipidab-9 and Ipidap-9, third and fourth, respectively, was expected. Ipidab-9 had 19% amphipathic, 3_{10} helicity in buffer but very little estimated 3_{10} helicity in SDS. Ipidap-9, on the other hand, lacked a well-defined structure in all of the solvent systems tested except the 100% organic solvent system, CH_3CN:TFE (9:1), in which α-helicity was mainly observed. Overall, the shortening of Ipi-10 (MIC, 7.7 μM) to make **3.1-3.3** resulted in diminished, but modest activity, against *E. coli* and no improvement in activity against *S. aureus*.

AcIpi-10 inhibits *E. coli* at approximately 7.4 μM; it also exhibited 41% 3_{10} helicity in SDS with a R value of 0.38. Shortening of AcIpi-10 to AcIpi-9 resulted in reduced activity. However, of the designed acetylated peptides (**3.5-3.8**), activity against *E. coli* was only observed for AcIpi-9 (**3.5**); it also had the highest estimated percent of amphipathic, 3_{10} helicity in 25 mM SDS. Practically no activity against *S. aureus* was

observed for any of the peptides. This may have been due in part to the much thicker cell wall (peptidoglycan) *S. aureus* possesses compared to *E. coli*. Although *E. coli* has a very thin peptidoglycan, it also has, as mentioned earlier, an additional outer membrane not present in S. aureus. However, the outer membrane is relatively permeable to small molecules.[3.40]

Overall, the shortening of the 10-mers, by removing the *N*-terminus, positively charged residue (Api) resulted in reduced 3_{10}-helicity as well as diminished antimicrobial activity against *E. coli*. The larger polar face associated with the non-acetylated 10-mer (Ipi-10), compared to the non-acetylated 9-mers, apparently has better peptide-membrane interactions in SDS and *E. coli*. Seemingly, only small, if any, repulsive forces between the charged Api residue and the *N*-terminal amine of the non-acetylated 10-mer exist. In any case, elimination of the adjacent charges, by removing the N-terminus Api, doesn't apparently improve helicity or bioactivity. However, acetylation of the 10-mer does improve 3_{10}-helicity and bioactivity. Therefore, the larger polar face of the 10-mer evidently overcomes any unfavorable like charge-charge effects.

The activity of our peptides against intracellular pathogens, like brucella, was not tested; however, their degree of toxicity to normal murine macrophages was examined. Macrophages are large white blood cells that ingest foreign particles and infectious microorganism by phagocytosis. Table 3.21 shows normal murine macrophage survival versus peptide concentration for the peptides **3.1-3.10**. Cell death was indicated by the enclosure of a trypan blue dye within a cell. Normal untreated murine macrophages have a survival rate of ~ 90%. No cytolytic effects were observed for Ipi-10; however, shortening it to the 9-mer peptides didn't lead to any significant cytotoxicity at

concentrations ≤ 100 μM. Ipiorn-9 wasn't significantly toxic up to the maximum concentration of 200 μM. However, **3.1** and **3.3-3.4** were slightly toxic at 200 μM. None of the tested acetylated peptides, based on the presence of a very few to zero blue cells, exhibited any significant cytotoxicity.

It is generally accepted that antimicrobial peptides selectively inhibit and kill bacteria over mammalian cells due to differences in their membranes.[3.20,3.41] The exterior membranes of mammalian cells are neutral, but bacteria cell exterior membranes are negatively charged. Because antimicrobial peptides are positively charged, they might preferentially bind to bacteria over mammalian cells. In a previous study,[3.17,3.26] the highest or optimum peptide dose, which was the maximum nontoxic to very slightly toxic dose, that showed $\geq 70\%$ macrophage survival was used as the starting dosage to determine if infected macrophages were selectively destroyed relative to non-infected macrophages; the average dose used in this study was 10 μM for amphipathic peptides of length 10-14 residues. For our 9-mer peptides, a starting dose as high as 200 μM could possibly be employed without significant toxicity to the normal macrophages.

The acetylated peptides showed very little cytotoxicity compared to non-acetylated peptides. It's desirable that this be translated into greater selectivity with good bioactivity for the acetylated peptides. It has been reported in other similar systems that short Aib-rich peptides (11-14 residues, acetylated and non-acetylated) kill infected macrophages significantly better than non-infected macrophages *in vitro*.[3.26] However, the acetylated peptides tended to be less effective than its respective non-acetylated versions at killing infected macrophages; this was especially observed, for these other systems, *in vivo*. For this above study, the acetylated peptides generally had less than

good activity against intracellular pathogens *in vivo*. *N*-terminus acetylation decreases the overall charge of a peptide while increasing the hydrophobicity, which may lessen the amount of peptide actually making it to the infected macrophages present in the spleen (*in vivo* study). It was hoped that our water-soluble, acetylated and non-acetylated 9-mers could overcome possible transport problems *in vivo*. Also, since our peptides are not very significantly toxic at concentrations as high as 200 μM, it is hoped that this

Table 3.20 Peptide antibacterial activity[a] and percent helicity

Peptide	*E. Coli*	*S. aureus*	% Helicity
3.1 Ipi-9	140	> 281	23,[b] 16[c]
3.2 Ipiorn-9	36	> 290	6,[b] 24[c]
3.3 Ipidab-9	149	> 300	4,[b] 19[c]
3.4 Ipidap-9	> 300	> 300	*d*
3.5 AcIpi-9	134	> 268	23[b]
3.6 AcIpiorn-9	> 277	> 277	11[b]
3.7 AcIpidab-9	> 285	> 285	8[b]
3.8 AcIpidap-9	> 295	> 295	*e*
3.9 Ipi-10	7.7	> 247	25[f]
3.10 AcIpi-10	7.4	> 237	41[b]

[a] These MIC (in μM) are corrected for the actual peptide concentration using quantitative amino acid analysis.
[b] % 3_{10}-helicity in 25 mM SDS at 25 °C
[c] % 3_{10}-helicity in buffer (pH = 7) at 25 °C
[d] Peptide 3.4 lacks well-defined structure in 25 mM SDS and neutral buffer.
[e] Peptide 3.8 lacks well-defined structure in 25 mM SDS.
[f] % 3_{10}-helicity in 25 mM SDS at 5 °C; it's only 5 % at 25 °C.

correlates with great selectively of bacterial killing over normal mammalian cells, which would have to be determined via *in vivo* and *in vitro* testings.

Table 3.21 Direct peptide toxicity effects on murine peritoneal macrophages

Peptide	200 μM	100 μM	50 μM	10 μM
3.1 Ipi-9	20 % Dead	95 % Viable	95 % Viable	95 % Viable
3.2 Ipiorn-9	90 % Viable	90 % Viable	95 % Viable	95 % Viable
3.3 Ipidab-9	20 % Dead	No Effect	No Effect	No Effect
3.4 Ipidap-9	20 % Dead	95 % Viable	95 % Viable	95 % Viable
3.5 AcIpi-9	No Effect	No Effect	No Effect	No Effect
3.6 AcIpiorn-9	Granular Appearance Very few blue Cells. 95 % Viability	Beginning to have granular appearance. 95 % Viability	"Fried looking cells present, but no blue cells. 95 % Viability	Less granular in appearance. No blue cells present. 95-100 % Viability
3.8 AcIpidap-9	Granular appearance. Very few blue cells. 95 % Viability	Beginning to have granular appearance. 95 % Viability	95 % Viability	95 % Viability
3.9 Ipi-10	Fewer cells but no lytic effects	Fewer cells but no lytic effects	Cells more granular in appearance	No Effect
3.10 AcIpi-10	No Effect	No Effect	No Effect	No Effect

3.3 Conclusions

Peptides **3.1-3.10**, which are rich in ααAAs (6 Aibs and 1 Api), were successfully prepared using solid-phase synthethic techniques. The *in situ* coupling reagent, PyAOP, was employed in our synthesis. The overall yields of the peptides were significantly improved when the dimer, Fmoc-Aib-Aib-OH, was used in the synthesis; however, the monomer, Aib, had to be employed, along with double coupling, for the first two Aibs in each peptide's sequence.

Peptides **3.1-3.8**, whose main-chains were based on the previously described Ipi-10 (3.9), were designed to be amphipathic, 3_{10}-helical peptides. The solvents effects on each peptide's 3_{10}-/α-helix equilibrium were measured in aqueous buffer, 25 mM SDS, and 50-100 % aqueous/organic solvent mixtures. For the non-acetylated peptides **3.1-3.3**, significant populations of both α-and 3_{10}-helices were observed in all of the solvent systems tested. Ipidap-9, which was composed of the shortest α-amino acid side-chains, was helical (mainly α-helix) only in the 90% organic solvent mixture. The amphipathic, 3_{10}-helical design was observed best, of peptides **3.1-3.4**, for **3.2** (Ipiorn-9, R = 0.48) in a neutral, aqueous buffer at 25 °C. We found that Ipi-10, which is apparently 3_{10}-helical (R = 0.32, 25% helicity) at low temperatures (0-5 °C) in 25 mM SDS and 100% organic solution (CH_3CN-TFE, (9:1)), is more α-helical at 25 °C in these solvent systems as well as under the other solvent conditions it was measured in. This wasn't a trend or tendency observed in the other peptides. However, the shortening of Ipi-10 to Ipi-9 did result in better 3_{10}-helical stabilization in 25 mM SDS at 25 °C.

Based on the absolute ellipticity values, a general decrease in stability was observed for the peptides in buffer upon heating to 70 °C. We found that the thermal

transition of each peptide was appreciably reversible. An isodichroic point was not observed during the temperature or solvent studies, which indicates that these are not simple two-state equilibria, but complex equilibria involving three or more folding intermediates.

The 3_{10}-helical, amphipathic design, based on R values, was observed best for the acetylated peptides, specifically **3.6** (AcIpiorn) and **3.10** (AcIpi-10). Peptide **3.6** folded appreciably into a 3_{10}-helix in 25 mM SDS and CH_3CN-TFE (9:1) and peptide **3.10**, in 25 mM SDS. AcIpidab-9 also folded considerably into a 3_{10}-helix in CH_3CN-TFE (9:1). In buffer, all of the acetylated peptides ($R \approx 1$) folded mainly into an α-helix.

The antimicrobial activity of our designed peptides was tested against *E. coli* and *S. aureus*. The shortening of Ipi-10 to **3.1-3.4** resulted in diminished but modest activity against *E. coli*. Of the non-acetylated peptides **3.1-3.4**, **3.2** (Ipiorn-9), which had the highest percent 3_{10}-helicity in neutral buffer, had the best activity against *E. coli*. AcIpi-9, which had the highest estimated 3_{10}-helicity in 25 mM SDS, was the only acetylated peptide of **3.5-3.8** to exhibit any activity against *E. coli*. Of all ten of the peptides, **3.10** (AcIpi-10), which displayed a R value of 0.38 and 41% 3_{10}-helicity in SDS micelles, had the best activity against *E.coli*. Practically no activity against *S. aureus* was observed for any of the peptides.

The shortening of Ipi-10 to the 9-mer peptides did not lead to any significant cytotoxicity in the concentration range of 10-100 uM. Peptides **3.1** and **3.3** were slightly toxic at 200 uM. None of the tested acetylated peptides exhibited any significant cytotoxicity. This may bode well for the potential selectivity of these peptides for lyses of infected/activated macrophages over non-infected/non-activated macrophages.[3.18]

3.4 Experimental

3.4.1 Peptide Synthesis

Peptides **3.1-3.10** were synthesized via solid-phase peptide synthesis using a Milligen 9050 peptide synthesizer on a PAL-PEG-PS (0.24 mmol/g) solid support. The peptides were prepared on a 0.24 mmol scale using the Fmoc-amino acids (0.96 mmol, 4 equiv.), preformed Fmoc-Aib-Aib-OH (0.96 mmol, 4 equiv.), PyAOP (0.96 mmol, 4 equiv.), DIEA (1.92 mmol, 8 equiv.), 1.2 h recycling time, and a jacket temperature of 50 °C. The monomer, Fmoc-Aib-OH, was employed only in the coupling of the first two Aibs in the peptide sequences. A double coupling was performed after each Fmoc-Aib-OH. A deblocking solution of 2% piperidine/2% 1,8-diazobicyclo[4.5.0]undec-7-ene (DBU) in DMF was used for Fmoc removal. Peptides **3.1-3.4** and **3.9** were acetylated on the solid support (0.12 mmol) by treatment with a 0.2 M solution of acetic anhydride in a 0.28 M solution of DIEA in DMF for 3 hours.

The peptides were simultaneously cleaved from the resin and side-chain deprotected using the following cleavage cocktail: 94% trifluoroacetic acid (TFA), 5% water, and 1% triisopropylsilane (TIPS). The resulting acidic solution was diluted with 30% acetic acid and lyophilized. The crude peptides were purified by reverse-phase preparative HPLC on a Waters 15 μM DeltaPak C-4 column using a mobile phase of water (0.05%, v/v, TFA) and acetonitrile (0.05%, v/v, TFA) and running a gradient of 10% to 50% of the organic phase over 1 hour; the absorption was monitored at 222 nm. Purities of the peptides were checked on a Vydac 5 μM C_{18} column running a similar mobile phase gradient and monitoring at 222 nm. The molecular weight of each purified

peptide was verified by matrix assisted laser desorption ionization (MALDI) mass spectrometry (Table 3.22).

3.4.2 N^1-tert-Butyloxycarbonyl-4-[N^2-(9-fluorenylmethoxycarbonyl) amino]-piperidine-4-carboxylic acid[3.42]

N^4,N^7,N^9-tris-tert-butyloxycarbonyl-8,10-dioxo-4,7,9-triazaspiro[5,4]cyclodecane was prepared from piperidine-4-spiro-5′-hydantoin according to a procedure described in reference 3.38. To a vigorously stirring suspension of N^4,N^7,N^9–tris-tert-butyloxycarbonyl-8,10-dioxo-4,7,9-triaza-spiro[5,4]cyclodecane (33 g, 71 mmol) in THF (300 mL) was added 2 N KOH (300 mL). After stirring for 18 hours, the two-layer clear solution was poured into a separatory funnel and then the aqueous layer was drained into

Table 3.22 Characterization of Peptides **3.1-3.10**

Peptide	t_R (min.)[a]	Calculated Mass	MALDI[b]
Ipi-9	22.6	910.16	910.99 $(M + H)^+$
Ipiorn-9	21.9	882.11	883.67 $(M + H)^+$
Ipidab-9	21.8	854.06	854.25 $(M)^+$
Ipidap-9	21.6	826.01	849.24 $(M + Na)^+$
AcIpi-9	29.4	952.21	953.21 $(M + H)^+$
AcIpiorn-9	29.1	924.15	925.47 $(M + H)^+$
AcIpidab-9	29.0	896.10	897.16 $(M + H)^+$
AcIpidap-9	28.5	868.05	869.01 $(M + H)^+$
Ipi-10	26.2	1036.32	1037.38 $(M + H)^+$
AcIpi-10	32.5	1078.36	1078.74 $(M + H)^+$

[a]Reverse-phase HPLC carried out on a C_4 column (8 x 100 mm) using a mobile phase of H_2O (0.05% TFA) and CH_3CN (0.05% TFA), gradient of 10 to 50% organic phase over 1h, and a flow rate of 1 mL/min.
[b]CCA matrix (CH_3CN-H_2O).

a round bottom flask. Residual THF was removed by rotary evaporation. The aqueous layer was acidified to pH 7 with 2 N HCl. The resultant white precipitate was filtered and dried *in vacuo* to yield 1-tert-butyloxycarbonyl-4-amino-piperidine-4-carboxylic acid. Yield: 15 g (88%). ^{1}H NMR (250 MHz, CD_3SOCD_3) δ 1.42 (s, 9 H) 1.90 (m, 4 H), 3.58 (m, 4 H).

According to Bolin's procedure,[3.33] under argon, anhydrous methylene chloride (150 mL) and DIEA (9.14 mL, 52.4 mmol) was syringed into a flask containing 1-tert-butyloxycarbonyl-4-amino-piperidine-4-carboxylic acid (5.12 g, 20.9 mmol). The reaction mixture stirred for 15 minutes at room temperature. Chlorotrimethylsilane (TMS-Cl) (5.32 g, 41.9 mmol) was then added dropwise , and the solution was heated to reflux for 3 hours. After cooling in an ice bath, 9-fluorenylmethyl chloroformate (5.45 g, 21.1 mmol) was added in one portion. The solution was stirred in the ice bath for 20 minutes and for 3 hours at room temperature. The solvent was evaporated, and the product was distributed between Et_2O (70 mL) and 2.5% Na_2CO_3 (300 mL). The aqueous layer was separated and washed with additional portions of Et_2O (2 x 30 mL). Residual Et_2O was removed from the aqueous layer by rotary evaporation and acidified to pH 2 in an ice bath using 2 N HCl. The precipitated free acid was extracted with EtOAc (100 mL) and additional portions of EtOAc (2 x 60 mL). The combined EtOAc fractions were dried over $MgSO_4$ and filtered. The solvent was removed by rotary evaporation, and the resulting yellow solid was dried *in vacuo*. Yield: 9 g (93%). ^{1}H NMR (250 MHz, CD_3OD) δ 1.40 (s, 9H), 1.75 (m, 2H), 1.96 (m, 2H), 3.04 (m, 2H), 3.76 (m, 2H), 4.37 (m, 3H), 7.25 (t, 2H), 7.30 (t, 2H), 7.70 (d, 2H), 7.90 (d, 2H). FABMS (NBA) m/e 465.3 $(M-H)^-$.

3.4.3 *N*-(9-Fluorenylmethoxycarbonyl)aminoisobutyric acid fluoride [Fmoc-Aib-F]

Under argon, Fmoc-Aib-OH (10 g, 30 mmol) was suspended in CH_2Cl_2 (100 mL) followed by the addition of pyridine (2.4 mL, 30 mmol) and cyanuric fluoride (5.1 mL, 61 mmol). The reaction mixture stirred at room temperature for 24 hours, and then it was diluted with CH_2Cl_2 (150 mL), poured onto ice-water, and filtered. The organic layer was extracted with ice water (2 x 200 mL), dried over $MgSO_4$, and evaporated in vacuo to yield the acid fluoride as a pink solid. The product was recrystallized from the solvent pair, CH_2Cl_2/hexane. Yield: 8 g (82%). ^{1}H NMR (250 MHz, $CDCl_3$) δ 1.45 (s, 6H), 4.25 (t, 1H), 4.46 (d, 2H), 7.42 (m, 5H), 7.78 (d, 2H), 7.95 (d, 2H).

3.4.4 Fmoc-Aib-Aib-OH

α-Aminoisobutyric acid (3.01 g, 29.2 mmol) was placed in a flask equipped with a condenser, heating mantle, and an argon inlet. Anhydrous CH_2Cl_2 (70 mL) was syringed into the reaction vessel followed by the addition of TMS-Cl (7.4 mL, 58.4 mmol). The mixture was refluxed for 2 hours and then cooled in an ice bath. DIEA (9.17 mL, 52.6 mmol) and Fmoc-Aib-F (6.37 g, 19.4 mmol) were added in succession. The reaction mixture was stirred with cooling for 20 minutes and then warmed to room temperature for 2 hours. The solvent was evaporated, and the resulting residue was distributed between Et_2O (160 mL) and 2.5% $NaHCO_3$ (210 mL). The aqueous layer was extracted with 2 x 50 mL of Et_2O. The aqueous layer was then acidified to pH 2 with 1 N HCl and extracted with EtOAc (3 x 80 mL). The combined EtOAc fractions were then dried over Na_2SO_4, filtered, concentrated, and dried *in vacuo*. The final product was recrystallized from the solvent pair, $CHCl_3$/hexane. Yield: 5.5 g (70%). ^{1}H NMR (250 MHz, CD_3SOCD_3) δ 1.33 (s, 12H), 4.25 (t, 1H), 4.4 (d, 2H), 7.32 (m, 4H), 7.56 (d, 2H),

7.83 (d, 2H), 12.24 (bs, 1H). MALDI (CCA) 411.34 $(M + H)^+$. Analysis calculated for $C_{23}H_{26}N_2O_5$: C, 67.32; H, 6.34; N, 6.83; Found: C, 67.51; H, 6.39; N, 6.77.

3.4.5 Amino Acid Analysis

The concentrations of the Peptides (**3.2-3.10**) were determined by quantitative amino acid analysis. Peptide samples containing a norleucine standard were hydrolyzed in 6 N HCl and 0.1% phenol for 24 h at 110 °C. This was followed by sodium cation exchange chromatography at 65 °C and post-column derivatization with ninhydrin at 130 °C. The peptide contents of lyophilized powders were between 67% and 80% peptide by weight.

3.4.6 Circular Dichroism Measurements

Circular dichroism measurements were performed on a (+)-camphor sulfonic acid calibrated Aviv 60DS spectropolarimeter at room temperature (except where noted). The measurements were recorded over a 250-180 range using a quartz cell of 0.1 cm path length, 1 nm bandwidth, 10 nm/min scan speed, and a 5 second time constant. Baseline corrections were performed by subtracting each sample spectrum from its respective, acquired background spectrum. Three repetitive scans were recorded and averaged to improve the signal to noise ratio. Ellipticity is reported as the mean residue ellipticity [θ] in units of deg cm^2 dm^{-1}, and it's derived from the formula, $[\theta] = [\theta]_{obs}$ (MRW/10*lc*), where $[\theta]_{obs}$ is the ellipticity measured in millidegrees, MRW is the mean residue molecular weight of the peptide (molecular weight divided by the number of peptide bonds), *c* is the concentration (mg/mL) of the sample, and *l* is the optical path length (cm) of the cell.

CD spectra of all peptides in this study were acquired in solvent systems ranging from 100% organic to 100% aqueous (0% organic). Final peptide concentrations of 0.2 mM were used for the experiments. The peptides were dissolved in acetonitrile for spectra taken in 9:1 CH_3CN:TFE and 10 mM phosphate buffer (pH 7) for spectra taken in SDS. The 10 mM phosphate buffer (pH 7) was also used as the aqueous component in the aqueous/organic experiments (CH_3CN/H_2O).

3.4.7 Minimum Inhibitory Concentration Assays

The MIC of peptides was determined against *E. Coli* American type culture collection (ATCC) 25922 and *S. aureus* ATCC 25723; they were employed as representative Gram-positive and Gram-negative bacteria, respectively. Bacterial cultures were grown to midlog phase in nutrient broth and were standardized to a McFarland turbidity tube before dilution. Peptide 1:2 serial dilutions were prepared from 512 μg/mL stock solutions to provide a range of peptide concentrations (256-2 μg/mL) in the culture media. 50 μL of the desired peptide solution was added to a sterile well containing 50 μL of 5 x 10^4 cells. The MIC is the lowest peptide concentration that prevents the growth of the cells as evidenced by the absence of turbidty after four hours. The MIC values are reported as the median assay value for at least three experiments.

3.4.8 Macrophage Assays

The peritoneal macrophages of the ten-week old BALB/c mice had to be extracted before toxicity studies with peptides. Briefly, following euthanasia using halothane, the cells were harvested by lavage from the peritoneal cavity of the mice using 8 mL of RPMI 1640 (Sigma) + 10% fetal calf serum (FCS) and Pen-Strep (Penicillin and Streptomycin). The cells were cultured in 96 well plates at a concentration of 5 x 10^5

cells per well in 200 μL of RPMI 1640 + 10% FCS at 37 °C in 5% CO_2. The cells were allowed to adhere overnight. The cell cultures were enriched for macrophages by washing away non-adherent cells, and then 200 μL of fresh media was added to the cultures.

For the toxicity studies, normal macrophage cultures were treated with 0 to 200 μM of the test peptide. The peptides were incubated with the cells for 60 minutes at 37 °C in 5% CO_2. The cells were washed 3 times with PBS (phosphate buffered saline) + 10% FCS to remove any residual peptide. Peptide treated cells were stained with 0.04% trypan blue in RPMI 1640 + 10% FCS and Pen-Strep. About 100 to 200 cells per well were counted using a hemocytometer and an inverted light microscope. Five wells were analyzed per peptide concentration; the number of blue stained cells was recorded. The enclosure of trypan blue dye within a cell is indicative of cell death. The percent survival was calculated by subtracting the number of blue cell from the total cells and normalized.

3.5 References

3.1 Toniolo, C.; Polese, A.; Formaggio, F.; Crisma, M.; Kamphuis, J. *J. Am. Chem. Soc.* **1996**, 118, 2744.

3.2 Millhauser, G. L. *Biochemistry* **1995**, 34, 3873.

3.3 Smythe, M. L.; Huston, S. E.; Marshall, G. R. *J. Am. Chem. Soc.* **1995**, 117, 5445.

3.4 Toniolo, C.; Benedetti, E. *Trends Biochem. Sci.* **1991**, 16, 350.

3.5 Smythe, M. L.; Nakaie, C. R.; Marshall, G. R. *J. Am. Chem. Soc.* **1995**, 117, 10555.

3.6 Otoda, K.; Kitagawa, Y.; Kimura, S.; Imanishi, Y. *Biopolymers* **1993**, 33, 1337.

3.7 Gerstein, M.; Chothia, C. *J. Mol. Biol.* **1991**, 220, 133.

3.8 Karle, I. L.; Flippen-Anderson, J. L.; Gurunath, R.; Balaram, P. *Biopolymers (Protein Sci.)* **1994**, 4, 1547.

3.9 Basu, G.; Bagchi, K.; Kuki, A. *Biopolymers* **1991**, 31, 1763.

3.10 Basu, G.; Kuki, A. *Biopolymers* **1993**, 33, 995.

3.11 Balaram, P. *Curr. Opin. Struct. Biol.* **1992**, 2, 845.

3.12 Karle, I. L.; Balaram, P. *Biochemistry* **1990**, 29, 6747.

3.13 Aleman, C.; Subirana, J. A.; Perez, J. J. *Biopolymers* **1992**, 32, 621.

3.14 Karle, I. L.; Flippen-Anderson, J. L.; Uma, K.; Balaram, H.; Balaram, P. *Proc. Natl. Acad. Sci. U. S. A.* **1989**, 86, 765.

3.15 Kennedy, D. F.; Crisma, M; Toniolo, C.; Chapman, D. *Biochemistry* **1991**, 30, 6541.

3.16 Formaggio, F.; Crisma, M.; Rossi, P.; Scrimin, P.; Kaptein, B.; Broxterman, Q. B.; Kamphuis, J.; Toniolo, C. *Chem. Eur. J.* **2000**, 6, 4498.

3.17 Yokum, T. S.; Gautheir, T. J.; Hammer, R. P.; McLaughlin, M. L. *J. Am. Chem. Soc.* **1997**, 119, 1167.

3.18 Yokum, T. S.; Elzer, P. H.; McLaughlin, M. L. *J. Med. Chem.* **1996** 39, 3603.

3.19 Branden, C.; Tooze, J. In *Introduction to Protein Structure*; Garland Publishing: New York, **1991**; pp. 8-15.

3.20 Javadpour, M. M.; Juban, M. M.; Lo, W. C. J.; Bishop, S. M.; Albertis, J. B.; Cowell, S. M.; Becker, C. L.; McLaughlin, M. L. *J. Med. Chem.* **1996**, 39, 3107.

3.21 Saberwal, G.; Nagaraj, R. *Biochem. Biophys. Acta* **1994**, 1197, 109.

3.22 Blondelle, S. E.; Houghten, R. A. *Biochemistry* **1992**, 31, 12688.

3.23 Manning, M. C.; Woody, R. W. *Biopolymers* **1991**, 31, 569.

3.24 Mayr, W.; Oekonomopoulos, R.; Jung, G. *Biopolymers* **1979**, 18, 425.

3.25 Jung, G.; Debischar, N.; Leibfritz, D. *Eur. J. Biochem.* **1975**, 54, 395.

3.26 Yokum, T. S. In *Dissertation*; Louisiana State University: **1998**; pp.57-100.

3.27 Kritana, C.; Johnson, W. C. *Analyt. Biochem.* **1997**, 253, 57.

3.28 Iwata, T.; Lee, S.; Oishi, O.; Aoyagi, H.; Ohno, M.; Anzai, K.; Kirino, Y.; Sugihara, G. *J. Biol. Chem.* **1994**, 269, 4928.

3.29 McLean, L. R.; Hagaman, K. A.; Owen, T. J.; Krstenansky, J. L. *Biochemistry* **1991**, 30, 31.

3.30 Carpino, L. A.; Choa, H. G.; Beyermann, M.; Bienert, M. *J. Org. Chem.* **1991**, 56, 2635.

3.31 Wenschuh, H.; Beyermann, M.; Haber, H.; Seydel, J. K.; Krause, E.; Bienert, M.; Carpino, L. A.; El-Faham, A.; Albericio, F. J. *J. Org. Chem.* **1995**, 60, 405.

3.32 Albericio, F.; Cases, M.; Alsina, J.; Triolo, S. A.; Carpino, L. A.; Kates, S. A. *Tetrahedron Lett.* **1997**, 38, 4853.

3.33 Bolin, D. R.; Sytwu, I. –I.; Humiec, F.; Meienhofer, J. *Int. J. Peptide Protein Res.* **1989**, 33, 353.

3.34 Wu, C. C.; Ikeda, K.; Yang, J. T. *Biochemistry* **1981**, 20, 566.

3.35 Scholtz, J. M.; Marqusee, S.; Baldwin, R. L.; York, E. J.; Stewart, J. M.; Santoro, M.; Bolen, D. W. *Proc. Natl. Acad. Sci. U.S.A.* **1991**, 88, 2854.

3.36 Kaneshina, S.; Kamaya, H.; Ueda, I. *Biochim. Biophys. Acta* **1982**, 685, 307.

3.37 Ramesh, V.; Labes, M. M. *J. Am. Chem. Soc.* **1986**, 108, 4643.

3.38 Stewart, J. M. In *The Amphipathic Helix*; Epand, R. M., Ed.; CRC Press: Florida, 1993; pp. 21-37.

3.39 Cornut, I.; Buttner, K.; Dasseux, J. –L.; Dufourcq, J. *FEBS Lett.* **1994**, 349, 29.

3.40 Brock, T. D.; Madigan, M. T.; Martinko, J. M.; Parker, J. In Biology of Microorganisms; 7th ed.; Prentice Hall: New Jersey 1994: pp. 45-65.

3.41 Opdenkamp, J. A. F. *Annu. Rev. Biochem.* **1979**, 48, 47.

3.42 Wysong, C. L.; Yokum, T. S.; Morales, G. A.; Gundry, R. L.; McLaughlin, M. L.; Hammer, R. P. *J. Org. Chem.* **1996**, 61, 7650.

Chapter 4

Summary and Future Studies

This dissertation focused on the synthesis and characterization of compounds from two classes of peptide analogs, phosphonopeptides and α,α-dialkylated amino acid-rich peptides. Compounds in both classes of analogs have been reported to exhibit significant bioactivity. The P (III) synthetic approach to phosphonopeptides provided a route to phosphonamide dipeptides **1a** and **1c** (Figure 4.1) which were previously unattainable by P (V) methods. Additionally, the use of reduced phosphorus intermediates allowed preparation of the related thiophosphamides **1b** and **1d** (Figure 4.1). Ten α,α-dialkylated amino acid (ααAA)-rich peptides, which were designed to be amphipathic and 3_{10}-helical, were successfully prepared using solid-phase synthetic methods. The helix preference of each peptide in different solvent environments were investigated as well as each peptide's antimicrobial activity and cytotoxicity.

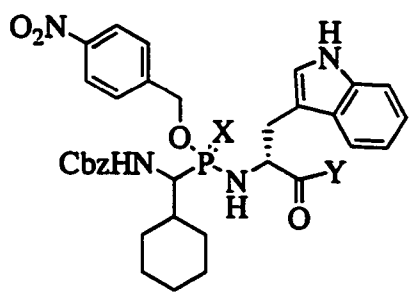

1a X = O, Y = NH_2
1b X = S, Y = NH_2
1c X = O, Y = OCH_3
1d X = S, Y = OCH_3

Figure 4.1 Main phosphonamide and thiophosphonamide synthetic targets

Phosphonamides are generally more difficult to prepare than phosphonate diesters. Phosphonamidate's poor synthetic accessibility has severely limited the use of this interesting class of compounds as tools in enzyme chemistry. Chapter 2 described

the conditions we developed, based on a one-pot activation-coupling-oxidation/sulfurization procedure, for preparation of sterically hindered phosphonamide and thiophosphonamide dipeptides. The commercially available Ph_3PCl_2 was used for activation of our air-stable precursor, Cbz-protected H-phosphinate amino acid ester [Cbz-CyhGly ψ (POH (OpNb)]. From a GC-MS study, it was determined that the presence of two equivalents of base (pyridine) during activation of the H-phosphinate amino acid ester with Ph_3PCl_2 was essential to preclude ester cleavage. However, as the number of equivalents of base increased from two to large excess (e.g., pyridine as solvent), the number and amount of side-products increased, as evident by ^{31}P NMR. The optimized activation step was generally high-yielding.

During the coupling step, a reactive phosphitylating agent, which we proposed to be an oxazaphospholine, formed and competed with the formation of the desired, intermediate phosphonamidites. Since the proposed oxazaphospholine was very reactive (electrophilic), it was purposely generated before the amine-coupling step. Each amine-nucleophile was coupled to the oxazaphospholine, instead of the initial activated P (III) species (a phosphonochloridite), to form two coupling, diastereomeric products instead of the possible four. This may have indicated a lack of stereoselectivity when amine adds directly to the phosphonochloridite.

Oxidation and sulfurization of the intermediate phosphonamidites were easily accomplished with t-butylhydroperoxide and elemental sulfur, respectively. Using our developed conditions, the previously inaccessible phosphonamide hapten precursor **1a** and related derivatives **1b-d** were prepared. In an alternate procedure, we found that the addition of 2 equivalents of an amine-nucleophile with 3.5 equivalents of DIEA to the

phosphonochloridite followed by sulfurization/oxidation could also form **1**, but as a mixture of four diastereomers instead of two. The former method, incorporating the oxazaphospholine, was also applied in the preparation of simpler phosphonamide and thiophosphonamide dipeptides and thiophosphonates.

The potential use of the non-urethane amine-protecting groups, Dde and Nbs, were also investigated in our phosphonopeptide syntheses. These amine-protecting groups were incorporated to lessen the formation of cyclized intermediates or oxazaphospholines, which is sometimes undesired in peptide synthesis. The coupling of an amine-nucleophile to a Nbs-protected phosphonochloridite results in the expectant diastereomeric mixture of phosphonamidites along with only a small amount of the proposed oxazaphospholine. However, with a Dde-protected phosphonochloridite, the formation of an oxazaphospholine isn't observed during amine-coupling, but the overall coupling reaction with this type of species doesn't proceed as well as the reaction with a Nbs-protected phosphonochloridite.

Future studies in the area of phosphonopeptide synthesis using reduced phosphorus species include the incorporation of non-participating amino protection (via solution-or solid-phase), use of milder activation agents, development of analytical conditions or techniques for separation of diastereomeric mixtures of phosphonopeptides, and solid-supported approaches. The amenability of the P (III) synthetic approach to solid-phase methods could be very valuable. In phosphonopeptides prepared by the P (III) protocol, diversity can be achieved around the phosphorus center as well as by the different side-chains of the α-amino acids coupled to them. Therefore, the next logical step, for the long-term, would be the adaptation of the solid-phase methodology to the

simultaneous synthesis (combinatorial chemistry) of several peptides, which could be beneficial in the search for therapeutic agents.

Chapter 4 described the synthesis of short, ααAA-rich peptides, the effects of different solvent environments on their 3_{10}-/α-helix equilibrium, and the peptides' *in vitro* antimicrobial activity and cytotoxicity. The peptides were designed to be amphipathic and 3_{10}-helical. They were prepared to test the hypothesis that shortened, amphipathic 3_{10}-helical peptides would retain biological activity while becoming increasingly selective (less cytotoxic) in bacterial killing over normal mammalian cells. This was based on the trend observed between the length of a peptide and cytotoxicity and helicity and bioactivity. The trend was that the shorter the peptide the higher and lower the selectivity and cytotoxcity, respectively, and the more helical the peptide the greater the activity.

Four homologous series of 9-mer, ααAA-rich peptides (and their acetylated versions) as well as previously described 10-mer peptide (and its acetylated version) were successfully prepared using solid-phase synthetic methods. The 9-mers were comprised of 78% ααAAs (6 Aibs and 1 Api) and two lysine or lysine-like residues, and the 10-mers were composed of 80% ααAAs (6 Aibs and 2 Api's) and two lysines. The 9-mers differed only in the length of their α-amino acid side-chains. The *in situ* coupling agent, PyAOP, was used in the synthesis. The coupling yields as well as the overall yields of the peptides were significantly improved when the dimer, Fmoc-Aib-Aib-OH, was employed in the synthesis; however, it was essential that the monomer, Aib, be incorporated, along with double coupling, for the first two Aibs in each peptide's sequence.

The solvent effects on each peptide's 3_{10}-/α-helix equilibrium were measured in aqueous buffer, 25 mM SDS, and 50-100% aqueous/organic solvent mixtures. Significant populations of both α- and 3_{10}-helices were generally observed for the non-acetylated 9-mer peptides under all of the solvent conditions tested. Ipidap-9, which was comprised of the shortest α-amino acid side-chains, was helical (mainly α-helix) only in CH_3CN:H_2O (9:1). The amphipathic, 3_{10}-helical design was observed best, of the non-acetylated 9-mers, for Ipiorn-9 (R = 0.48) in neutral, aqueous buffer at 25 °C. Interestingly, Ipi-10, which is apparently 3_{10}-helical (R = 0.32) at 5 °C in SDS micelles and CH_3CN-TFE (9:1), is more α-helical at 25 °C under these solvent conditions as well as in the other solvent environments it was measured in. This wasn't a trend observed in the other peptides. Further shortening of Ipi-10 to Ipi-9, however, did result in the better 3_{10}-helical stabilization in 25 mM SDS at 25 °C.

A temperature study was also conducted on the 9-mer peptides. A general decrease in stability, based on absolute ellipticity values, was observed for the peptides in buffer upon heating to 70 °C. However, the thermal transition of each peptide was appreciably reversible. Furthermore, during the temperature studies as well as the solvent studies no isodichroic point was observed.

The 3_{10}-helical, amphipathic design, based on R values, was observed best for the acetylated peptides, specifically AcIpiorn-9 and AcIpi-10. AcIpiorn-9 folded appreciably into a 3_{10}-helix in 25 mM SDS and CH_3CN-TFE (9:1) and AcIpi-10, in 25 mM SDS. AcIpidab-9 also adopted the 3_{10}-helical conformation to a substantial extent in CH_3CN-TFE (9:1). In buffer, all of the acetylated peptides (R ≈1) folded mainly into an α-helix.

The antimicrobial activity of our designed peptides was tested against *E. coli* and *S. aureus*. The shortening of Ipi-10 to the 9-mer peptides resulted in diminished but modest activity against *E. coli*. Of the non-acetylated peptides, Ipiorn-9, which had the highest percent 3_{10}-helicity in neutral buffer, had the best activity against *E. coli*. AcIpi-9, which had the highest estimated 3_{10}-helicity in 25 mM SDS, was the only acetylated peptide of the acetylated-9-mers to exhibit any activity against *E. coli*. Of all ten of the peptides, AcIpi-10, which displayed a R value of 0.38 and 41% 3_{10}-helicity in SDS micelles, had the best activity against *E.coli*. Practically no activity against *S. aureus* was observed for any of the peptides.

The shortening of Ipi-10 to the 9-mer peptides did not lead to any significant cytotoxicity in the concentration range of 10-100 uM. Ipi-9 and Ipidab-9 were only slightly toxic at 200 uM. None of the tested acetylated peptides exhibited any significant cytotoxicity.

Potential future studies include the introduction of a suitable transition metal or salt bridges for possible induction of helical stabilization (preferably 3_{10}-helix) in the 9-mer, ααAA-rich peptides and the determination of the effects (e.g., helix preference and stability, bioactivity, etc.) of increasing the length of the side-chains of the 9-mers (starting from Ipi-9). The *in vitro* and *in vivo* testing of the 9-mers (acetylated and non-acetylated) against intracellular pathogens, like Brucella, is also a potential future area of investigation.

Vita

Sheila Denise Rushing was born December 30, 1973, in Hollandale, Mississippi. After receiving her high school diploma in 1992 from Simmons High School in Hollandale, she attended Tougaloo College, Jackson, Mississippi, where she received her bachelor of science degree in chemistry. In 1996 she began graduate school at Louisiana State University under the direction of Dr. Robert P. Hammer. Currently, she is a candidate for the degree of Doctor of Philosophy in the Department of Chemistry, which will be awarded at Spring Commencement, 2001.

DOCTORAL EXAMINATION AND DISSERTATION REPORT

Candidate: Sheila Denise Rushing

Major Field: Chemistry

Title of Dissertation: Synthesis of Phosphonopeptides and Alpha, Alpha-Dialkylated Amino Acid-Rich Peptides

Approved:

Major Professor and Chairman

Dean of the Graduate School

EXAMINING COMMITTEE:

Date of Examination:

March 20, 2001